Engineering and Applied Science Theses & Dissertations

McKelvey School of Engineering

Spring 5-15-2019

Exploring Methodologies to Improve Lignin Utilization in Biorefineries

James Meyer
Washington University in St. Louis

Recommended Citation

WASHINGTON UNIVERSITY IN ST. LOUIS

McKelvey School of Engineering

Department of Energy, Environmental, & Chemical Engineering

Dissertation Examination Committee:
Marcus B. Foston, Chair
Milorad Dudukovic
John D. Fortner
John T. Gleaves
Grigoriy Yablonsky

Exploring Methodologies to Improve Lignin Utilization in Biorefineries

by
James R. Meyer

A dissertation presented to
The Graduate School
of Washington University in
partial fulfillment of the
requirements for the degree
of Doctor of Philosophy

May 2019
St. Louis, Missouri

Table of Contents

List of Figures

List of Tables

<u>Acknowledgments</u>

I would like to thank my advisor, Dr. Foston, for taking a chance on me, introducing me to the field of lignocellulosic biorefineries, and guiding me as I learned how to be a researcher. I would like to thank Yu Gao, an amazing lab partner and friend for all of his help, suggestions, and support through our years together. To all of my friends at Washington University, particularly Ray Henson, thank you for the conversations and friendships.

My deepest appreciation to my parents, Ted and Linda, and family, Nic, Rae, Luke, Mitch, and Kelly for their unending support. And to my wife, Anna, your endless support and love has given me the strength to pull through all the tough moments and persevere to the finish.

James R Meyer

Washington University in St. Louis

March 2019

Dedicated to my loving wife, Anna.

ABTRACT OF THE DISSERTATION

Exploring Methodologies to Improve Lignin Utilization in Biorefineries

By James R. Meyer

Doctor of Philosophy in Energy, Environmental, & Chemical Engineering

Washington University in St. Louis, 2019

Assistant Professor Marcus B. Foston, Chair

The increasing world population, coupled with an improving quality of life, has driven a rapidly increasing demand for fuels, chemicals, and materials. Fossil carbon feedstocks, such as petroleum, are currently being consumed to meet these demands. The utilization of these feedstocks has negative impacts on human and environmental health, which are undoubtedly intensifying as a result of the increased reliance required to meet these demands. As an alternative way to meet these demands, biorefineries generate a wide range of fuels, chemicals, and materials from biomass, a renewable and sustainable resource. Current second-generation biorefineries use a plant-based feedstock, lignocellulosic biomass, comprised of three main components: cellulose, hemicellulose, and lignin. Second-generation biorefineries focus on converting cellulose and hemicellulose into fermentative fuels, discarding lignin as waste. Lignin is a complex and recalcitrant random co-polymer that is difficult to isolate and process, but it is comprised of molecular sub-unit structures that are analogous to many high value components of petroleum. If biorefineries are to compete against and mitigate the harmful effects of petroleum refineries, they must efficiently utilize all three major biomass components to increase product diversity, value, and yields.

This dissertation explores extracting and upgrading lignin to improve its utilization in biorefineries. The first study investigates the use of a series of organic solvent mixtures to extract usable lignin from the waste stream of an ammonia fiber explosion extraction (AFEX) biorefinery. It focuses on understanding the solvent characteristics that control the lignin yield and resulting physochemical properties. An ethanol:water mixture effectively separates lignin from the waste, with high yields and only minor chemical modifications. By utilizing a current waste stream, the technology is easily adopted without disrupting the biorefinery operation. The dissertation next explores the reactions occurring during organosolv pretreatment that control the lignin extraction efficiency, as well as reactions associated with key physiochemical characteristics. A 'pseudo-first order in series' reaction model was applied to nuclear magnetic resonance (NMR) data of extracted lignin and kinetics constants for lignin yields and the chemical moieties related to important physicochemical properties were elicited. This study provides guiding principles for designing future organosolv processes that obtain lignin streams with desired qualities. In a final study, Fourier Transform Ion Cyclotron Resonance High Resolution Mass Spectrometry (FT-ICR HRMS) is used to analyze lignin breakdown products after catalytic upgrading. FT-ICR HRMS overcomes many problems other characterization methods face, but a single analysis results in thousands of data points, making processing the data difficult, thus a petroleomic analysis is adopted to easily track key characteristics. In the study, FT-ICR HRMS and a petroleomic analysis are applied to a catalysis and stabilizing co-solvent system that effectively fragments the lignin while preserving important chemical moieties, as shown by petroleomic analysis of the FT-ICR HRMS data. All three of the technologies explored within this dissertation offer avenues to improve the technical and economic viability of biorefineries.

Chapter 1: Introduction

1.1   Overview

The increasing world population, coupled with an improving quality of life, has driven rapidly increasing demand for fuels, chemicals, and materials.[1-3] Currently, most fuels, chemicals, and materials are derived from fossil resources,[5] whose recovery, processing, and comsumption impose a high cost in terms of human and environmental health.[1] While pollution from sources such as strip mining, ash ponds, and toxic discharge/leaks is detrimental to human and environmental well-being, a larger concern is the release of sequestered carbon from fossil resources in the form of carbon dioxide and methane, into the atmosphere, leading to irreparable global damage and climate change.[9-14] The biorefinery is being considered as a promising option for producing energy, chemicals, and materials from sustainable resources and preventing the release of sequestered carbon.

A biorefinery is analogous to current petroleum refineries, housing several unit operations that together are capable of producing a wide-range of fuels, chemicals, and materials. However, instead of petroleum, biorefineries utilize biomass as the feedstock.[3, 6, 15] Biorefineries combine integrated thermal, chemical, and biological conversion processes to efficiently utilize all of the materials and energy contained within lignocellulosic biomass. Biomass, as a feedstock for fuel, chemical, and material production, presents a sustainable carbon recycling pathway. Sources of biomass and fossil carbon (i.e., petroleum, coal, and natural gas) both represent sequestered atmospheric CO_2. However, the rate at which atmospheric CO_2 is sequestered into fossil carbon sources is so slow in comparison to the rate of fossil carbon source utilization that sources of fossil carbon are not considered renewable, and their consumption is causing atmospheric CO_2

accumulation at an alarming rate. By utilizing a feedstock such as biomass, whose rates of atmospheric CO_2 sequestration and utilization are on similar time-scales, biorefineries provide an opportunity to meet growing energy and material demands while mitigating the impacts associated with fossil carbon-related atmospheric CO_2 accumulation.

Current first-generation biorefineries produce mainly fuels (e.g., bio-ethanol) and have been introduced on a demonstration scale in several countries.[16] Because first-generation biorefineries require feedstocks like food crops (e.g. corn, sugar cane, or sugar beets) that contain readily fermentable sugars, their large-scale and world-wide deployment could negatively impact food supplies and prices.[16-17] Hence, efforts have shifted towards developing second-generation biorefineries, which utilize lignocellulosic materials (e.g., agricultural and forest residues, as well as dedicated energy crops) that are abundant and cheap feedstocks.[16] Lignocellulosic biomass is comprised of carbohydrates, made up of cellulose and hemicellulose, and lignin. Current second-generation pilot-scale biorefinery outputs do not suggest that a large-scale biorefinery could meet the required process performance and cost metrics for profitable operation. To date, most second-generation biorefineries rely on the fermentation of hydrolyzed sugars derived from carbohydrates to generate various products (e.g., ethanol [18-19], butanol [20], and long chain hydrocarbons [21-22]), chemicals/monomers [23] (e.g., succinic acid [24] and lactic acid [25]), and materials/polymers (e.g., polyhydroxyalkanoates [26]). In the current processing paradigm, lignin remains relatively under-utilized.[6, 15]

1.2 Motivation

The utilization of lignin is crucial to the economic viability and minimal environmental footprint of biorefineries and the ultimate displacement of petroleum feedstocks. In an engineering analysis of the production process for a potential state-of-the-art bio-ethanol plant, where the lignin

is only burned for process energy, the minimum selling price for ethanol would have to be $2.15 per gallon, equivalent to the performance of gasoline at $3.27 per gallon.[27] In the analysis, lignin was burnt to produce electricity, providing a value of about $57 per ton of lignin, and very little other economic contribution to the overall viability of the biorefinery. [27] Yet because lignin is comprised of molecular sub-unit structures that are analogous to many high value components of petroleum (i.e., aromatic and phenolic compounds), it has been proposed as a potential source for the production of a wide-range of chemicals and materials.[28] Smolarski et al. postulate that if lignin is converted into benzene, toluene, or xylene (BTX) at ~$1,200 per ton, or phenol at ~$1,800 per ton, the economics of a biorefinery are greatly improved. In fact, to meet 2022 US fuel targets, fermentative biorefineries would have to produce 16 billion gallons of second-generation biofuels from approximately 223 million tons of lignocellulosic biomass, generating a projected 62 million tons per year of lignin waste and providing a great economic opportunity.[6] Nevertheless, there are still technological challenges to producing demanded volumes of lignin-derived chemicals at market rates. For biorefineries to be economically competitive, the development of second generation biorefineries that focus on the efficient use of lignin as well as the carbohydrate fractions will be needed to generate a broader portfolio of value-added products, similar to that derived from petroleum. Simply stated, more valuable products and a broader range of products must be efficiently derived from not only the carbohydrate fraction of biomass but also from the lignin fraction. Such product diversification will minimize the risk associated with "front-end" operations and mitigate fluctuations in commodity fuel markets.

1.3 Lignin

1.3.1 What is lignin?

Plant cell walls are comprised of three major polymers: cellulose, hemicellulose, and lignin, respectively making up ~40-50%, ~10-30%, and 15-30% of the dry weight. Cellulose, comprised of glucose monomers joined by β-1,4-glucan linkages forms long (rectangular, 100-200 nm long and 5-10 nm wide) fibril structures. Hemicellulose, comprised of several possible pentose and hexose sugars, typically connects the lignin and cellulose structures, as seen in Figure 1-1. Lignin, interwoven between the cellulose fibrils, provides structural integrity, facilitates vascular
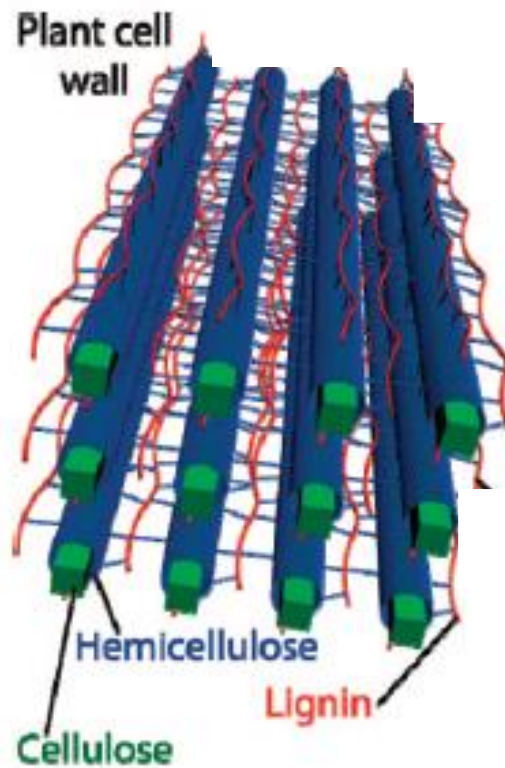
Figure 1-1. Simplified graphical representation of cell wall structure with the three main constituents, cellulose, hemicellulose, and lignin.[8] (Reproduced with permission. Copyright 2010, American Chemical Society)

water transport, and is part of the plant's native defense system.[29-31] Plants have evolved a lignin structure that is inherently recalcitrant, rigid, and insoluble so that it provides structural support

and is naturally resistant to biological and environmental mediated degradation. These same properties also make lignin difficult and, thus far, cost-prohibitive to industrially convert into value-added products.[30]

1.3.2 Lignin structure

Lignin is described as a three-dimensional, random, co-polymer network mostly comprised of variously linked hydroxycinnamyl alcohol monomers, differing mainly in their degree of methoxylation (e.g., coniferyl, sinapyl, and p-coumaryl alcohol). Lignification of the plant cell wall is mediated through radical coupling reactions. The lignin monomers are enzymatically dehydrogenated to produce radicals that are then excreted into the plant cell wall, where these radicals undergo uncontrolled radical-coupling polymerization to produce a lignin molecule that is primarily linear but contains some branched polymer topologies.[29] Typically, coniferyl, sinapyl, and p-coumaryl alcohol monolignols are incorporated into lignin as guaiacyl (G), syringyl (S), and p-hydroxyphenyl (H) moieties (i.e., phenylpropanoid units), as shown in Figure 1-2. Since the
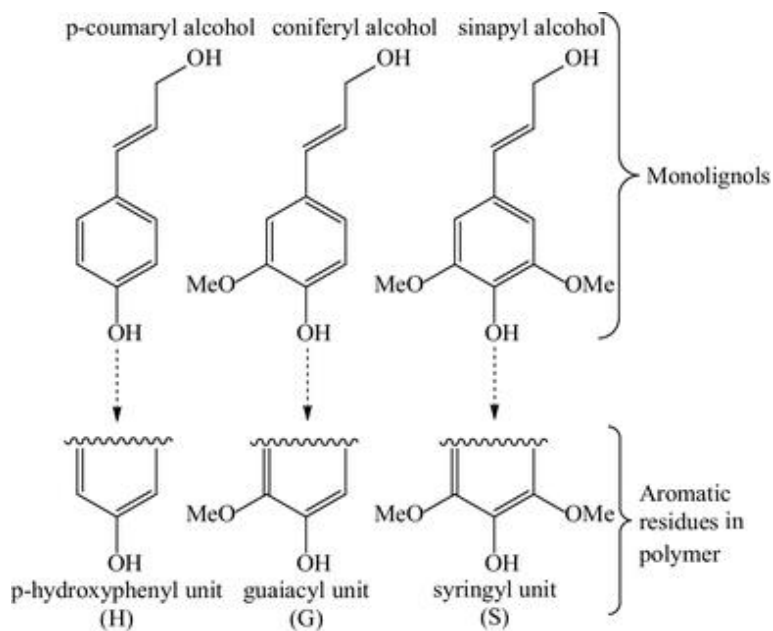
Figure 1-2. Hydroxycinnamyl alcohol monomers in the biosynthesis of lignin and their resulting lignin moieties.[7] (Figure is reproduced under Creative Commons CC BY License)
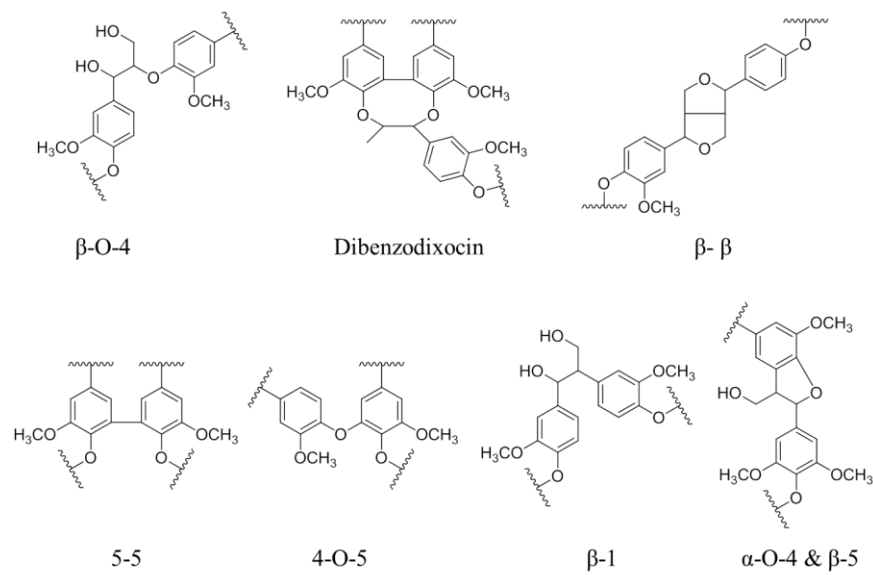
Figure 1-3. Types of linkages between dimers in lignin.[4]

radical coupling between the monomers is uncontrolled, the polymerization results in a number of different inter-unit linkages. Several of the common types are illustrated in Figure 1-3, and a representative lignin molecule is depicted in Figure 1-4.

In response to both genetic and transcriptional (i.e., environmental) factors, the composition and quantity of lignin varies significantly from species to species, although large variations in lignin composition and quantity are also observed genotype to genotype, between clones, and even between different tissues within the same plant.[29-30] Although the exact structure of lignin varies greatly, hardwood lignin tends to have a high methoxy content, consisting of roughly equal amounts of guaiacyl and syringyl units; softwood lignin is mainly guaiacyl units; and grass lignin is composed of similar amounts of guaiacyl and syringyl units, along with some *p*-hydroxyphenyl units.[29]
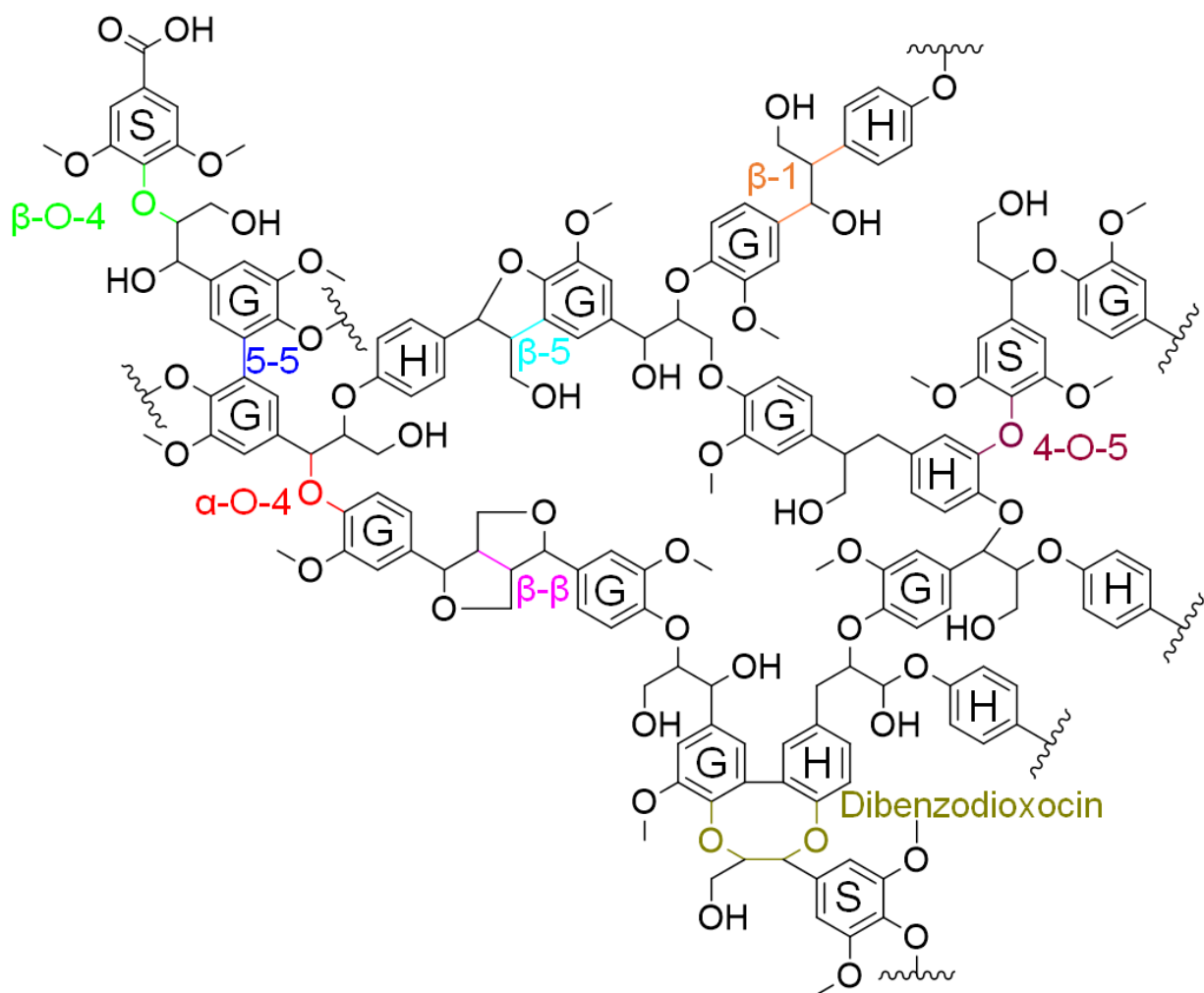
Figure 1-4. Graphical depiction of a possible lignin structure.[4]

The variation in lignin structure and inter-unit linkage distributions is, in part, due to biosynthesis genes and environmental factors, but is largely due to the random nature of radical coupling reactions and the apparent lack of biochemical control of lignin synthesis.[29-31] Certain inter-unit linkages, however, have favorable thermodynamic energetics, and thus are present at a higher percentage within the cell wall. Major inter-unit linkage distributions in the lignin of softwoods and hardwoods are shown in Table 1-1.[29] The most frequent inter-unit linkage is the β-O-4 (an aliphatic-aryl ether) linkage, comprising about half of the total linkages in both softwood and hardwood lignin.[29] The formation of C-O bonds is favored over the formation of C-C bonds,

7

thus, the β-O-4 linkage is the most prevalent linkage formed. Hardwood lignin has a slightly higher percentage of β-O-4 linkages than softwood lignin, due to the greater number of syringyl units, which have a lower chance of forming β-5, 5-5, and 4-O-5 linkages during lignification due to the protection of the additional methoxy group. The resulting functional groups associated with the various lignin substructures, inter-unit linkages, and terminal sites (i.e., methoxyl, phenolic and aliphatic hydroxyl, benzyl alcohol, non-cyclic benzyl ether, and carbonyl groups) have major influences on the solubility, reactivity, and fractionation of lignin.[15] For example, the β-O-4 linkage is one of the most easily cleaved chemically; however, linkages with C-C bonds, such as β-5, β-β, 5-5, and β-1 linkages, are more resistant to chemical degradation.

The overall structure and structural subunits of lignin (including their heterogeneity) evolved in plants over millions of years, in part as a defensive structure to protect cell wall carbohydrates from fungal and microbial attack and/or to protect the plant from chemical degradation by the environment. This evolved recalcitrance, inherent structural heterogeneity, and plant-to-plant variability of lignin represents a major obstacle to harnessing lignin efficiently for the production of desired and specific chemicals. [32-33]

Table 1-1. Percent of inter-unit linkages in softwood and hardwood lignin.[15]

Linkages	Softwood (spruce)	Hardwood (birch)
β-O-4, aryl ether	46%	60%
α-O-4, aryl ether	6-8%	6-8%
4-O-5, diaryl ether	3.5-4%	6.5%
β-5, phenyl coumaran	9-12%	6%
5-5, biphenyl	9.5-11%	4.5%
β-1, 1,2-Diarylpropane	7%	7%
β-β, Resinol	2%	3%
Others	13%	5%

1.4 Biorefineries

At the turn of the 20th century, the petroleum industry started by producing an alternative for lamp oil, kerosene, to meet one of the main energy needs of the time. Gasoline and other petroleum products initially were waste.[34] Similarly, at the turn of the 21st century, biorefineries initially focused on replacing one of the main energy demands of our time, transportation fuels, especially gasoline and diesel. Lignin is currently a waste product, useful only to generate process heat, but as the early petroleum refineries discovered, biorefineries have also realized that waste streams can be turned into a variety of profitable products.[35]
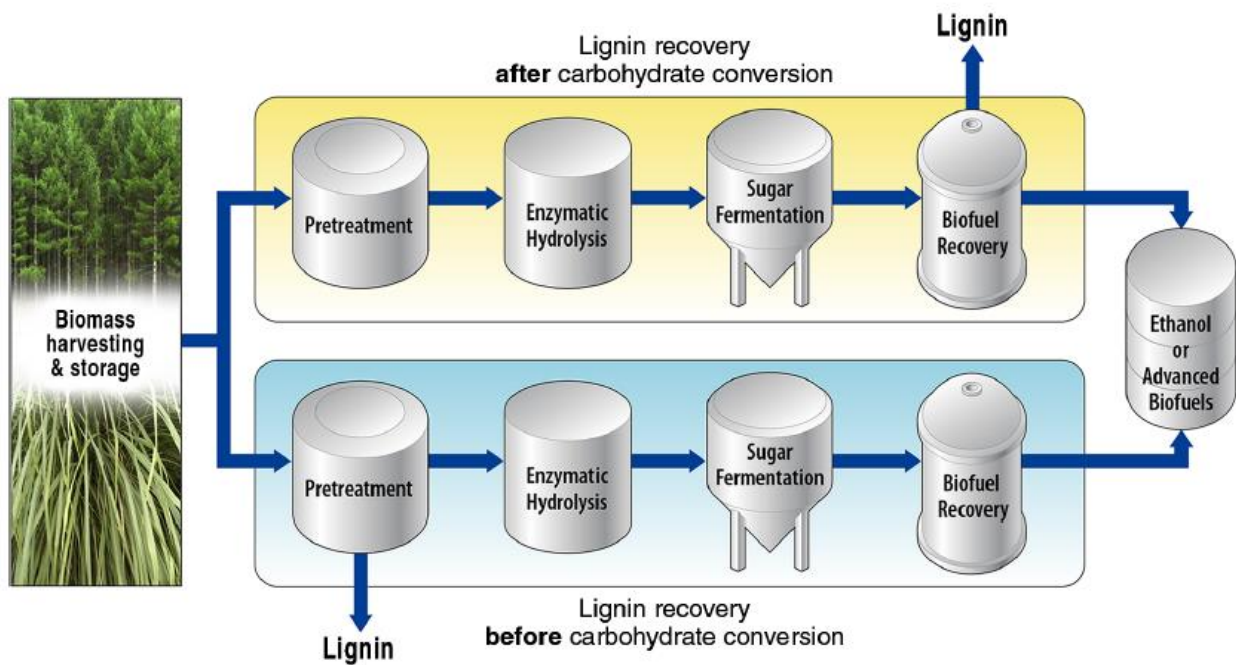
Figure 1-5. The two main process flows for second-generation biorefineries, providing the opportunity for lignin recovery[6] (Reproduced with permission. Copyright 2014, American Association for the Advancement of Science)

A current second-generation biorefinery utilizes three basic processes: (1) feedstock pretreatment, (2) hydrolysis and fermentation, (3) and product separation. The initial process, feedstock pretreatment, typically includes two steps: first, mechanical size reduction, and then a chemical pretreatment. Pretreatment reduces the natural resistance of carbohydrates within the biomass to deconstruction and increases enzymatic sugar yields, typically by increasing enzymatic

access to the cell wall cellulose via biomass pore structure expansion or lignin/hemicellulose removal. The carbohydrate-rich fraction then undergoes hydrolysis, either enzymatic or chemical, to break it into sugars. The remaining solids (i.e., residual lignin, enzymes, and unhydrolyzed carbohydrates) are separated at this point. The sugar-rich stream is then fed to microbial systems to be fermented into products. The final step is to separate the desired products from the waste or recycle streams. While each step is critical to achieving overall process efficiency, the pretreatment process has the largest effect on the biorefinery.

1.4.1 Current Technologies

In the early stages of development, second generation biorefineries adopted many technologies from the pulp and paper industry, which had long made high quality cellulose fibers from lignocellulosic material. Several different pulping processes (e.g., Kraft pulping, alkaline pulping, sulfite pulping, organic solvent (organosolv) pulping, and steam explosion) were adopted as pretreatment methods to increase enzymatic hydrolysis yield and rate via delignification, with little concern for the resulting lignin structures. These pretreatments have since been modified into other biomass fractionation technologies, designed to separate cellulose, hemicellulose, and lignin cell wall components for downstream recovery of all or some of the fractions of biomass. In general, many biomass pulping, fractionation, and pretreatment technologies (for example, organosolv pulping, organosolv extraction, or organosolv pretreatment) differ only in their process severity and applications. For example, biomass pretreatment is designed to reduce the inherent resistance of biomass carbohydrates to enzymatic hydrolysis via delignification with little regard for the removed lignin fraction. Whereas an extraction process is lignin-focused by design. Each delignification process creates a lignin stream with different molecular modifications, affecting not only the molecular structure and chemistry of the fractionated lignin but also the resulting

molecular/physical (e.g., size, reactivity, and solubility), mechanical, and thermal properties, and ultimately possible end uses. [36-39]

This dissertation explores two approaches to separating lignin and the carbohydrate fractions of lignocellulosic biomass that limit the detrimental effects of the pretreatment/extraction process on the resulting lignin. The first pretreatment/extraction process explored is ammonia fiber expansion (AFEX). It offers several advantages, such as milder processing conditions (120 $^{\circ}$C), significant recovery and reuse of the ammonia catalyst, minimal water utilization, and increased enzymatic hydrolysis yields (80-90%) at industrially relevant high solid loadings (18% or higher).[40] Most importantly, for further unhydrolyzed solids (UHS) and lignin utilization, AFEX pretreatments minimize alterations to native lignin linkages and functionalities.[41-42] The other process explored in this dissertation is organosolv processing, extracting lignin from lignocellulosic material with an organic solvent system. Originally developed to be more environmentally friendly than Kraft or sulfite pulping, it produces a less modified lignin stream.[43] Organosolv extractions are highly dependent on the organic solvent used and its acidity, water content, solubility parameter, and polarity.[44-48] The temperature and time profile of the extraction also has a significant effect on organosolv extractions of lignin.[49-50] Generally, organosolv processes have been optimized either as a pretreatment to maximize enzymatic sugar yields and bioethanol production or as a pulping method to isolate cellulosic substrates and maximize cellulosic substrate yield and quality, while providing an option for lignin optimization.[51-53] Both of these processes produce a minimally altered and clean (i.e., free of carbohydrates and without contamination, such as sulfur) lignin, making them ideal pretreatments for advanced second-generation biorefineries.

1.5 Downstream Processes

Lignin has a naturally complex structure that only increases in complexity and variety during extraction processes, thus further complicating the use and our understanding of lignin.[54] Extracted lignin contains a variety of inter-monomer linkages, some of which are specific to the extraction process, linkage sequence, molecular weight, and topology, with varying chemical reactivities.[55-58] There are few direct uses for extracted lignin, thus further upgrading is typically required to produce base chemicals that can be 'dropped in' to current processes producing higher value chemicals, fuels, or materials. Isolated lignin streams for the production of chemicals can undergo two processes: depolymerization and upgrading. Depolymerization selectively breaks inter-unit linkages and prevents unwanted linkages from forming. Upgrading modifies functionality and chemical moieties into more desirable chemical moieties. There are several current methods by which lignin streams are depolymerized and upgraded, typically varying only in process intensity: thermal methods (i.e., pyrolysis or gasification), catalytic oxidative or reductive fragmentation, and solvolytic cleavage. Typically, the more selective the process, the lower the yield of desired product. All the processes yield a large range of desired and undesired products.[59-62] Two of the challenges in designing and optimizing technologies for lignin valorization are accurately understanding the molecular structures and the overall composition of lignin-derived products.

Currently, several methods are used to characterize lignin and lignin-derived products. Gel permeation chromatography characterizes the size distribution of the lignin molecules, indicating the progress of depolymerization processes, but provides no chemical information. Nuclear magnetic resonances (NMR) can give very detailed structural information, but requires a large sample size and gives only averages across a sample. For sufficient sample amounts, several different NMR techniques are useful in characterizing lignin-derived products. Carbon (^{13}C) NMR

can provide quantitative information on the types of chemical moieties and can also provide information on specific inter-unit linkages, using 2D NMR techniques such as ^{1}H-^{13}C heteronuclear single quantum coherence (HSQC).   Gas chromatography, typically coupled with mass spectroscopy, is another commonly used technique for analyzing the volatile components of the product mixtures. Unfortunately, many components of the lignin-derived products, which are oligomeric, oxygen-rich, and polar, are not volatile enough to be separated.[63] Additionally, typical mass spectrometers do not have the resolution to separate all the components.   Liquid chromatography is used to overcome the challenge of the lower volatility of many lignin breakdown products, but typically it cannot separate the mixture adequately and takes an impractically long time for a single sample.

Fourier-transform ion cyclotron resonance with high resolution mass spectroscopy (FTICR-HRMS) offers a detailed understanding of lignin breakdown products. Short run time, high sensitivity, high resolution, and ability to analyze larger molecular weight molecular analytes make FTICR-MS a powerful tool for analyzing lignin breakdown products. Although FTICR-HRMS is only semi-quantitative due to the ionization bias of individual compounds, by utilizing several different ionization methods a more complete picture of the compounds within a lignin-derived mixture can be obtained.[64]

1.6 Objectives and Approach

The main objective of this dissertation is to study technologies that improve lignin utilization and valorization within a biorefinery. The dissertation explores three different technologies, two processes and a lignin characterization method, all with the potential to improve lignin utilization within biorefineries.

Study 1: The first study explores a route to better recover and use lignin from a common waste stream of second-generation biorefineries. Unhydrolyzed solids (UHS), the post-enzymatic hydrolysis waste stream from an AFEX process, were extracted with a series of solvents. The lignin from the four highest yielding solvent extractions was highly characterized to develop value-added product streams.

Study 2: The second study examines adapting a common pretreatment process, organosolv, as an extraction process. A key aspect is developing a deep understanding of the lignin reaction kinetics during the extraction, so that a process can be designed with a desired lignin in mind, instead of the resulting carbohydrates, as in a pretreatment.

Study 3: The third study utilizes FTICR-HRMS to analyze lignin and lignin breakdown products from catalytically depolymerized, organosolv extracted lignin. FTICR-HRMS provides a comprehensive picture of the products resulting from three time series of depolymerizations, (1) catalytic depolymerization, (2) catalytic depolymerization with a stabilizing co-solvent, and (3) a depolymerization without any catalysis as a control.

1.7 Dissertation Outline

This dissertation contains five chapters: an introduction to the field of biorefineries, a chapter on each study, and a chapter describing my thoughts on the future direction of the biorefinery field. References are provided at the end of each chapter, with some references cited multiple times within the dissertation.

The first chapter gives a broad overview of lignocellulosic biomass and biorefineries, along with several state-of-the-art technologies for biorefineries. The motivation, specific objectives, and layout of the dissertation are also presented in this chapter. The second chapter is based on Study 1, exploring a new process to be added onto existing second-generation biorefineries that utilizes

a waste stream to produce a useful lignin stream. An AFEX biorefinery process is used as a model system to exhibit the potential of the new process. The third chapter is based on Study 2, adapting an organosolv pretreatment to a lignin extraction process, shifting the processing paradigm to emphasize lignin rather than carbohydrates. Understanding the lignin reaction kinetics occurring during organosolv extractions will allow the process to be designed to optimize the lignin product stream. The fourth chapter details Study 3, FTICR coupled with high resolution mass spectroscopy that tracks the chemical makeup of different lignin depolymerization mixtures with a level of detail that is hard to gain by any other means. The final chapter delivers a perspective on the future directions of the field. It discusses possible lignin extraction technologies and avenues for upgrading lignin streams into value-added products.

1.8 References

1.   Bentley, R. W., Global oil & gas depletion: an overview. *Energy Policy* **2002,** *30* (3), 189-205.

2.   Qu, Y.; Zhu, M.; Liu, K.; Bao, X.; Lin, J., Studies on cellulosic ethanol production for sustainable supply of liquid fuel in China. *Biotechnology Journal* **2006,** *1* (11), 1235-1240.

3.   Ragauskas, A. J.; Williams, C. K.; Davison, B. H.; Britovsek, G.; Cairney, J.; Eckert, C. A.; Frederick, W. J.; Hallett, J. P.; Leak, D. J.; Liotta, C. L., The path forward for biofuels and biomaterials. *Science* **2006,** *311* (5760), 484-489.

4.   Gao, Y., Lignin Conversion to Value-added Products via Heterogeneous Catalysts. **2018**.

5.   Ren21, R., Global status report. *Renewable Energy Policy Network for the 21st Century, Paris, France* **2010**.

6.   Ragauskas, A. J.; Beckham, G. T.; Biddy, M. J.; Chandra, R.; Chen, F.; Davis, M. F.; Davison, B. H.; Dixon, R. A.; Gilna, P.; Keller, M., Lignin valorization: improving lignin processing in the biorefinery. *Science* **2014,** *344* (6185), 1246843.

7.   Guadix-Montero, S.; Sankar, M., Review on Catalytic Cleavage of C–C Inter-unit Linkages in Lignin Model Compounds: Towards Lignin Depolymerisation. *Topics in Catalysis* **2018,** *61* (3), 183-198.

8.   Zakzeski, J.; Jongerius, A. L.; Bruijnincx, P. C. A.; Weckhuysen, B. M., Catalytic Lignin Valorization Process for the Production of Aromatic Chemicals and Hydrogen. *ChemSusChem* **2012,** *5* (8), 1602-1609.

9.   Barbir, F.; Veziroğlu, T.; Plass, H., Environmental damage due to fossil fuels use. *International Journal of Hydrogen Energy* **1990,** *15* (10), 739-749.

10.   Barreto, L.; Makihira, A.; Riahi, K., The hydrogen economy in the 21st century: a sustainable development scenario. *International Journal of Hydrogen Energy* **2003,** *28* (3), 267-284.

11.   Klass, D. L., *Biomass for renewable energy, fuels, and chemicals*. Academic Press: 1998.

12.   Panwar, N.; Kaushik, S.; Kothari, S., Role of renewable energy sources in environmental protection: a review. *Renewable and Sustainable Energy Reviews* **2011,** *15* (3), 1513-1524.

13.   Von Blottnitz, H.; Curran, M. A., A review of assessments conducted on bio-ethanol as a transportation fuel from a net energy, greenhouse gas, and environmental life cycle perspective. *Journal of Cleaner Production* **2007,** *15* (7), 607-619.

14.   Coumou, D.; Rahmstorf, S., A decade of weather extremes. *Nature Climate Change* **2012,** *2* (7), 491-496.

15.   Pandey, M. P.; Kim, C. S., Lignin depolymerization and conversion: a review of thermochemical methods. *Chemical Engineering & Technology* **2011,** *34* (1), 29-41.

16.   Hahn-Hägerdal, B.; Galbe, M.; Gorwa-Grauslund, M.-F.; Lidén, G.; Zacchi, G., Bio-ethanol–the fuel of tomorrow from the residues of today. *Trends in Biotechnology* **2006,** *24* (12), 549-556.

17.   Sims, R.; Taylor, M.; Saddler, J.; Mabee, W., From 1st-to 2nd-generation biofuel technologies. *Paris: International Energy Agency (IEA) and Organisation for Economic Co-Operation and Development* **2008**.

18.   de Jong, E.; Higson, A.; Walsh, P.; Wellisch, M., Bio-based chemicals value added products from biorefineries. *IEA Bioenergy, Task42 Biorefinery* **2012**.

19.   Lau, M. W.; Dale, B. E., Cellulosic ethanol production from AFEX-treated corn stover using Saccharomyces cerevisiae 424A (LNH-ST). *Proceedings of the National Academy of Sciences* **2009,** *106* (5), 1368-1373.

20.   Zheng, J.; Tashiro, Y.; Wang, Q.; Sonomoto, K., Recent advances to improve fermentative butanol production: genetic engineering and fermentation technology. *Journal of bioscience and bioengineering* **2015,** *119* (1), 1-9.

21.   Zakzeski, J.; Bruijnincx, P. C.; Jongerius, A. L.; Weckhuysen, B. M., The catalytic valorization of lignin for the production of renewable chemicals. *Chemical reviews* **2010,** *110* (6), 3552-3599.

22.   Fortman, J.; Chhabra, S.; Mukhopadhyay, A.; Chou, H.; Lee, T. S.; Steen, E.; Keasling, J. D., Biofuel alternatives to ethanol: pumping the microbial well. *Trends in biotechnology* **2008,** *26* (7), 375-381.

23. Lee, S. Y.; Hong, S. H.; Lee, S. H.; Park, S. J., Fermentative production of chemicals that can be used for polymer synthesis. *Macromolecular bioscience* **2004,** *4* (3), 157-164.

24. Kim, D. Y.; Yim, S. C.; Lee, P. C.; Lee, W. G.; Lee, S. Y.; Chang, H. N., Batch and continuous fermentation of succinic acid from wood hydrolysate by Mannheimia succiniciproducens MBEL55E. *Enzyme and Microbial Technology* **2004,** *35* (6), 648-653.

25. Patel, M.; Ou, M.; Ingram, L.; Shanmugam, K., Fermentation of sugar cane bagasse hemicellulose hydrolysate to L (+)-lactic acid by a thermotolerant acidophilic Bacillus sp. *Biotechnology letters* **2004,** *26* (11), 865-868.

26. Khanna, S.; Srivastava, A. K., Recent advances in microbial polyhydroxyalkanoates. *Process Biochemistry* **2005,** *40* (2), 607-619.

27. Humbird, D.; Davis, R.; Tao, L.; Kinchin, C.; Hsu, D.; Aden, A.; Schoen, P.; Lukas, J.; Olthof, B.; Worley, M. *Process design and economics for biochemical conversion of lignocellulosic biomass to ethanol: dilute-acid pretreatment and enzymatic hydrolysis of corn stover*; National Renewable Energy Lab.(NREL), Golden, CO (United States): 2011.

28. Holladay, J. E.; White, J. F.; Bozell, J. J.; Johnson, D. *Top Value-Added Chemicals from Biomass-Volume II—Results of Screening for Potential Candidates from Biorefinery Lignin*; Pacific Northwest National Laboratory (PNNL), Richland, WA (US): 2007.

29. Boerjan, W.; Ralph, J.; Baucher, M., Lignin biosynthesis. *Annual Review of Plant Biology* **2003,** *54* (1), 519-546.

30. Campbell, M. M.; Sederoff, R. R., Variation in lignin content and composition. *Plant Physiology* **1996,** *110*, 3-13.

31. Freudenberg, K., Biosynthesis and Constitution of Lignin. *Nature* **1959,** *183* (4669), 1152-1155.

32.   Argyropoulos, D. S.; Menachem, S. B., Lignin. In *Biotechnology in the Pulp and Paper Industry*, Springer: 1997; pp 127-158.

33.   Gosselink, R. J.; Teunissen, W.; Van Dam, J. E.; De Jong, E.; Gellerstedt, G.; Scott, E. L.; Sanders, J. P., Lignin depolymerisation in supercritical carbon dioxide/acetone/water fluid for the production of aromatic chemicals. *Bioresource Technology* **2012,** *106*, 173-177.

34.   Berger, B. D.; Anderson, K. E., Modern petroleum: a basic primer of the industry.[contains glossary]. **1978**.

35.   Aditiya, H.; Mahlia, T.; Chong, W.; Nur, H.; Sebayang, A., Second generation bioethanol production: A critical review. *Renewable and sustainable energy reviews* **2016,** *66*, 631-653.

36.   Vishtal, A. G.; Kraslawski, A., Challenges in industrial applications of technical lignins. *BioResources* **2011,** *6* (3), 3547-3568.

37.   Negro, M.; Manzanares, P.; Oliva, J.; Ballesteros, I.; Ballesteros, M., Changes in various physical/chemical parameters of Pinus pinaster wood after steam explosion pretreatment. *Biomass and Bioenergy* **2003,** *25* (3), 301-308.

38.   Trajano, H. L.; Engle, N. L.; Foston, M.; Ragauskas, A. J.; Tschaplinski, T. J.; Wyman, C. E., The fate of lignin during hydrothermal pretreatment. *Biotechnol. Biofuels* **2013,** *6* (1), 110.

39.   Stewart, D., Lignin as a base material for materials applications: Chemistry, application and economics. *Industrial crops and products* **2008,** *27* (2), 202-207.

40.   Jin, M.; da Costa Sousa, L.; Schwartz, C.; He, Y.; Sarks, C.; Gunawan, C.; Balan, V.; Dale, B. E., Toward lower cost cellulosic biofuel production using ammonia based pretreatment technologies. *Green Chemistry* **2016,** *18* (4), 957-966.

41.   Chundawat, S. P.; Donohoe, B. S.; da Costa Sousa, L.; Elder, T.; Agarwal, U. P.; Lu, F.; Ralph, J.; Himmel, M. E.; Balan, V.; Dale, B. E., Multi-scale visualization and characterization of

lignocellulosic plant cell wall deconstruction during thermochemical pretreatment. *Energy & Environmental Science* **2011,** *4* (3), 973-984.

42.   Singh, S.; Cheng, G.; Sathitsuksanoh, N.; Wu, D.; Varanasi, P.; George, A.; Balan, V.; Gao, X.; Kumar, R.; Dale, B. E., Comparison of different biomass pretreatment techniques and their impact on chemistry and structure. *Frontiers in Energy Research* **2015,** *2*, 62.

43.   Mabee, W. E.; Gregg, D. J.; Arato, C.; Berlin, A.; Bura, R.; Gilkes, N.; Mirochnik, O.; Pan, X.; Pye, E. K.; Saddler, J. N. In *Updates on softwood-to-ethanol process development*, Twenty-Seventh Symposium on Biotechnology for Fuels and Chemicals, Springer: 2006; pp 55-70.

44.   Parajo, J. C.; Alonso, J. L.; Santos, V., Kinetics of catalyzed organosolv processing of pine wood. *Industrial & engineering chemistry research* **1995,** *34* (12), 4333-4342.

45.   Bozell, J. J.; Black, S. K.; Myers, M.; Cahill, D.; Miller, W. P.; Park, S., Solvent fractionation of renewable woody feedstocks: Organosolv generation of biorefinery process streams for the production of biobased chemicals. *biomass and bioenergy* **2011,** *35* (10), 4197-4208.

46.   Quesada-Medina, J.; López-Cremades, F. J.; Olivares-Carrillo, P., Organosolv extraction of lignin from hydrolyzed almond shells and application of the δ-value theory. *Bioresource technology* **2010,** *101* (21), 8252-8260.

47.   Bauer, S.; Sorek, H.; Mitchell, V. D.; Ibáñez, A. B.; Wemmer, D. E., Characterization of Miscanthus giganteus lignin isolated by ethanol organosolv process under reflux condition. *Journal of agricultural and food chemistry* **2012,** *60* (33), 8203-8212.

48.   Cybulska, I.; Brudecki, G.; Rosentrater, K.; Julson, J. L.; Lei, H., Comparative study of organosolv lignin extracted from prairie cordgrass, switchgrass and corn stover. *Bioresource technology* **2012,** *118*, 30-36.

49.   Sidiras, D.; Koukios, E., Simulation of acid-catalysed organosolv fractionation of wheat straw. *Bioresource technology* **2004,** *94* (1), 91-98.

50.   Sluiter, A.; Hames, B.; Ruiz, R.; Scarlata, C.; Sluiter, J.; Templeton, D.; Crocker, D., Determination of structural carbohydrates and lignin in biomass. *Laboratory analytical procedure* **2008,** *1617*, 1-16.

51.   Pan, X.; Xie, D.; Gilkes, N.; Gregg, D. J.; Saddler, J. N. In *Strategies to enhance the enzymatic hydrolysis of pretreated softwood with high residual lignin content*, Twenty-Sixth Symposium on Biotechnology for Fuels and Chemicals, Springer: 2005; pp 1069-1079.

52.   Pan, X.; Arato, C.; Gilkes, N.; Gregg, D.; Mabee, W.; Pye, K.; Xiao, Z.; Zhang, X.; Saddler, J., Biorefining of softwoods using ethanol organosolv pulping: preliminary evaluation of process streams for manufacture of fuel-grade ethanol and co-products. *Biotechnology and bioengineering* **2005,** *90* (4), 473-481.

53.   Goh, C. S.; Tan, H. T.; Lee, K. T.; Brosse, N., Evaluation and optimization of organosolv pretreatment using combined severity factors and response surface methodology. *biomass and bioenergy* **2011,** *35* (9), 4025-4033.

54.   DeMartini, J. D.; Pattathil, S.; Miller, J. S.; Li, H.; Hahn, M. G.; Wyman, C. E., Investigating plant cell wall components that affect biomass recalcitrance in poplar and switchgrass. *Energy & Environmental Science* **2013,** *6* (3), 898-909.

55.   Azadi, P.; Inderwildi, O. R.; Farnood, R.; King, D. A., Liquid fuels, hydrogen and chemicals from lignin: A critical review. *Renewable and Sustainable Energy Reviews* **2013,** *21*, 506-523.

56. Calvo-Flores, F. G.; Dobado, J. A.; Isac-García, J.; Martín-Martínez, F. J., *Lignin and lignans as renewable raw materials: chemistry, technology and applications*. John Wiley & Sons: 2015.

57. Bhagia, S.; Li, H.; Gao, X.; Kumar, R.; Wyman, C. E., Flowthrough pretreatment with very dilute acid provides insights into high lignin contribution to biomass recalcitrance. *Biotechnology for biofuels* **2016,** *9* (1), 245.

58. Zhao, X.; Cheng, K.; Liu, D., Organosolv pretreatment of lignocellulosic biomass for enzymatic hydrolysis. *Appl Microbiol Biotechnol* **2009,** *82* (5), 815.

59. Tuck, C. O.; Pérez, E.; Horváth, I. T.; Sheldon, R. A.; Poliakoff, M., Valorization of biomass: deriving more value from waste. *Science* **2012,** *337* (6095), 695-699.

60. Esposito, D.; Antonietti, M., Redefining biorefinery: the search for unconventional building blocks for materials. *Chemical Society Reviews* **2015,** *44* (16), 5821-5835.

61. Li, C.; Zhao, X.; Wang, A.; Huber, G. W.; Zhang, T., Catalytic transformation of lignin for the production of chemicals and fuels. *Chemical reviews* **2015,** *115* (21), 11559-11624.

62. Schutyser, W.; Renders, T.; Van den Bosch, S.; Koelewijn, S.-F.; Beckham, G. T.; Sels, B. F., Chemicals from lignin: an interplay of lignocellulose fractionation, depolymerisation, and upgrading. *Chemical Society Reviews* **2018,** *47* (3), 852-908.

63. Panda, S. K.; Andersson, J. T.; Schrader, W., Mass-spectrometric analysis of complex volatile and nonvolatile crude oil components: a challenge. *Analytical and bioanalytical chemistry* **2007,** *389* (5), 1329-1339.

64. Hertzog, J.; Carré, V.; Jia, L.; Mackay, C. L.; Pinard, L.; Dufour, A.; Mašek, O. e.; Aubriet, F. d. r., Catalytic Fast Pyrolysis of Biomass over Microporous and Hierarchical Zeolites:

Characterization of Heavy Products. *ACS Sustainable Chemistry & Engineering* **2018,** *6* (4), 4717-

4728.

Chapter 2: Isolation of Lignin from Ammonia Fiber Expansion (AFEX) Pretreated Biorefinery Waste

This chapter was adapted from the following publication:

2.1 Abstract

Rapidly improving the efficiency of biorefineries and lignin utilization requires adapting technologies from existing processes. This chapter describes experiments to isolate lignin from unhydrolyzed solids (UHS), a by-product stream of second-generation biofuel production, with organic solvent solutions. Under reflux conditions, aqueous solutions of acetone, ethanol (EtOH), acetic acid (AcOH), and γ-valerolactone (GVL) displayed approximately 53, 51, 53, and 65 % yields of extractable solids, respectively, from corn stover UHS after ammonia fiber expansion (AFEX) pretreatment and subsequent enzymatic hydrolysis. Detailed chemical characterization, including nuclear magnetic resonance, gel permeation chromatography, and thermogravimetric analysis, showed that material extracted from UHS using EtOH:H_2O and acetone:H_2O contained a lignin fraction that most resembled native lignin; although, the material extracted using acetone:H_2O contained a significant carbohydrate component. These results suggest that solvent polarity, rather than solvent reflux temperature, is a more significant factor determining the mass yields of extractable solids from UHS.

2.2 Introduction

As second-generation biorefineries start to come online, it important to remember that it has taken years of engineering, financing, and construction to accomplish. In many current pilot biorefineries, the potential of lignin is not fully realized.[1-2] Therefore, to quickly implement lignin upgrading technology, existing material streams and process designs must be adapted. This chapter describes how such an adaptive approach can upgrade a waste stream into a potential source of valuable fuels, chemicals, and materials.

An ammonia fiber expansion (AFEX) pretreatment was used as the model system because it is currently in pilot-scale development as a lignocellulosic biomass pretreatment technology for second-generation bioethanol production. AFEX pretreatment is known to increase total enzymatic sugar yields from and enzyme accessibility to lignocellulosic cell wall carbohydrates, via fiber decompression as well as hemicellulose and lignin solubilization/rearrangement.[3] AFEX offers several advantages over other pretreatment technologies, such as milder processing conditions (120°C), significant recovery and reuse of the ammonia catalyst, minimal water utilization, decreased production of fermentative inhibitory compounds (e.g., hydroxymethylfurfural, furfural, lignin degradation products), and increased enzymatic hydrolysis yields (80-90%) at industrially relevant high solid loadings (18% or higher).[4] Most importantly, the milder processing conditions utilized in AFEX pretreatment limits the modification of lignin.

In previous efforts, an AFEX pretreatment was modified (i.e., extractive ammonia (EA) pretreatment) to facilitate enzymatic hydrolysis and generate a lignin-rich ammonia extractive product.[5-6] This ammonia-soluble lignin-rich extractive, easily isolated from the pretreatment solvent via evaporation, could potentially undergo water/ethanol-based fractionation to produce several lignin product streams with attractive commercial

applications. Yet, following enzymatic hydrolysis of the AFEX pretreated biomass, the unhydrolyzed solids (UHS) left behind, which are enriched in lignin (up to 50%), remain under-utilized.[4] The lignin-rich UHS is similar to the industrial lignin cake produced during second-generation biofuel production. Thus, to generate co-products from the lignin in UHS, AFEX pretreatment and its reduced severity (e.g., time, temperature, and pH), is ideal because the lignin structure appears very similar to ''native'' lignin.[3, 5]

A typical AFEX lignocellulosic biorefinery, processing 2000 tons of biomass per day, will leave behind approximately 400 to 450 thousand tons of UHS in a year.[4] For maximum economic efficiency of an AFEX biorefinery, the production of value-added products from soluble lignin isolated from UHS (by removing residual carbohydrates).[7] For example, the mild depolymerization of lignin into renewable aromatics is dependent on the removal of carbohydrates and the abundance of ether lignin monomer linkages.[8-13]. Similarly, the thermo-rheological behavior of lignin, which determines its melt-processability and mechanical properties (e.g., lignin-derived carbon fibers), is highly affected by the presence of residual carbohydrates and the abundance of non-native condensed (C-C) lignin monomer linkages.[14] The isolation methods applied to fractionate the lignin and residual carbohydrate fractions in the UHS tend to have more significant impacts on the structure and quality of the extracted lignin than the AFEX pretreatment. Basically, the processing history of lignin can highly affect its downstream processing and applications.

The thermal, physical, and chemical properties of the extracted lignin, and thus its quality and applicability for specific applications, depend not only on the structure of the lignin within the UHS, but also on the isolation method and conditions used to remove unwanted carbohydrates, proteins, and ash in the UHS from its lignin fraction. While lignin

extraction from lignocellulose [15-16] or black liquor [17-18] has been extensively explored, lignin extraction from residues after pretreatment and enzymatic hydrolysis [19-20] has garnered only limited attention.

In this chapter, various organic solvents under reflux were screened for the extraction of lignin from UHS generated by the enzymatic hydrolysis of AFEX-pretreated corn stover. The goal was to understand the effect of solvent on the extraction of lignin from UHS and on the resulting structure and properties of that lignin.
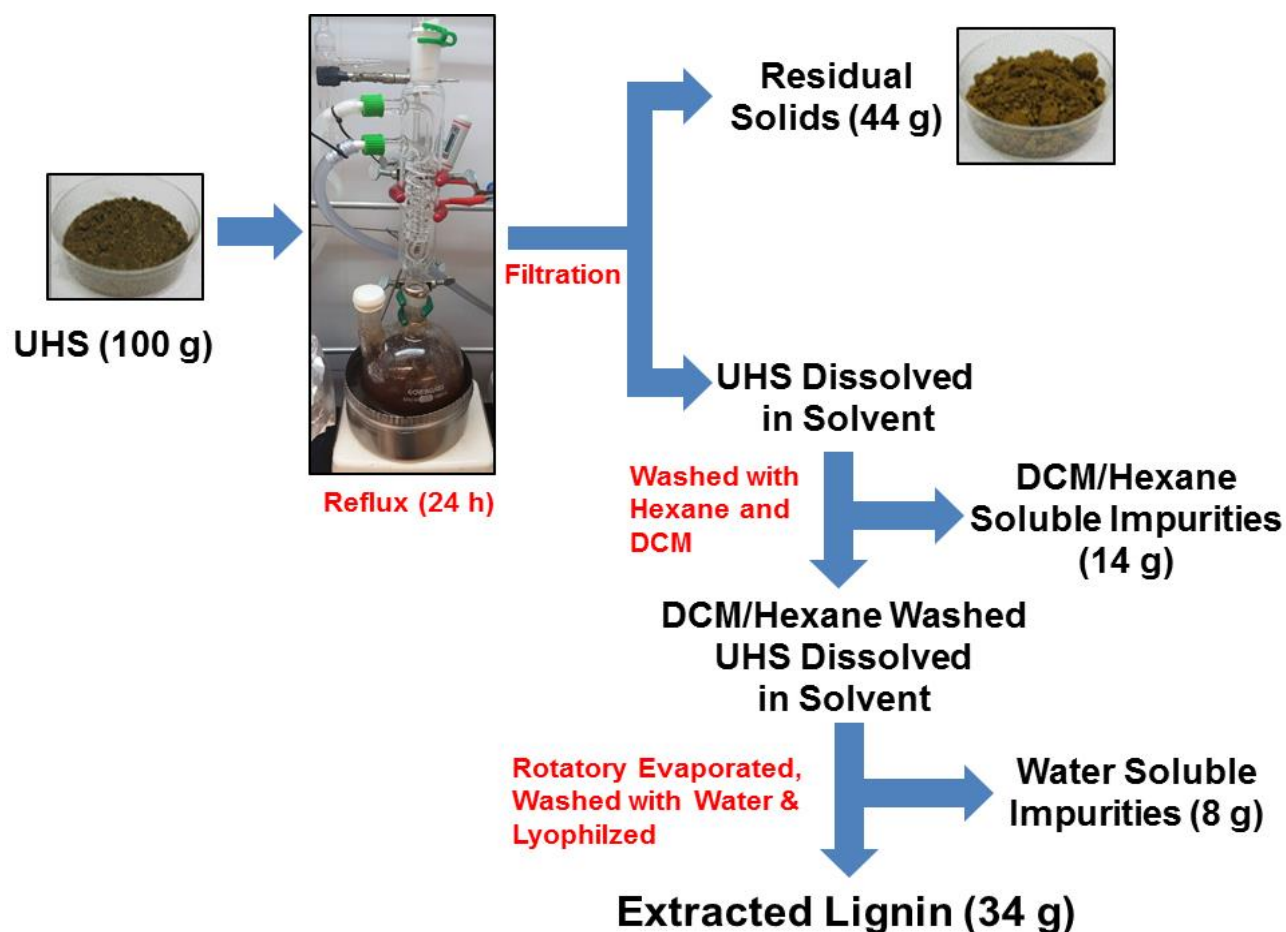
Scheme 2-1: Schematic diagram of the lignin isolation process from UHS after the modified AFEX pretreatment and enzymatic hydrolysis with an acetic acid:H_2O (2:1) solvent system.

2.3. Materials and Methods

2.3.1. Materials

Corn stover (Pioneer 36H56), harvested in September 2010 in Wisconsin (USA), was oven dried at 50 °C for approximately two weeks. The biomass was further passed through a 5 mm screen installed in a Christy hammer mill (Christison Scientific LTD, England) and stored at 4 °C in heat-sealed bags prior to utilization. The moisture content of the dried and milled corn stover was approximately 6% on a wet weight basis. On a dry weight basis, we experimentally determined that the untreated corn stover contained approximately 31% glucan, 19% xylan, 1% galactan, 3% arabinan, 13% Klason lignin, 1% acid soluble lignin, and 13% acid insoluble ash. All chemicals, buffers, and fractionation solvents used in this chapter were purchased from Sigma Aldrich (St. Louis, MO, USA). The enzymes Cellic® CTec2 (138 mg protein/mL, batch number VCNI 0001) and Cellic® HTec2 (157 mg protein/mL, batch number VHN00001) were generously provided by Novozymes (Bagsvaerd, Denmark), and Multifect Pectinase® (72 mg protein/mL, batch number 4861295753) was generously provided by DuPont (formerly Genencor, Palo Alto, CA). The protein concentrations of the enzymes were determined by estimating the protein content (and subtracting the non-protein nitrogen contribution) using the Kjeldahl nitrogen analysis method (AOAC Method 2001.11, Dairy One Cooperative Inc., Ithaca, NY, USA).

2.3.2. Methods

2.3.2.1. Ammonia Fiber Expansion (AFEX) Pretreatment

The AFEX pretreatment was carried out as previously described.[21] Pretreatments were conducted at a 1:1 ammonia-to-biomass ratio (dry biomass weight basis) with 60 wt% biomass moisture and run at a temperature of 120 °C for a residence time of 30 min. The pretreated biomass was stored dried (at 10 wt% moisture) in zip sealed bags at 4 °C in a refrigerator prior to further usage.

2.3.2.2. Enzymatic Hydrolysis

Enzymatic hydrolysis of the AFEX pretreated corn stover was performed at 6.0% glucan loading. The enzymatic hydrolysis was carried out for 96 h in a 4L bioreactor at 50 °C, with a buffered pH of 4.8. A total protein loading of 20 mg protein per g biomass was used. The commercial enzymes and their respective dosages used were Ctec2 (28.5 mL per kg CS), Htec2 (16.0 mL per kg CS), and Multifect Pectinase (38.2 mL per kg CS), based on values described previously.[21] The mass balance around the enzymatic hydrolysis was constructed as described previously.[21]

2.3.2.3. Isolation of Extracted Materials from Unhydrolyzed Solids (UHS)

To remove adsorbed sugars and proteins, the UHS obtained after enzymatic hydrolysis were washed three times (100 mL for 10 g) with distilled water. Each time, the slurry was stirred for 3 h and centrifuged at 4000 rpm for 30 min. The UHS was dried at 80 °C for 48 h and then milled through a 0.1 mm sieve. The desired amounts of UHS (10 g) and solvent (200 mL) were refluxed for 24 h as shown in the schematic representation of Scheme 1 (yields are reported in Table 1). After refluxing, the solids were filtered and washed with distilled water (200 mL). The filtrate was washed twice with 100 ml of hexane and dichloromethane (except for extractions involving GVL and GVL:H_2O) to remove impurities like fatty acid sugars, and then concentrated to 50 ml under vacuum in a rotary evaporator at 50 °C. Next, 10 mL of water was added and the filtrate was centrifuged at 4000 rpm. The centrifuged solids were lyophilized. In the case of extractions involving GVL or a GVL:H_2O mixture, after the filtrate was concentrated under reduced pressure, ethyl acetate was added to precipitate the lignin, and the entire mixture was centrifuged at 4000 rpm for 30 min, and then lyophilized. For all the mixed solvent systems (i.e., benzene:EtOH, acetone:H_2O, EtOH:H_2O, glycerine:H_2O, GVL:H_2O, and AcOH:H_2O) a 2:1

29

volume ratio of organic solvent to water was used. The solvents were chosen based on solvent polarity, boiling point, and pH.

2.3.2.4. Isolation of Standard Lignin

The standard lignin sample (used as a control) was prepared according to the reported procedure of Guerra et al. and Holmtman et al.[22-23] The UHS was extracted with dioxane: H_2O (96% dioxane by volume) in a shaker at 100 rpm for 24 h at 27 °C in the dark. This extraction was performed three times, each time using 200 ml of solvent per g of UHS. The dioxane: H_2O extracts were combined, and the solvents were removed at 35°C under reduced pressure. The solid lignin was then dissolved in 90% acetic acid (50 mg/ml) and precipitated in deionized water. The precipitated lignin was freeze dried, dissolved in 1,2 dichloroethane:ethanol (2:1 v/v), and precipitated in hexane, then washed with cold hexane. The sample was dried overnight at 40°C. The yield of standard lignin extracted from UHS through this procedure was 12.6% ± 0.5%.

2.3.2.5. Determination of Carbohydrate and Lignin Content

The carbohydrate, acid insoluble lignin, and acid insoluble ash contents of UHS and the materials extracted from UHS were measured according to methods reported by NREL[24-25]. Carbohydrate analysis was conducted using high performance liquid chromatography (HPLC) equipped with an automatic sampler (LC2010; Shimadzu Scientific Instruments, Columbia, MD, USA) and refractive index detector (Waters RI Detector, 410; Waters Corporation, Milford, MA, USA). A two-stage hydrolysis protocol was employed on UHS and extracted lignin to convert structural carbohydrates into monosaccharides. Stage one of the carbohydrate digestion involved using 72% sulfuric acid at 30 °C for 60 min, while stage two began after dilution of the acid to a 4% concentration and included heating to 121 °C for 60 min. The released monosaccharides were profiled using an HPLC and HPX-87H

Aminex column (Bio-Rad, Hercules, CA, USA) maintained at 65°C, with a 5.0 mM sulfuric acid-based mobile phase (flow rate of 0.6 mL/min). Total glucan, xylan, and arabinan values were calculated from the released monosaccharides (i.e., glucose, xylose, and arabinose) concentrations based on quantification by external standards. The Klason or acid insoluble lignin contents were the solids that remained after the two-stage hydrolysis protocol and after correction for the mass of residual acid insoluble ash. Acid-insoluble ash contents were determined based on the weight loss that occurred after dry acid-insoluble lignin was heated in a muffle furnace at 575 °C for 24 hours. Duplicate carbohydrate, acid-insoluble lignin, and ash content analyses were performed, and the averages were rounded to the nearest whole number. Standard deviations for all values were less than one percent.

2.3.2.6. Gel Permeation Chromatography (GPC) Analysis

Before gel permeation chromatography analysis, the materials extracted from UHS were acetylated according to a slightly modified published procedure.[26] In brief, the dried extracted material from UHS (15 mg) was dissolved in a 1:1 (v/v) mixture of acetic anhydride/pyridine (2.00 mL) and stirred at room temperature overnight. Anhydrous ethanol (5 mL) was then added, and after 30 min, the solvent was removed by rotary evaporation. The residue was repeatedly diluted with ethanol and evaporated under reduced pressure until all traces of acetic acid and pyridine were removed from the product. The residue was dissolved in a minimum quantity of chloroform (2 mL) and precipitated with diethyl ether. The precipitate was centrifuged, washed with diethyl ether (×3), and dried under vacuum overnight.

The acetylated extracted materials from UHS were then dissolved in tetrahydrofuran (THF, 0.5 mg/ml) and filtered through a 0.45-μm nylon membrane filter. GPC analysis was

31

carried out using a Waters 2590 chromatography system with an ultraviolet detector on a three-column sequence of Waters™ Styragel HR1, HR3, and HR4 columns. THF was used as eluent, and the flow rate was 0.8 ml/min. Polystyrene standards were used for calibration. A calibration curve was constructed based on six narrow polystyrene standards ranging in molecular weight from 1.5×10^3 to 3.6×10^6 g/mol.

2.3.2.7. Nuclear Magnetic Resonance (NMR) Analysis

NMR tubes for quantitative 1D ^{13}C NMR of materials extracted from UHS were prepared by first making a solvent mixture of DMSO-d_6 with 0.05% wt. of both 1,3,5 trioxane as an internal standard and chromium(III) acetylacetonate as a T_1 relaxing agent. Then mixing the solvent mixture and materials extracted from UHS were mixed in a 10:1 w/w ratio and added to the NMR tube. NMR samples for 2D ^{1}H-^{13}C heteronuclear single quantum coherence (HSQC) of materials extracted from UHS were made by adding only DMSO-d_6 as the solvent in a 10:1 ratio. Whole cell HSQC NMR samples of the solid remaining after extraction from UHS were prepared by following a procedure developed by Mansfield et al. [27]. All ^{13}C and ^{31}P NMR spectra were acquired using a Varian Unity Inova-600 MHz and a Varian Unity Plus-300 MHz spectrometers, respectively. HSQC NMR spectra were recorded by a Varian Unity Inova-600 spectrometer. The HSQC analysis was performed using a standard Varian gradient HSQC pulse sequence with a 90° pulse, 0.11 s acquisition time, 1.5 s recycle delay, 521 scans, a J_{C-H} of 145 Hz, and acquisition of 256 data points at 45 °C . ^{31}P NMR spectra were acquired after *in-situ* derivatization of materials extracted from UHS samples with 2-chloro-4,4,5,5-tetramethyl-1,3,2-dioxaphospholane (TMDP). N–Hydroxy–5–norborene–2,3–dicarboximide was used as an internal standard. The conditions for ^{31}P NMR spectra were as follows: a 45° pulse angle, 0.1 s acquisition time, 25 s recycle delay, and 256 scans at room temperature.[28-29] The quantitative ^{13}C NMR spectra were collected at 45 ºC,

using a z-restored spin-echo sequence and inverse-gated ^{1}H decoupling with a 90° pulse, 0.87 s acquisition time, 10 s recycle delay, and 128 scans. Inversion-Recovery experiments were run prior to insure the quantitative nature of the experiments.

2.3.2.8. Thermogravimetric Analysis (TGA)

Thermogravimetric analysis was performed using a TGA Q500 series thermogravimetric analyzer (TA Instruments, USA) with a heating rate of 20 K/min in a flowing nitrogen environment at 2.0 mL/min.[30]

2.4. Results and Discussion

2.4.1. Mass Yield

Generally, more severe solvent extraction conditions, such as high/low pH and higher temperatures, are associated with greater lignin extraction mass yields due to increased lignin solubility, lignin fragmentation, and/or carbohydrate depolymerization.[31] For example, severe solvent extraction conditions can also cause carbohydrate depolymerization, resulting in a high percent mass conversion of UHS. However, after the aqueous washing steps, mass related to water-soluble oligosaccharides and/or monosaccharides will be lost and the percent mass yield of extracted material will decrease. In this case, the extracted material precipitated from the organic solvent, most likely, will be lignin. Equally important, more severe solvent extraction conditions will promote unwanted chemical and molecular alteration to the lignin being extracted, such as inter-monomer linkage cleavage reactions (e.g., aryl ether hydrolysis) and condensation reactions (e.g., electrophilic carbocations forming C-C bond).[32]

Table 2-1 reports the percent mass yields resulting from the extraction of UHS with various solvents under reflux for 24 h. These results suggest that, on average, solvent

systems with higher solvent extraction (reflux) temperatures resulted in higher mass yields. However, the data in Table 2-1 also suggest that solvent factors that determine lignin/carbohydrate-solvent interactions (e.g., various solvent and lignin/carbohydrate solubility parameters, solvent pKa, solvent hydrogen bond basicity, and solvent dipolarity/polarizability) play a more important role in determining the mass yield of extractable material from UHS. The AcOH:H_2O solvent system gave the highest extraction yield, followed by GVL:H_2O > EtOH:H_2O > acetone:H_2O. Extensive studies have investigated the addition of water to organic solvents, such as methyl isobutyl ketone and/or EtOH:H_2O[33-34], AcOH and/or formic acid:H_2O[35-37], and acetone:H_2O[38-40], to augment lignin removal from biomass. The addition of water to a polar organic solvent (miscible) seems to increase the extraction mass yield, which matches observations by several other researchers[41-42], either due to an increase of reflux temperature or an alteration in lignin/carbohydrate-solvent interactions. The significant difference between the extraction percent mass yield of acetone and acetone:H_2O, EtOH and EtOH:H_2O, and GVL and GVL:H_2O solvent systems with respect to the small increase in reflux temperature suggests water is altering the lignin/carbohydrate-solvent interactions so as to increase extraction yield. The polar solvents were found to have higher percent mass yields of extraction from UHS than the non-polar solvents.

Table 2-2. Percent mass yields of material extracted from UHS with various solvents. The four highest yielding solvent systems are bolded.

Solvent	Refluxing Temp. (°C)	% Mass Yield
Dichloromethane (DCM)	40	2.9
Benzene:Ethanol (2:1)	50	26.3
Acetone	56	6.3
Acetonitrile (ACN)	82	22.4
Acetone:H_2O (2:1)	**57**	**52.6**
Hexane	60	0.6

1,4 Dioxane	75	27.4
Benzene	78	3.8
Ethyl acetate	78	4.3
Ethanol (EtOH)	79	32.7
EtOH:H$_2$O (2:1)	**81**	**51.3**
Glycerine:H$_2$O (2:1)	100	33.9
1,4 Dioxane:H$_2$O (2:1)	100	37.1
Water	100	38.7
γ−Valerolactone (GVL)	100	38.9
Acetic Acid (AcOH)	100	48.2
AcOH:H$_2$O (2:1)	**100**	**65.5**
GVL:H$_2$O (2:1)	**100**	**53.5**

From a processing standpoint, optimizing the mass extraction yields from UHS is critical. However, in the context of isolating a "native" lignin or a lignin with specific properties for further application, understanding the effect of extraction on the chemical and molecular structure of the material extracted is of equal or greater importance. Thus, for each of the four extraction solvent systems that gave the highest percent mass yields (acetone:H$_2$O, EtOH:H$_2$O, GVL:H$_2$O, and AcOH:H$_2$O), the soluble materials extracted were characterized to determine their chemical and molecular properties and compared to a standard lignin as a control (a dioxane extraction from UHS, not requiring heating for comparison[43]).

2.4.2. Compositional Analysis

To determining the relative proportions of carbohydrates, Klason (acid-insoluble) lignin, and ash, compositional analysis was conducted on the UHS, the solid residues remaining after extraction, and the material extracted from UHS, (see Tables 2-2 and 2-3). A more detailed accounting of the relative proportion of carbohydrates (i.e., glucan, xylan, and arabinan) can be found in the Appendix I, Tables I-1 and I-2. Klason lignin is the solid residue that remains after a

two-stage acid hydrolysis procedure, corrected for residual ash. Both significant residual carbohydrates and ash are generally considered detrimental to further utilization of lignin.[16]

Table 2-2 gives the results from the compositional analysis for the material extracted from UHS using acetone:H_2O, EtOH:H_2O, GVL:H_2O, and AcOH:H_2O. The ratio of carbohydrates to Klason lignin is lowest for material extracted with AcOH:H_2O, followed by lignin extracted with EtOH:H_2O, which indicates those samples were mostly lignin. In comparison, material extracted with GVL:H_2O or acetone:H_2O is more carbohydrate-rich than the original UHS. Note the ash contents for all extracted materials are negligible.

Table 2-2. Relative compositional analysis of the material extracted from UHS with various solvents.

Solvent	% Carbohydrates (± 2%)	% Klason Lignin (± 2%)	% Ash (± 1%)
Acetone:H_2O (2:1)	38	62	0.7
Ethanol:H_2O (2:1)	4	96	0.3
AcOH:H_2O (2:1)	2	98	0.2
GVL:H_2O	55	45	0.9

Compositional analysis of the solid residues remaining after extraction from UHS can also be used to assess the ability of the screened solvents to selectively dissolve and extract lignin. Since the mass yields of the solid residues remaining after extraction were at least 50% for all solvents, conducting compositional analysis on those solids (as opposed to material extracted from UHS) was much easier (due to the smaller sample size) and is reported in Table 2-3. For example, the mass yield of material extracted from UHS with DCM was 2.9% (or 290 mg from 10 g of UHS), which was simply not enough material to conduct compositional analysis. However, the mass of solid residues remaining after extraction of UHS with DCM was sufficient.

On average, the ratio of carbohydrates to Klason lignin in the solid residues remaining after extraction decreases with increasing extraction temperature: only the solid residues remaining after

extraction with glycerine:H_2O, H_2O, GVL, AcOH, and GVL:H_2O showed a ratio lower than UHS.

Thus, thirteen of the eighteen screened solvent systems displayed the ability to extract more lignin

than carbohydrates from UHS, which is expected because carbohydrates have a low solubility in

most organic solvents. The material extracted from UHS with GVL:H_2O showed the highest

percent mass yield, but also a high carbohydrate to Klason lignin ratio, and thus the lowest

selectively for lignin. Xue et al. showed that in co-solvent systems with GVL, a well-known

solvent for biomass [44], its hydrogen bond basicity parameter (β-value) plays an important role in

solubilizing both lignin and cellulose.[45] The high solubility of both lignin and cellulose in GVL

leads to a low selectively of the extraction for lignin from UHS. An alternative explanation

involves the chemical and molecular modification of carbohydrates, facilitating their increased

solubility. For example, refluxing in AcOH could acetylate the carbohydrates in UHS and increase

their extractability in organic solvents, lowering the selectively for the extraction of lignin from

UHS.

Table 2-3. Relative compositional analysis of the solids remaining after extraction of carbohydrates and lignin from UHS (solids which are not dissolved) with various solvents. The highest yielding solvent systems are in bold.

Solvent	% Carbohydrates (± 2%)	% Klason Lignin (± 2%)	% Ash (± 1%)
Dichloromethane	29	41	29
Benzene:Ethanol (2:1)	24	39	37
Acetone	23	43	34
Acetonitrile	24	41	35
Acetone:H_2O (2:1)	**21**	**39**	**40**
Hexane	31	41	28
1,4 Dioxane	21	38	41
Benzene	30	42	27
Ethyl acetate	30	43	28
Ethanol (EtOH)	19	40	41
EtOH:H_2O (2:1)	**20**	**27**	**52**
Glycerine:H_2O (2:1)	12	51	36

1,4 Dioxane:H$_2$O (24:1)	21	36	43
Water (H$_2$O)	13	52	35
γ-Valerolactone (GVL)	10	44	46
AcOH	15	46	40
AcOH:H$_2$O (2:1)	**19**	**13**	**68**
GVL:H$_2$O (2:1)	**2**	**65**	**33**
UHS	**25**	**52**	**23**

Assuming that the ash in UHS is not soluble, the absolute mass of ash found in UHS and in the solid residues remaining after extraction will not change. As a result, one method to compare the relative compositions of solid residues remaining after extraction and determine the amount of carbohydrates and lignin solubilized is to normalize the compositions based on the ash content. For example, the relative composition of UHS is 25% carbohydrates, 52% lignin, and 23% ash by mass (or 2.5 g of carbohydrates, 5.2 g of lignin, and 2.3 g of ash for 10 g of UHS). Assuming the extraction began with 10 g of UHS and the mass of ash in the solid residue remaining after extraction of UHS is the same as the mass of ash in the UHS before extraction, then the solid residue remaining after extraction of UHS with hexane has 2.5 g of carbohydrates, 3.4 g of lignin, and 2.3 g of ash. In other words, extraction with hexane does not remove any carbohydrates from UHS, but does remove ~1.8 g of lignin (a 35% decrease) which does not show up in the washed hexane precipitant. Table 2-4 lists the percent change in the absolute amount of carbohydrates and lignin in the solids remaining after extraction with various solvents.

Table 2-4. Percent change in the absolute amounts of carbohydrates and lignin remaining in the residual solids after extraction. The highest yielding solvent systems are in bold

Solvent	% Δ for Carbohydrates	% Δ for Lignin
Dichloromethane	-9	-38
Benzene:Ethanol (2:1)	-41	-53
Acetone	-38	-45
Acetonitrile	-39	-49

Acetone:H$_2$O (2:1)	**-52**	**-57**
Hexane	-1	-35
1,4 Dioxane	-54	-59
Benzene	-1	-33
Ethyl acetate	-4	-32
Ethanol (EtOH)	-58	-57
EtOH:H$_2$O (2:1)	**-65**	**-77**
Glycerine:H$_2$O (2:1)	-70	-38
1,4 Dioxane:H$_2$O (24:1)	-56	-63
Water (H$_2$O)	-67	-35
γ-Valerolactone (GVL)	-80	-58
AcOH	-67	-49
AcOH:H$_2$O (2:1)	**-75**	**-91**
GVL:H$_2$O (2:1)	**-96**	**-13**

Though the percent mass yields were low, the extractions with DCM, hexane, benzene, and ethyl acetate were highly selective for lignin. On the other hand, though the percent mass yields were high, the extraction with GVL:H$_2$O was not selective for lignin. The data in Table 2-4 also indicated that the extraction with acetone:H$_2$O, dioxane, EtOH, EtOH:H$_2$O, glyercine:H$_2$O, dioxane:H$_2$O, H$_2$O, GVL, AcOH, GVL:H$_2$O, and AcOH:H$_2$O resulted in at least a 50% decrease in both carbohydrates and lignin. This finding suggests that these solvents have a significant capacity to solubilize and/or depolymerize carbohydrates and lignin. Table 2-4, also shows that the extraction of UHS with AcOH:H$_2$O removes ~75% of the carbohydrates and ~91% of the lignin, however, the material extracted from UHS with AcOH:H$_2$O contains almost no carbohydrates. This result suggests that the AcOH:H$_2$O UHS extraction generated water-soluble oligosaccharides and/or monosaccharides that were removed during the extraction washing steps. A similar loss of mass due to aqueous washing was observed for the material extracted from UHS with EtOH:H$_2$O.

2.4.3. Gel Permeation Chromatography (GPC)

The molecular weight of a lignin, in part, determines many of its physical properties, such as its thermal transition temperatures (e.g., glass transition temperature), mechanical properties (e.g., strength), and flow behavior.[46] If the molecular weight is too low or too high, these physical properties will not overlap with the material property requirements for an application, thus, inter-monomer cleavage and condensation reactions, which generally occur quite easily in treatments such as high temperature extractions must be taken into account for lignin extractions.[46] In addition, different solvents can selectively solubilize and extract different fractions of the lignin molecular weight distribution. Herein, GPC was applied to understand possible changes in lignin molecular weight distributions as a function of the extraction.

The molecular weights of the materials extracted from UHS using acetone:H_2O, EtOH:H_2O, GVL:H_2O, and AcOH:H_2O were determined via GPC in tetrahydrofuran (THF) following their acetylation. Acetylation facilitates dissolution for GPC analysis. Figure 2-1 displays the resulting chromatograms, as well as the corresponding number average molecular weight (M_n, relative to polystyrene standards in g/mol) and dispersity (Đ). The molecular weight distributions of the materials extracted had Đ values between 1.4 and 1.8. The highest molecular weight materials resulted from extraction with GVL:H_2O, which may be variously attributed to selective removal of higher molecular weight fractions, to condensation reactions that result from the higher temperature used for extraction, and/or to residual carbohydrates. Though similar to the standard lignin with respect to M_n and Đ, the material extracted with acetone:H_2O demonstrated the lowest molecular weight, evident in its chromatogram and the absence of a shoulder at a retention time of 20 min. Trends with respect to molecular weight display similar changes for lignin after organosolv pretreatment or fractionation.[47]
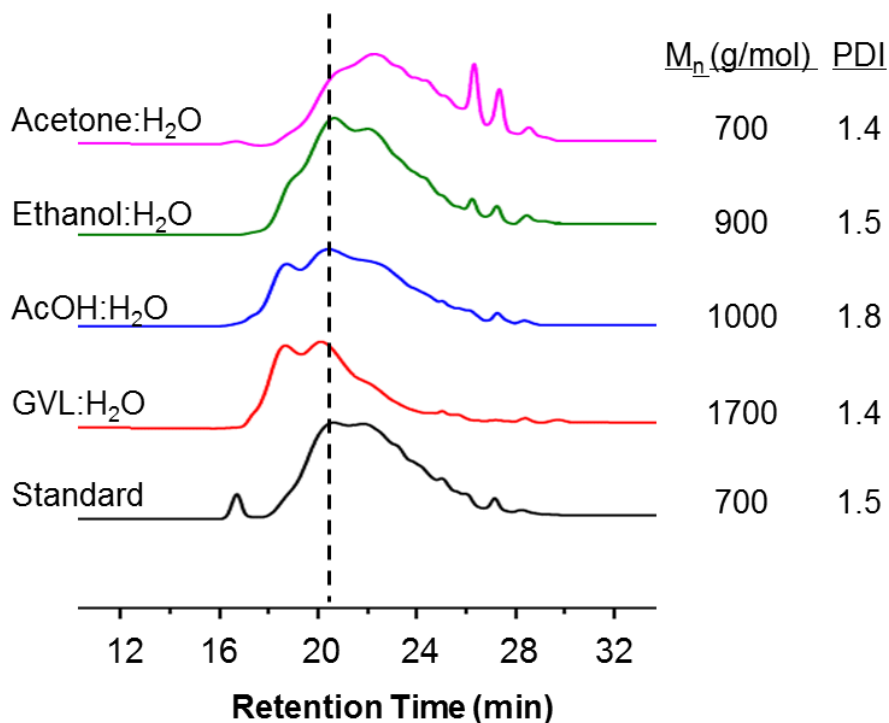
Figure 2-1: Gel permeation chromatograms of material extracted from UHS with various solvents (with the standard lignin for comparison). The dotted line is only a reference to visually indicate shifts in the chromatographs

2.4.4. Nuclear Magnetic Resonance (NMR) Analysis

In an effort to understand the effect of each extraction solvent system on the chemical and molecular structure of the material extracted from UHS, a series of nuclear magnetic resonance (NMR) experiments were conducted. NMR is a powerful analytical tool for lignin, facilitating both functional and sub-structural unit analysis and illuminating the chemical changes that occur to lignin during its extraction from UHS.

2D ^{1}H-^{13}C heteronuclear single quantum coherence (HSQC) NMR was performed on the UHS, standard lignin, solid residues remaining after extraction from UHS, and material extracted from UHS. 2D ^{1}H-^{13}C HSQC NMR can be used to resolve the overlapping ^{1}H or ^{13}C spectral features of lignin or material extracted from UHS in the ^{13}C and ^{1}H spectral dimensions. In general, 2D

HSQC NMR is not quantitative, but rather indicates the presence of a wide array of lignin-related sub-structures. Figure 2-2 and 2-3 include the HSQC NMR spectra of the standard lignin and materials extracted from UHS, displaying the aromatic region (^{1}H: 5.8-8.3 ppm and ^{13}C: 90-150 ppm) in Figure 2-2 and the aliphatic region (^{1}H: 2.8-6.0 ppm and ^{13}C: 50-100 ppm) in Figure 2-3. The aromatic region for the standard lignin (representing native lignin) shows the presence of various lignin sub-structural units that are aromatic monomers, including ferulate (FA), *p*-coumarate (*p*CA), *p*-hydroxybenzyl (PB), guaiacyl (G), oxidized guaiacyl (G'), 4-hydroxyphenyl (H), syringyl (S), and oxidized syringyl (S') units. Furthermore, the aliphatic region for the standard lignin shows various lignin sub-structural units that are linkages between aromatic monomers, including β-O-4 aryl ether (A), phenylcoumaran (β-5) (B), and resinol (β-β) (C) linkages, as well as cinnamyl alcohol (X1) end groups. The aromatic and aliphatic region spectra for the standard lignin are characterized by intense cross-peaks and the appearance of multiple cross-peaks for the same sub-structural unit. For example, β-O-4 aryl ether linkages are detectable by cross-peaks for carbon-hydrogen correlations at the α-, β- and γ-carbon positions. Generally, due to its favorable NMR relaxation behavior, the cross-peak for the γ-carbon position is most prevalent. As degradation occurs and the concentration of β-O-4 aryl ether linkages is reduced, the cross-peak for the α- and β-carbon positions disappear first, followed by the γ-carbon cross-peak. Appendix I, Table I-3 includes the ^{1}H-^{13}C HSQC chemical shifts of these lignin-related sub-structural units and their assignments, including whether each sub-structural unit was detected in the ^{1}H-^{13}C HSQC NMR spectra of the standard lignin and materials extracted from UHS. The whole cell HSQC NMR spectra of the UHS and solids remaining after extraction of UHS are shown in Appendix I, Figures I-1 and I-2. These spectra clearly show strong lignin-related cross-

peaks, indicating the presence of G, S, and β-O-4 aryl ether sub-structural units in all the solids remaining after extraction of UHS.

The HSQC NMR spectrum, in both the aromatic and aliphatic regions, for the material extracted from UHS with acetone:H_2O was nearly identical to the HSQC NMR spectrum of standard lignin, indicating their significant chemical similarity. The HSQC NMR spectrum of the material extracted from UHS with acetone:H_2O contains relatively unaltered cross-peaks. These cross-peaks indicate the presence of inter-monomer linkages and monomer units, and even those sub-structural units susceptible to degradation or chemical alteration, such as X1, FA, and *p*CA. Accordingly, the material extracted from UHS with EtOH:H_2O also is very similar to standard
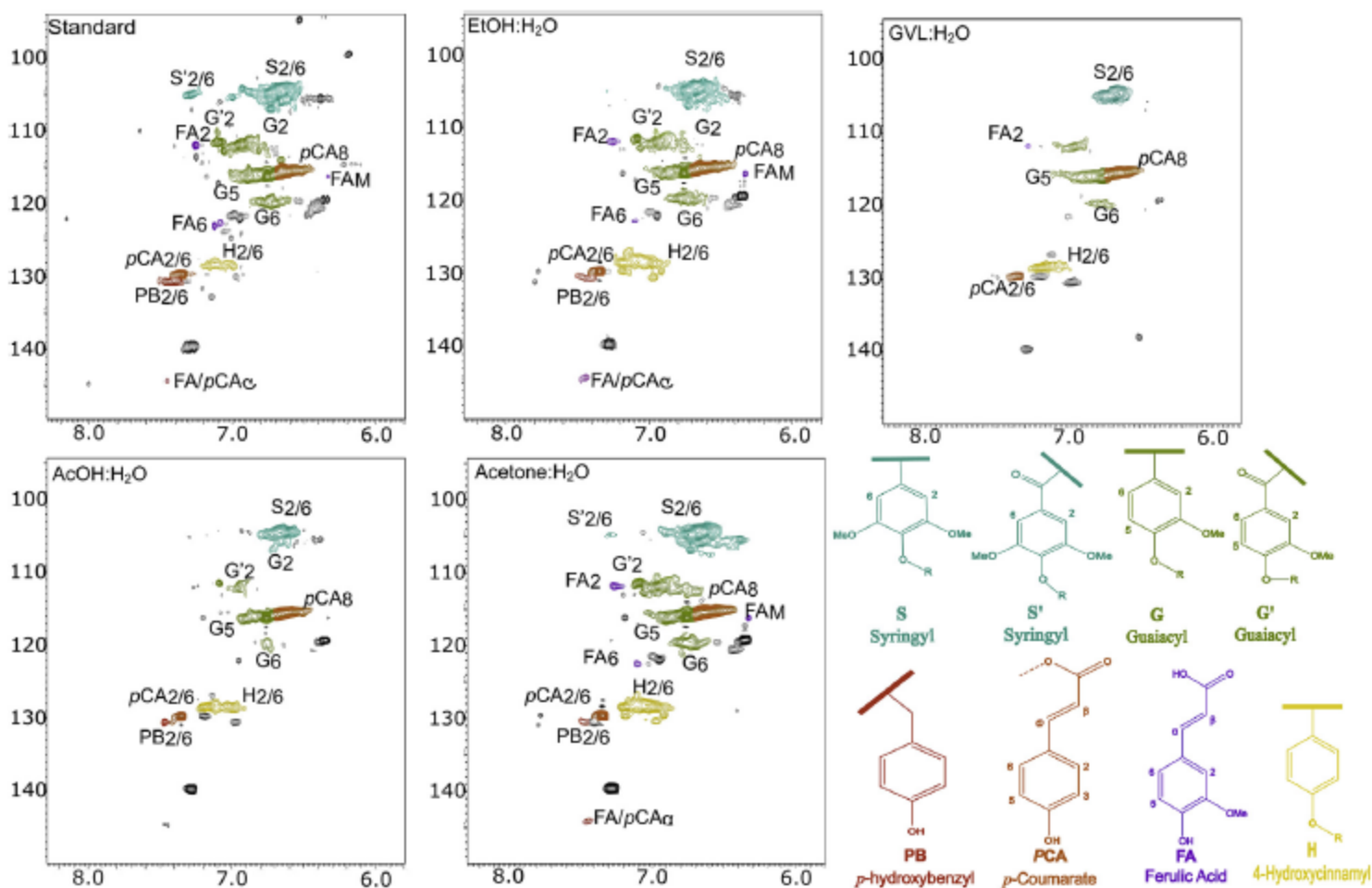
Figure 2-2. Aromatic region of the 2D ^1H-^{13}C HSQC NMR spectra of the standard lignin and material extracted from UHS with various solvents.

lignin. In the aromatic and aliphatic regions of the HSQC NMR spectra of material extracted from UHS with AcOH:H_2O and GVL:H_2O, the reduction or disappearance of various cross-peaks suggests that degradation occurred during extraction. The complete disappearance of cross-peaks attributed to B, C, and X1 sub-structures in the HSQC NMR spectrum of material extracted from UHS with AcOH:H_2O suggests this extraction resulted in the most significant degradation or chemical alteration. Lastly, the aliphatic region of the HSQC NMR spectra of material extracted from UHS with GVL:H_2O, and to a lesser degree, material extracted from UHS with acetone:H_2O,
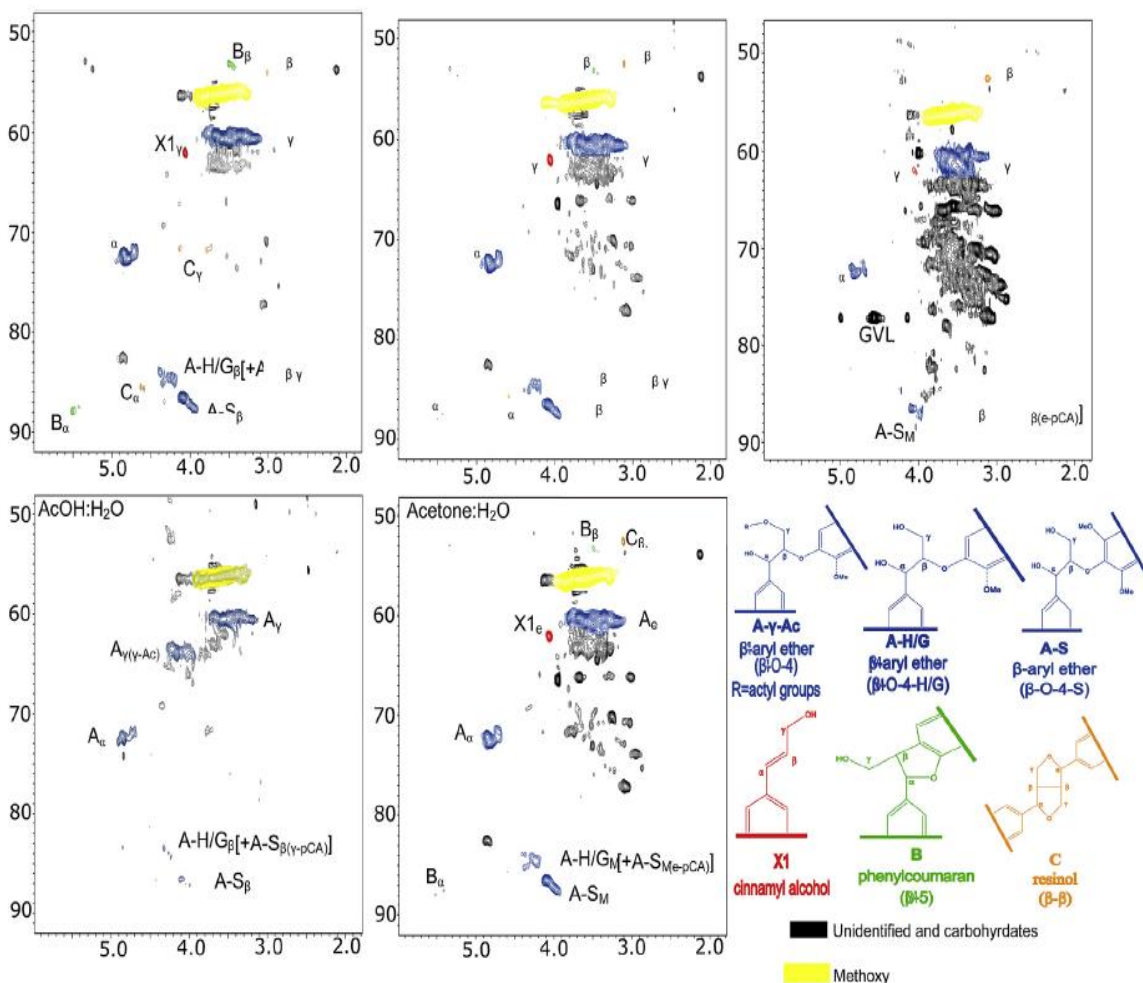
Figure 2-3. Aliphatic region of the 2D ^{1}H-^{13}C HSQC NMR spectra of the standard lignin and material extracted from UHS with various solvents.

show the presence of non-lignin related aliphatic C-O cross-peaks, presumably from carbohydrates.
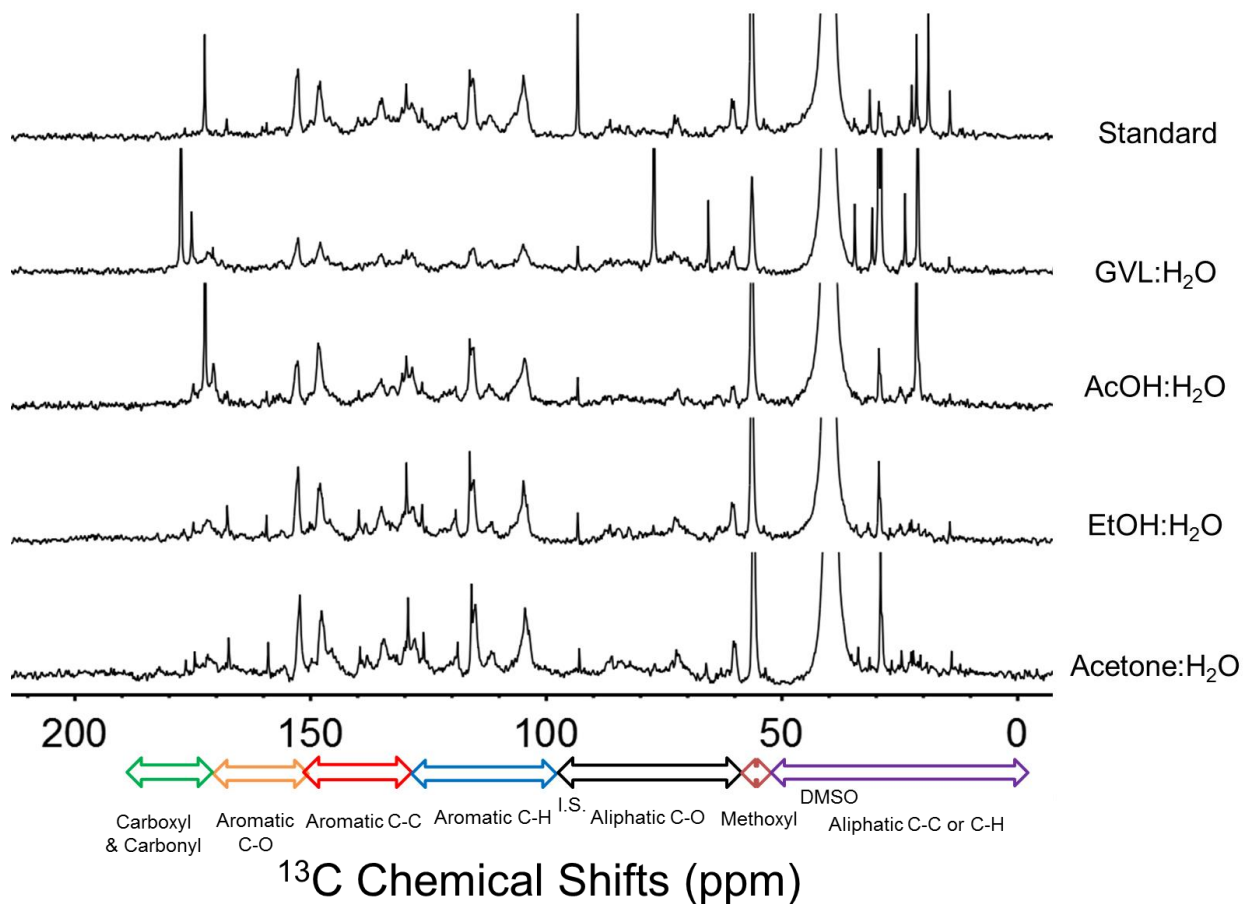
Figure 2-4. ^{13}C NMR spectra of material extracted from UHS in aqueous solutions of acetone, ethanol, acetic acid, and γ-valerolactone (GVL). Note the spectrum of extracted lignin from UHS in aqueous GVL has ^{13}C NMR resonances from residual GVL at 177, 77, 29, and 21 ppm.

Quantitative ^{13}C NMR spectra of the standard lignin and material extracted from UHS with EtOH:H$_2$O, GVL:H$_2$O, AcOH:H$_2$O, and acetone:H$_2$O are shown in Figure 2-4. The ^{13}C NMR chemical shifts and functional group assignments for lignin are listed in Appendix I, Table I-4, along with the amount of carbon attributed to carbonyl and carboxyl, methoxyl, aromatic C-H, aromatic C-C, aromatic C-O, aliphatic C-O, and aliphatic C-C functionalities. Figure 2-5 shows the relative percentage of carbon attributed to carbonyl and carboxyl, methoxyl, aromatic C-H, aromatic C-C, aromatic C-O, aliphatic C-O, and aliphatic C-C carbon functionalities. The

spectrum of material extracted from UHS in GVL:H$_2$O has ^{13}C NMR resonances from residual

GVL at 177, 77, 29, and 21 ppm, indicating ~33 % of the material extracted from UHS in

GVL:H$_2$O (on a % carbon basis) is GVL. No other spectrum suggested a similar type of solvent

contamination. The material extracted from UHS in GVL:H$_2$O displays the highest percentage of

aliphatic C-O carbon, 25 %, and has an aromatic carbon to aliphatic C-O carbon ratio of 1.7

(compared to the 4.8 ratio observed for standard lignin and the >3.2 ratio observed for the materials

extracted from UHS with other solvents). Along with the 2D HSQC NMR results, the relatively

high percentage of aliphatic C-O carbon can be, in part, attributed to the presence of carbohydrates.

The percentage of aromatic carbons that are aromatic C-C carbons in material extracted from UHS

in GVL:H$_2$O is ~26% compared to the ~30% observed for standard lignin and the materials

extracted from UHS with other solvents. At the conditions for organic solvent extraction of lignin,

the formation of highly reactive groups on lignin (e.g., benzylic carbocations) can cause inter- and

intra-molecular condensation reactions.[48] Since aromatic C-C bonds form as a result of these

condensation reactions, the fact that material extracted from UHS in GVL:H$_2$O displays a lower

percentage of aromatic carbons that are aromatic C-C carbons suggests that its lignin component

has undergone the least amount of condensation. The strong presence of ^{13}C NMR resonances at

178 and 21 ppm, representing carboxyl and acetal methyl carbons respectively, in the ^{13}C NMR

spectrum of material extracted from UHS with AcOH:H$_2$O confirms that acetylation has occurred.

Integration of the ^{13}C NMR resonances at 178 and 21 ppm suggests that ~10 % of the carbon in

the material extracted from UHS with AcOH:H$_2$O is the result of this acetylation. When comparing

materials extracted from UHS with AcOH:H$_2$O and EtOH:H$_2$O, the percentage of aliphatic C-O

carbon is lower for the material extracted from UHS with AcOH:H$_2$O. This result suggests that the

material extracted from UHS with $AcOH:H_2O$ undergoes more degradation at aliphatic C-O linkages than the material extracted from UHS with $EtOH:H_2O$.
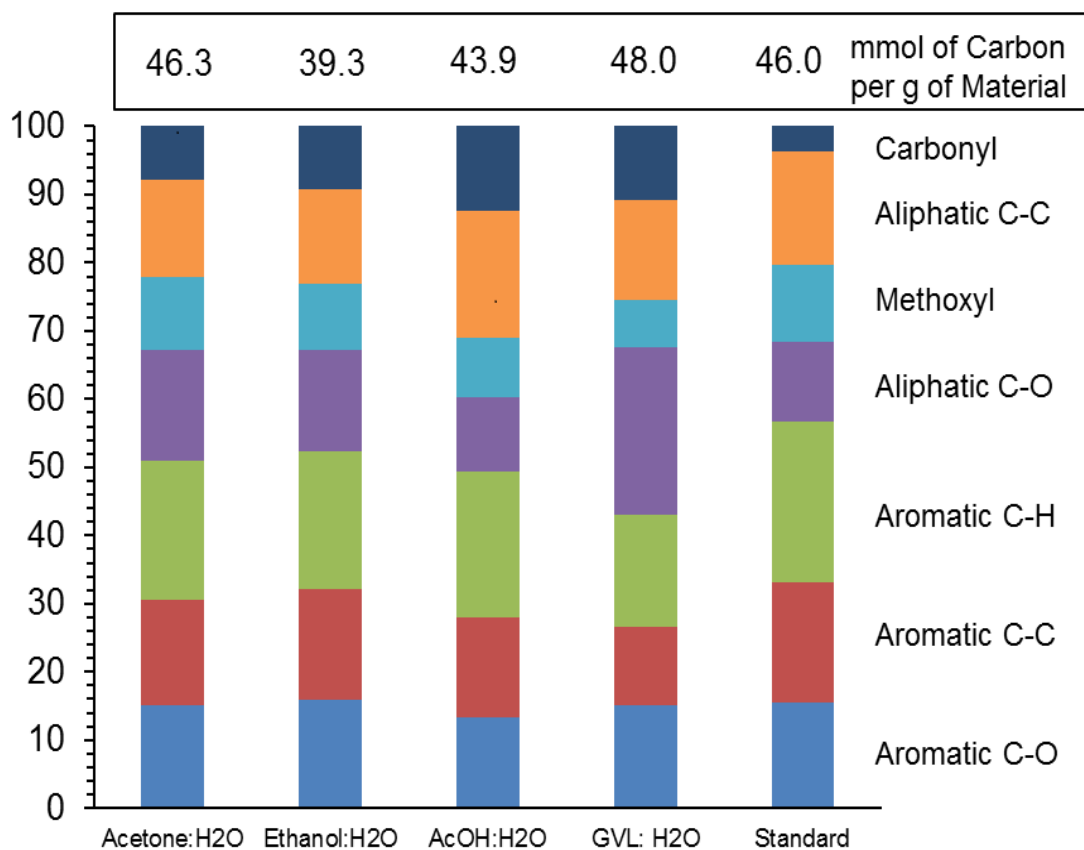
Figure 2-5. Amounts of carbon attributed to various functional groups on material extracted from UHS with various solvents as determined by ^{13}C NMR

To profile the change in terminal phenolic monomer units and overall hydroxyl group distribution, quantitative ^{31}P NMR on material extracted from UHS following phosphorylation with 2–chloro–4,4,5,5–tetramethyl–1,3,2–dioxaphospholane (TMDP) was conducted. This methodology is used to routinely determine the content of aliphatic, phenolic (i.e., guaiacyl, syringyl, C5-substituted guaiacyl phenolics, catechols, *p*–hydroxyphenols, etc.), and carboxylic acid hydroxyl groups on lignin. Quantitative ^{31}P NMR spectra of the phosphorylated material extracted from UHS are shown in Appendix I, Figure I-3. The ^{31}P NMR chemical shifts and

functional group assignments are listed in Appendix I, Table I-5, along with the hydroxyl content (mmol of OH per g of lignin) for the materials extracted from UHS.

Table 2-5 displays total, aliphatic, and aromatic hydroxyl contents for the materials extracted from UHS. Hydroxyls can be attributed to lignin chain ends (4-position phenolic hydroxyls), lignin inter-monomer linkages (2 per β-O-4 or β-1 and 1 per phenylcourmaran/spirodienone), or residual carbohydrates (3 or 4 per sugar monomer). In the case of lignin, the greater amount of aromatic hydroxyls per mass of lignin suggest more chain ends, which in turn indicate a lower molecular weight. Therefore, an increase in total hydroxyl content with respect to the standard lignin can suggests three possibilities: (1) chain scission at aryl ether linkages that produce a phenolic hydroxyls, (2) selective extraction of small molecular weight lignin, and/or (3) the presence of a higher percentage of residual carbohydrates. On the other hand, decreases in total hydroxyl content can suggest (1) selective extraction of large molecular weight lignin, (2) disruption of lignin inter-monomer linkages that leads to or is accompanied by reduction in aliphatic hydroxyls, (3) hydroxyl groups that have undergone chemical modification (i.e., acetylation), and/or (4) the presence of a lower percentage of residual carbohydrates.

Table 2-5. OH content (mmol of OH/g of extracted material) determined by ^{31}P NMR spectral intensities of phosphorylated lignin extracted from UHS with various solvents.

Assignment	OH content (mmol/g)				
	Std	Acetone:H_2O	EtOH:H_2O	AcOH:H_2O	GVL:H_2O
Total OH	9.6	10.4	8.4	5.8	7.4
Aliphatic OH	4.7	7.6	5.4	1.9	3.6
Aromatic OH	3.8	1.9	2.2	2.8	2.6

2.4.5. Thermogravimetric Analysis (TGA)

The thermal stability and decomposition of lignin are important physical properties for a variety of applications and are typically determined using thermogravimetric analysis (TGA). TGA measure the percentage of total weight lost as a function of increasing

temperature and shows the onset temperature of degradation. The TGA curves of the material extracted from UHS with acetone:H_2O, EtOH:H_2O, AcOH:H_2O, and GVL:H_2O are shown in Appendix I, Figure I-4, and the total weight loss percentage, residue mass percentage, onset temperature of thermal degradation, and end temperature of thermal degradation are in Table 2-6. The TGA curves of all the materials extracted from UHS are very similar as are the corresponding total weight loss percentages and residue mass percentages.

Table 2-6. TGA results for the lignin extracted from UHS with various solvents.

Sample	T_{onset} (°C)	T_{end} (°C)	Total weight loss % (+/- 2%)	Residue mass % (+/- 2%)
Acetone:H_2O	182	437	52	41
EtOH:H_2O	225	445	53	40
AcOH:H_2O	253	449	51	42
GVL:H_2O	247	445	53	43
Standard	253	441	53	41

2.5. Conclusions

While the work reported in this chapter was performed on a process that utilized an AFEX pretreatment and corn stover feedstock, the knowledge gained can be extended to most second-generation biorefineries, because all will have a waste stream of UHS, regardless of the pretreatment method and biomass feedstock. While other pretreatments and feedstocks will ultimately dictate the final structure of the lignin molecules and resulting UHS, the underlying extraction principles will be transferable.

Mass yields of materials extracted from UHS were higher for polar and high-reflux temperature solvents. The addition of water to polar organic solvents improved the mass yields of materials extracted from UHS. Due to the small increases in reflux temperature upon adding water, the results suggest lignin-solvent interactions that determine solubility (e.g., solvent H-bonding properties) are important when considering a solvent for lignin extraction from UHS. These results

correspond well with other studies that focus on aqueous/organic solvent systems as a means to improve biomass pretreatment[42], lignin extraction from biomass[47], or lignin separation into fractions [49-50]. Other factors, such as a solvent's propensity to perform chemical modifications (e.g., acetylation), must also be considered. Although low mass yields are unwanted, it is important to note that non-polar solvents were highly selective for lignin extraction from UHS, and could potentially provide a high value stream, depending on the compounds extracted. The AcOH:H_2O solvent system gave the maximum mass yield of material extracted from UHS, and was highly selective for lignin extraction. However, the AcOH:H_2O solvent system did cause acetylation and the most significant degradation to lignin–related aliphatic C-O sub-structures. Most likely the acidity of AcOH caused significant chemical degradation, and produced water-soluble oligosaccharides and/or monosaccharides that were removed during the extraction washing steps. The GVL:H_2O solvent system had the second highest mass yield of material extracted from UHS, but also produced an extracted material that was carbohydrate-rich. The EtOH:H_2O solvent system gave a high mass yield of material extracted from UHS and a high selectively for lignin extraction (after water washes), while producing material extracted from UHS with a relatively unaltered lignin structure. Extracting UHS with organic solvents provides an opportunity to valorize currently unutilized lignin.

2.6 References

1.   Brown, T. R.; Brown, R. C., A review of cellulosic biofuel commercial-scale projects in the United States. *Biofuels, bioproducts and biorefining* **2013,** *7* (3), 235-245.

2.   Efficiency, E.; Energy, R.; Reserves, O. S.; Reserve, S. P.; Reserve, N. H. H. O., FY 2015 Congressional Budget Request.

3.   Chundawat, S. P.; Donohoe, B. S.; da Costa Sousa, L.; Elder, T.; Agarwal, U. P.; Lu, F.; Ralph, J.; Himmel, M. E.; Balan, V.; Dale, B. E., Multi-scale visualization and characterization of lignocellulosic plant cell wall deconstruction during thermochemical pretreatment. *Energy & Environmental Science* **2011,** *4* (3), 973-984.

4.   Jin, M.; da Costa Sousa, L.; Schwartz, C.; He, Y.; Sarks, C.; Gunawan, C.; Balan, V.; Dale, B. E., Toward lower cost cellulosic biofuel production using ammonia based pretreatment technologies. *Green Chemistry* **2016,** *18* (4), 957-966.

5.   da Costa Sousa, L.; Foston, M.; Bokade, V.; Azarpira, A.; Lu, F.; Ragauskas, A. J.; Ralph, J.; Dale, B.; Balan, V., Isolation and characterization of new lignin streams derived from extractive-ammonia (EA) pretreatment. *Green Chemistry* **2016**.

6.   da Costa Sousa, L.; Jin, M.; Chundawat, S. P.; Bokade, V.; Tang, X.; Azarpira, A.; Lu, F.; Avci, U.; Humpula, J.; Uppugundla, N., Next-generation ammonia pretreatment enhances cellulosic biofuel production. *Energy & Environmental Science* **2016,** *9* (4), 1215-1223.

7.   Liu, W.-J.; Jiang, H.; Yu, H.-Q., Thermochemical conversion of lignin to functional materials: a review and future directions. *Green Chemistry* **2015,** *17* (11), 4888-4907.

8.   Zakzeski, J.; Bruijnincx, P. C.; Jongerius, A. L.; Weckhuysen, B. M., The catalytic valorization of lignin for the production of renewable chemicals. *Chemical reviews* **2010,** *110* (6), 3552-3599.

9.   Huber, G. W.; Iborra, S.; Corma, A., Synthesis of transportation fuels from biomass: chemistry, catalysts, and engineering. *Chemical reviews* **2006,** *106* (9), 4044-4098.

10.   Energy, E. E. R., BioEnergy Technologies Office: Multi-Year Program Plan. Energy, U. S. D. o., Ed. 2013.

11.   Holladay, J. E.; White, J. F.; Bozell, J. J.; Johnson, D. *Top Value-Added Chemicals from Biomass-Volume II—Results of Screening for Potential Candidates from Biorefinery Lignin*; Pacific Northwest National Laboratory (PNNL), Richland, WA (US): 2007.

12.   Kleinert, M.; Barth, T., Towards a lignincellulosic biorefinery: direct one-step conversion of lignin to hydrogen-enriched biofuel. *Energy & Fuels* **2008,** *22* (2), 1371-1379.

13.   Collinson, S.; Thielemans, W., The catalytic oxidation of biomass to new materials focusing on starch, cellulose and lignin. *Coordination chemistry reviews* **2010,** *254* (15), 1854-1870.

14.   Harper, D.; Foston, M., Melt-processability of lignin. *Unpublished raw data* **2014**.

15.   Ragauskas, A. J.; Beckham, G. T.; Biddy, M. J.; Chandra, R.; Chen, F.; Davis, M. F.; Davison, B. H.; Dixon, R. A.; Gilna, P.; Keller, M., Lignin valorization: improving lignin processing in the biorefinery. *Science* **2014,** *344* (6185), 1246843.

16.   Vishtal, A. G.; Kraslawski, A., Challenges in industrial applications of technical lignins. *BioResources* **2011,** *6* (3), 3547-3568.

17.   Tomani, P.; Axegård, P.; Berglin, N.; Lovell, A.; Nordgren, D., Integration of lignin removal into a kraft pulp mill and use of lignin as a biofuel. *Cellulose Chemistry and Technology* **2011,** *45* (7), 533.

18.   Klett, A. S., Purification, Fractionation, and Characterization of Lignin from Kraft Black Liquor for Use as a Renewable Biomaterial. **2017**.

19.   Leskinen, T.; Kelley, S. S.; Argyropoulos, D. S., Refining of ethanol biorefinery residues to isolate value added lignins. *ACS Sustainable Chemistry & Engineering* **2015,** *3* (7), 1632-1641.

20.   Zoia, L.; Salanti, A.; Tolppa, E.-L.; Ballabio, D.; Orlandi, M., Valorization of side-streams from a SSF biorefinery plant: Wheat straw lignin purification study. *BioResources* **2017,** *12* (1), 1680-1696.

21.   Uppugundla, N.; da Costa Sousa, L.; Chundawat, S. P.; Yu, X.; Simmons, B.; Singh, S.; Gao, X.; Kumar, R.; Wyman, C. E.; Dale, B. E., A comparative study of ethanol production using dilute acid, ionic liquid and AFEX™ pretreated corn stover. *Biotechnology for biofuels* **2014,** *7* (1), 1.

22.   Guerra, A.; Mendonça, R.; Ferraz, A.; Lu, F.; Ralph, J., Structural characterization of lignin during Pinus taeda wood treatment with Ceriporiopsis subvermispora. *Applied and environmental microbiology* **2004,** *70* (7), 4073-4078.

23.   Holtman, K. M.; Chang, H. m.; Jameel, H.; Kadla, J. F., Quantitative 13C NMR characterization of milled wood lignins isolated by different milling techniques. *Journal of wood chemistry and technology* **2006,** *26* (1), 21-34.

24.   Sluiter, A.; Hames, B.; Ruiz, R.; Scarlata, C.; Sluiter, J.; Templeton, D.; Crocker, D., Determination of structural carbohydrates and lignin in biomass. *Laboratory analytical procedure* **2008,** *1617*, 1-16.

25.   Sluiter, A.; Hames, B.; Ruiz, R.; Scarlata, C.; Sluiter, J.; Templeton, D., Determination of ash in biomass (NREL/TP-510-42622). *National Renewable Energy Laboratory, Golden* **2005**.

26.   Lin, S. Y.; Dence, C. W., *Methods in lignin chemistry*. Springer Science & Business Media: 2012.

27.   Mansfield, S. D.; Kim, H.; Lu, F.; Ralph, J., Whole plant cell wall characterization using solution-state 2D NMR. *Nature protocols* **2012,** *7* (9), 1579.

28.   Pu, Y.; Cao, S.; Ragauskas, A. J., Application of quantitative 31P NMR in biomass lignin and biofuel precursors characterization. *Energy & Environmental Science* **2011,** *4* (9), 3154-3166.

29.   Granata, A.; Argyropoulos, D. S., 2-Chloro-4, 4, 5, 5-tetramethyl-1, 3, 2-dioxaphospholane, a reagent for the accurate determination of the uncondensed and condensed phenolic moieties in lignins. *Journal of Agricultural and Food Chemistry* **1995,** *43* (6), 1538-1544.

30.   Sahoo, S.; Seydibeyoğlu, M.; Mohanty, A.; Misra, M., Characterization of industrial lignins for their utilization in future value added applications. *Biomass and bioenergy* **2011,** *35* (10), 4230-4237.

31.   Pandey, M. P.; Kim, C. S., Lignin depolymerization and conversion: a review of thermochemical methods. *Chemical Engineering & Technology* **2011,** *34* (1), 29-41.

32.   Chen, J.; Lu, F.; Si, X.; Nie, X.; Chen, J.; Lu, R.; Xu, J., High Yield Production of Natural Phenolic Alcohols from Woody Biomass Using a Nickel-Based Catalyst. *ChemSusChem* **2016,** *9* (23), 3353-3360.

33.   Huijgen, W.; Telysheva, G.; Arshanitsa, A.; Gosselink, R.; De Wild, P., Characteristics of wheat straw lignins from ethanol-based organosolv treatment. *Industrial Crops and Products* **2014,** *59*, 85-95.

34.   Pan, X.; Kadla, J. F.; Ehara, K.; Gilkes, N.; Saddler, J. N., Organosolv ethanol lignin from hybrid poplar as a radical scavenger: relationship between lignin structure, extraction conditions, and antioxidant activity. *Journal of agricultural and food chemistry* **2006,** *54* (16), 5806-5813.

35.   Xu, F.; Sun, J.-X.; Sun, R.; Fowler, P.; Baird, M. S., Comparative study of organosolv lignins from wheat straw. *Industrial crops and products* **2006,** *23* (2), 180-193.

36.   Shui, T.; Feng, S.; Yuan, Z.; Kuboki, T.; Xu, C. C., Highly efficient organosolv fractionation of cornstalk into cellulose and lignin in organic acids. *Bioresource technology* **2016,** *218*, 953-961.

37.   Snelders, J.; Dornez, E.; Benjelloun-Mlayah, B.; Huijgen, W. J.; de Wild, P. J.; Gosselink, R. J.; Gerritsma, J.; Courtin, C. M., Biorefining of wheat straw using an acetic and formic acid based organosolv fractionation process. *Bioresource technology* **2014,** *156*, 275-282.

38.   Jiménez, L.; De la Torre, M.; Bonilla, J.; Ferrer, J., Organosolv pulping of wheat straw by use of acetone-water mixtures. *Process Biochemistry* **1998,** *33* (4), 401-408.

39.   Jafari, Y.; Amiri, H.; Karimi, K., Acetone pretreatment for improvement of acetone, butanol, and ethanol production from sweet sorghum bagasse. *Applied Energy* **2016,** *168*, 216-225.

40.   Huijgen, W. J.; Reith, J. H.; den Uil, H., Pretreatment and fractionation of wheat straw by an acetone-based organosolv process. *Industrial & Engineering Chemistry Research* **2010,** *49* (20), 10132-10140.

41.   Bozell, J. J.; Black, S. K.; Myers, M.; Cahill, D.; Miller, W. P.; Park, S., Solvent fractionation of renewable woody feedstocks: Organosolv generation of biorefinery process streams for the production of biobased chemicals. *biomass and bioenergy* **2011,** *35* (10), 4197-4208.

42.   Quesada-Medina, J.; López-Cremades, F. J.; Olivares-Carrillo, P., Organosolv extraction of lignin from hydrolyzed almond shells and application of the δ-value theory. *Bioresource technology* **2010,** *101* (21), 8252-8260.

43.   Wu, S.; Argyropoulos, D., An improved method for isolating lignin in high yield and purity. *Journal of Pulp and Paper Science* **2003,** *29* (7), 235-240.

44.   Luterbacher, J. S.; Rand, J. M.; Alonso, D. M.; Han, J.; Youngquist, J. T.; Maravelias, C. T.; Pfleger, B. F.; Dumesic, J. A., Nonenzymatic sugar production from biomass using biomass-derived γ-valerolactone. *Science* **2014,** *343* (6168), 277-280.

45.   Xue, Z.; Zhao, X.; Sun, R.-C.; Mu, T., Biomass-Derived γ-Valerolactone-Based Solvent Systems for Highly Efficient Dissolution of Various Lignins: Dissolution Behaviour and Mechanism Study. *ACS Sustainable Chemistry & Engineering* **2016**.

46.   Tolbert, A.; Akinosho, H.; Khunsupat, R.; Naskar, A. K.; Ragauskas, A. J., Characterization and analysis of the molecular weight of lignin for biorefining studies. *Biofuels, Bioproducts and Biorefining* **2014,** *8* (6), 836-856.

47.   Balogh, D.; Curvelo, A.; De Groote, R., Solvent effects on organosolv lignin from Pinus caribaea hondurensis. *Holzforschung-International Journal of the Biology, Chemistry, Physics and Technology of Wood* **1992,** *46* (4), 343-348.

48.   Shuai, L.; Amiri, M. T.; Questell-Santiago, Y. M.; Héroguel, F.; Li, Y.; Kim, H.; Meilan, R.; Chapple, C.; Ralph, J.; Luterbacher, J. S., Formaldehyde stabilization facilitates lignin monomer production during biomass depolymerization. *Science* **2016,** *354* (6310), 329-333.

49.   Jääskeläinen, A.-S.; Liitiä, T.; Mikkelson, A.; Tamminen, T., Aqueous organic solvent fractionation as means to improve lignin homogeneity and purity. *Industrial crops and products* **2017,** *103*, 51-58.

50.   Domínguez-Robles, J.; Tamminen, T.; Liitiä, T.; Peresin, M. S.; Rodríguez, A.; Jääskeläinen, A.-S., Aqueous acetone fractionation of kraft, organosolv and soda lignins. *International journal of biological macromolecules* **2018,** *106*, 979-987.

Chapter 3: Understanding Fragmentation and Condensation Reaction Kinetics during Organosolv Extractions

This chapter was adapted from the following manuscript in preparation for publication:

Meyer, James R. et al. "Understanding Fragmentation and Condensation Reaction Kinetics during Organosolv Extractions" (2019)

3.1 Abstract

A current biorefinery approach to lignin valorization relies on a high temperature extraction using organic solvents, or organosolv extraction. However, the extraction severity (i.e., extraction residence time and temperature profile) required to obtain high lignin extraction yields generally results in a lignin that has undergone significant molecular and morphological alteration and that no longer has the desirable properties for further downstream processing into valuable products. To better understand reaction pathways that lead to these undesirable chemical and molecular alterations, organosolv extractions were conducted at increasing extraction temperatures of 150, 180, and 210 °C. Lignin was collected at extraction residence times of 0.25, 1.0, 2.5, 5.5, 12.0, and 25.0 h for each extraction temperature. The collected lignin was analyzed using nuclear magnetic resonance (NMR) techniques which quantitatively determine the concentration of key chemical moieties known to correlate with lignin chain fragmentation and condensation pathways as well as to affect lignin properties. Kinetics of the generation and consumption of key NMR detectable chemical moieties on lignin extracted from poplar biomass during an organosolv extraction with ethanol has been modeled in terms of two reactions in-series. In this model, it is assumed that the concentration of chemical moieties on extracted lignin can be described via a

pseudo first-order reaction that results in the appearance of lignin chemical moieties and then a pseudo first-order reaction that that results in the disappearance of lignin chemical moieties. Arrhenius parameters have been obtained to describe the rate constants of these lignin chemical moiety generation and consumption reactions.

3.2 Introduction

In the previous chapter, an extraction process which upgrades an existing waste stream to produce a more valuable lignin product stream was developed. The downstream process of a previously designed biorefinery was investigate so that the process would be rapidly deployable and a fraction of the valuable lignin could be recuperated; but to truly achieve the full potential lignin can offer to the viability of biorefineries, it must be considered throughout the entire process. Irreparable degradation (i.e., the formation of certain C-C condensed inter-unit linkages) can result from pretreatment processes, lowering the possible downstream uses and thus value. Organosolv extractions are a promising approach to separate lignin from lignocellulosic biomass with minimal drawbacks for downstream upgrading. The process performance is highly dependent on (1) whether an acid catalyst is used, (2) the properties of the organic solvent (e.g., acidity, water content, solubility parameter, and/or polarity)[1-5], and (3) the temperature and time profile of the extraction.[6-7] Generally, organosolv processes have been optimized either as a pretreatment to maximize enzymatic sugar and/or fermentative bio-product yields or as a pulping method to isolate cellulosic substrates and maximize cellulosic substrate yield and quality.[8-10] In most pulping, pretreatment, or fractionation processes, the primary target is cell wall carbohydrates and thus little attention is paid to its effect on the resulting lignin.

In the past, the effect of organosolv extraction conditions on lignin properties has been explored by correlating reaction conditions (e.g., extraction time, extraction temperature, and acid

concentration) with extraction performance (e.g., lignin yield and carbohydrate content), lignin molecular properties (e.g., oxygen content, aromaticity, antioxidant content), or lignin molecular/physical proprieties (e.g., size, thermal stability, degradation temperature).[11-16] While these models provide insights, their correlations are highly dependent on the specific biomass source and reactor setup. Most other lignin extraction kinetic models seek only to describe the apparent rate of soluble lignin generation, which fails to account for the molecular changes that happen to the lignin as a result of secondary reaction pathways occurring during prolonged extraction times (or reactor residence time) in a batch reactor configuration.[17-20] In this study, the kinetics of the generation and consumption of key NMR detectable chemical moieties on extracted lignin as a function of organosolv extraction time and temperature for a hybrid poplar (*populus deltoides* x *trichocarpa*) are deconvoluted. The terminology used to describe lignin extraction in the literature is often treated as exchangeable; however, this makes a precise discussion of the complex phenomena occurring difficult. Therefore, in this study, extraction is refers to the unit operation used to separate lignin from biomass, fractionation is defined as the molecular process of lignin leaving the biomass cell wall matrix, precipitation is defined as the molecular process of lignin precipitating from solvent due to a change in solvent and/or lignin properties; whereas, lignin chain fragmentation is defined as a set of reactions that manifest as the breaking or cleavage of inter-monomer linkages in a lignin molecule and lignin chain condensation is defined as a set of reactions that manifest as the inter- or intra-molecular condensation of a lignin molecule(s). Our goal is to kinetically model the appearance and disappearance of key chemical moieties whose presence or removal is indicative of lignin chain fragmentation and condensation reaction pathways occurring during organosolv extraction.

3.3 Experimental Section

3.3.1 Materials. All chemicals were purchased from Sigma Aldrich (St. Louis, MO) and used as received, except for the deuterated solvents, which were purchased from Cambridge Isotope Laboratories, Inc. (Tewksbury, MS).

3.3.2 Biomass Preparation. The hybrid poplar (*populus deltoides x trichocarpa)* wood chips were received from GreenWood Resources, Inc. (Clatskanie, OR). They were air-dried, milled to 35-45 mesh with a Wiley mill, sieved twice, Soxhlet extracted for 18 h with toluene:ethanol (2:1), Soxhlet extracted ethanol for 18 h, dried, and stored in a freezer until use.

3.3.3 Organosolv Extraction. A set of organosolv extractions was run at three temperatures: 150, 180, and 210 °C. In each set, an extraction was run for each of six durations: 0.25, 1.0, 2.5, 5.5, 12, and 25 h, for a total of 18 extractions. All the extractions were carried out in a 300 mL Parr reactor (Series 4560 Mini Reactor). 50 mL of a 65% aqueous ethanol solution and 5 g of biomass (10 mL:1 g v/w solvent to biomass ratio) was added to a 300 mL Parr glass reactor liner. The reactor was preheated to the extraction temperature for 20 min. The empty hot reactor was opened, the glass liner with the reaction mixture was placed in the reactor, and the reactor was re-sealed and heated to the extraction temperature all within five minutes. By preheating the reactor, the desired reaction temperature was rapidly reached and a more consistent ramp-up time achieved, regardless of the extraction temperature. At the end of the extraction process, the reactor was quenched by flowing cooling water through an internal cooling loop and submerging the reactor in an ice bath. Once the reactor had cooled to 60 °C, it was opened and the extraction mixture was immediately filtered. The filtride was washed twice with 30 mL of 65% aqueous ethanol solution warmed to 75 °C, air dried, and weighed. The dried filtride made up the cellulose-rich residual biomass fraction. The liquid filtrate recovered was washed in a separatory funnel with 25 mL of

```
        ┌──────────┐
        │ Biomass  │
        └──────────┘
              │
              ▼
1)  Organosolv Extraction
2)  Ethanol/Water Washing          ┌──────────────────┐
3)  Filtration          ─────────▶ │ Residual Biomass  │
                                   │      Solids       │
                                   └──────────────────┘
              │
              ▼
        ┌──────────────┐
        │Liquid Filtrate│
        └──────────────┘
              │
              ▼
                                   ┌──────────────────┐
4) Hexane Washing      ─────────▶  │  Hexane Solubles  │
                                   └──────────────────┘
              │
              ▼
5) Solvent Removal                 ┌──────────────────┐
6) Water Wash          ─────────▶  │ Aqueous Solubles  │
                                   └──────────────────┘
              │
              ▼
        ┌──────────┐
        │  Lignin  │
        └──────────┘
```
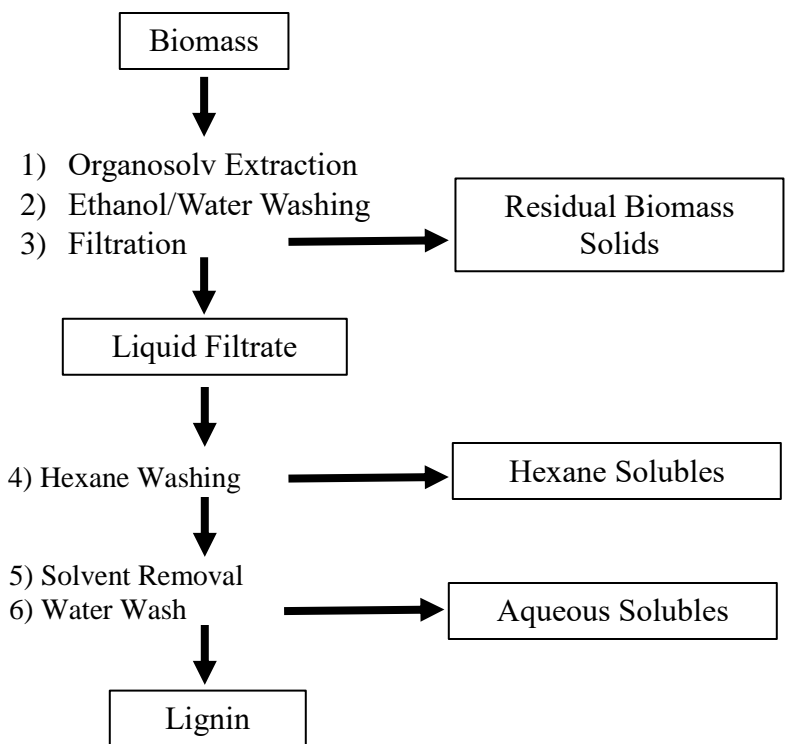
Figure 3-1: Organosolv extraction work-up, highlighting the production of a residual biomass (carbohyrate-rich) solids and lignin.

hexane to remove small hydrophobic molecules. The reaction solvent was removed from the filtrate using rotary evaporation, causing a lignin-rich solid to precipitate. This solid was washed with 50 mL of deionized water to remove aqueous-soluble components from the precipitated lignin. To complete the mass balance, rotary evaporation was again used to remove the water to produce the aqueous soluble fraction.

3.3.4 Gel Permeation Chromatography. To prepare the GPC sample, the lignin was dried at 35 ℃ and 0.1 Torr for 18 h, dissolved in tetrahydrofuran (THF, ~10 mg/ml), and filtered through a 0.45 μm nylon membrane filter. GPC analysis was carried out using a Waters e2695 system with a 2489 ultraviolet detector (260 nm) on a four-column sequence of Waters[TM] Styragel columns (HR0.5, HR1, HR3, and HR5). THF was used as eluent at a flow rate of 1.0 ml/min. A calibration

curve was constructed based on six narrow polystyrene standards and two small molecules (diphenylmethane and toluene), ranging in molecular weight from 3.4×10^4 to 92 g/mol.

3.3.5 ^{31}P-NMR. In preparation for ^{31}P NMR analysis, the lignin samples were dried at 35 ºC at 0.1 Torr for 18 h. Under the protection of argon, ~40 mg of lignin was dissolved in a mixture of anhydrous pyridine and deuterated chloroform (Py/CDCl$_3$, 1.6/1.0, v/v) containing a relaxation agent (chromium (III) acetylacetonate) and an internal standard (N-hydroxy-5-norbornene-2,3-dicarboximide). In a small vial containing a small stir bar, the mixture was stirred for 30 min at room temperature. Then 2-chloro 4,4,5,5-tetramethyl-1,3,2-dioxaphospholane (TMDP) (~200 µL) was added and the mixture was stirred for another 30 min. The reaction mixture was transferred into a 5 mm NMR tube for ^{31}P NMR analysis. Quantitative ^{31}P NMR spectra were collected, using a 500 MHz Varian Unity Inova, at room temperature with a 90° inverse gated decoupling pulse, a 15 s relaxation delay, and 128 scans (for a total experiment time of 32 min) were collected for each spectra. The TMDP hydrolysis product signal (132.2 ppm) was chosen as a reference.

3.3.6 ^{13}C-NMR. In preparation for ^{13}C NMR analysis, the extracted lignin samples were dried at 35 ºC at 0.1 torr for 18 h. About 80-100 mg of the lignin sample was added into a dry NMR tube, followed by ~1.5 mL of DMSO-d_6, which contained ~4 mg/ml of 1,3,5 trioxane as an internal standard and ~3 mg/ml chromium acetylacetonate as a relaxation agent. The samples were covered in foil, vortexed, and allowed to rest to insure complete dissolution. The quantitative ^{13}C NMR spectra were collected at 45 ºC with a z-restored spin-echo sequence and a relaxation delay of 60 seconds on a 600 MHz Varian NMR equipped with a HCN cold probe. A total of 2048 scans were collected for each spectra (for a total experiment time of 34.1 hours). [13]C inversion-recovery experiments were conducted on select samples to ensure the recycle delay was set properly.

3.3.7 Modeling Mass Yield Kinetics. Initially, lignin yield was modeled as described by Vázquez et al.[21] This "reaction-in-series" model utilizes pseudo first-order kinetics to represent each reaction: I, the initial amount of lignin within the biomass. Lignin within the biomass undergoes fractionation to produce F, the portion of lignin that has been fractionated out of the biomass and is soluble in the extraction solvent. As the extraction continues, N, the portion of fractionated lignin that has undergone a secondary reaction pathway (i.e., fragmentation) that produces lower molecular weight molecules or another secondary reaction pathway (i.e., condensation) that produces higher molecular weight molecules that may become so large or molecularly condensed that they precipitate out of the extraction solvent.

$$I \xrightarrow{k_F} F \xrightarrow{k_P} N \tag{1}$$

$$C_F = \frac{C_{Io} * k_F}{k_P - k_F} (e^{-k_F t} - e^{-k_P t}) + C_{Fo} e^{-k_P t} \tag{2}$$

Here, C_F is the concentration of the fractionated lignin, C_{Fo} is the concentration of fractionated lignin at t = 0, k_F is the rate constant of fractionation, k_P is the rate constant of lignin precipitating out of solution, and C_{Io} is the initial concentration of lignin that can be fractionated from biomass. It is important to note that t=0 is when the reactor reaches the extraction temperature. As a result, C_{Fo} is not zero, as some lignin has been extracted during the reactor heating temperature ramp. Equation 2 was fitted to the data with Igor Pro version 6.3.7.2.

3.3.8 Modeling Chemical Kinetics. The modeled described by Vázquez et al.[21] was then extended to chemical functional group or moieties within the fractionated lignin. For this model, A represents NMR observable functional groups or chemical moieties of interest on the fractionated lignin. P represents all the possible functional groups or chemical moieties on lignin within the

cell wall matrix that are able to be converted to A on the fractionated lignin. D represents functional groups or chemical moieties which A is converted into due to molecular changes that occur to fractionated lignin as a result of extraction conditions in a batch reactor configuration.

$$P \xrightarrow{k_A} A \xrightarrow{k_D} D \tag{3}$$

$$C_A = \frac{C_{Po}*k_A}{k_D - k_A}(e^{-k_A t} - e^{-k_D t}) + C_{Ao}e^{-k_D t} \tag{4}$$

Here, C_A is the concentration of a NMR observable functional group or chemical moiety on the fractionated lignin denoted as A, C_{Ao} is the concentration of chemical moiety A in the fractionated lignin at t = 0, k_A is the rate constant for the appearance of A, k_D is the rate constant for the disappearance of A, and C_{Po} is the concentration of all of the different functional groups or chemical moieties on lignin that have the potential of becoming functional group or chemical moiety A on the fractionated lignin at t = 0. Similar to Equation 1, C_{Ao} is not zero, as some lignin has been extracted during the reactor heating temperature ramp , and thus the moiety exist in the fractionated lignin at t=0. The Equation 4 was fitted to the data with Igor Pro version 6.3.7.2.

3.4 Results and Discussion

Organosolv lignin extraction is a very complex set of concurrent and sequential processes that involves (1) mass transfer of extraction media (e.g., organic solvent and water) into the biomass cell wall structure, (2) a complex series of heterogeneous chemical reactions between cell wall polymers and extraction media, and (3) mass transfer of solubilized lignin out of the cell wall via the extraction media.[22]   Once the extraction media is transported to the region of extraction, chemical phenomena occur that facilitate lignin fractionation including carbohydrate depolymerization, fragmentation of lignin, and cleavage of chemical linkages and physical entanglements between lignin and carbohydrates.[23]   Lignin fractionation primarily involves on

solvolytic cleavage of ether and ester bonds (i.e., lignin-carbohydrate complexes, lignin fragmentation via aryl ether inter-monomer linkages, and carbohydrate glycosidic linkages). The solubility of lignin in many of the solvents used in organosolv extraction is relatively low.[24] Generally however, smaller molecular weight polymers tend to have higher solubilities than their high molecular weight counterparts.[25] Thus, the initial fragmentation of lignin not only helps to free lignin from the biomass cell wall matrix but also helps to solubilize lignin.

Lignin fractionation, which requires chemical reactions, represents the minimum modification of lignin (with respect to its native molecular structure) required for soluble lignin to appear. Due to the complexity of biomass and lignin, some lignin molecules in the biomass cell wall will readily fractionate, while others require more time and energy. As a result during organosolv extraction, the solubilized lignin molecules that are easily released and transported from the cell wall matrix at short extraction residence times are subjected to extraction conditions for a significant portion of the total extraction residence time required to achieve high yields. During this period, the population of already fractionated lignin molecules can undergo secondary reaction pathways (i.e., secondary to the chemical reactions required for fractionation). The secondary reaction pathways that can occur to fractionated lignin can be classified as reactions that cause (1) chain fragmentation, (2) intra- or inter-chain condensation, or (3) some other chemical modification not effecting chain topology or molecular weight (Figure 2). Fragmentation reaction pathways of fractionated lignin are generally associated with lignin inter-monomer ether cleavage and molecular weight reduction. In contrast, proposed condensation reaction pathways of fractionated lignin involve the formation of aryl-aryl or aryl-aliphatic C-C linkages.[26-29] Both intra-molecular and inter-molecular condensation reactions can occur, though only inter-molecular

condensation reactions result in increased molecular weight. In some cases, the lignin molecule can become so condensed that it is no longer soluble, precipitating out of the extraction media back onto the biomass and lowering the overall lignin extraction yields.[30]

3.4.1 Lignin Extraction Yield. The mass of lignin, the residual carbohydrate-rich, and the water soluble fraction (as described in Figure 3-1) was reported as a function of extraction time and temperatures in Supplementary Figure II-1. Note that as extraction severity increases, the percent of total mass recovery decreases. This was primarily attributed to the increased formation of a

Soluble Lignin

Condensation

Biomass → **Fractionation** → Lower MW Lignin ⇄ Higher MW Lignin → **Precipitation** → Insoluble Lignin

Fragmentation
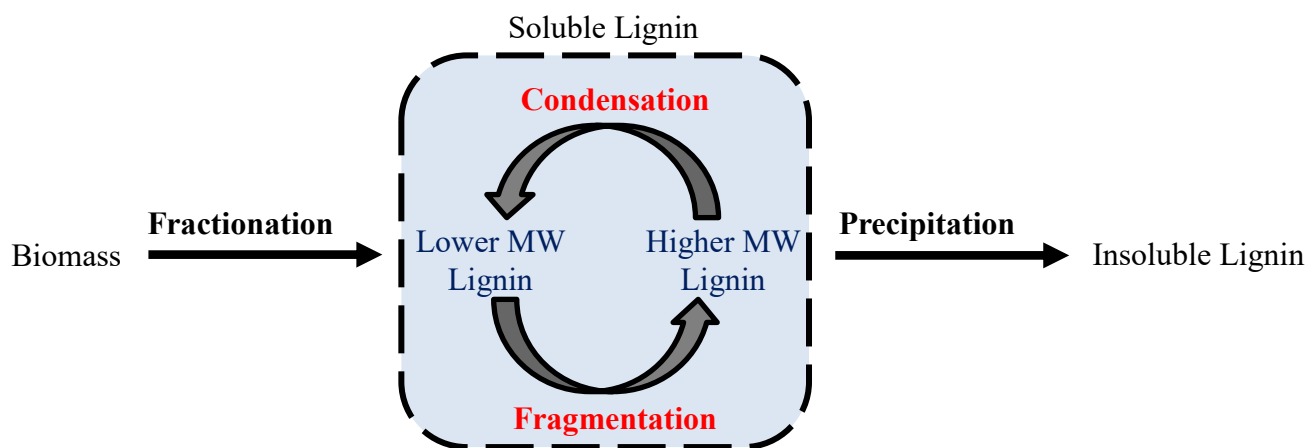
Figure 3-2: A schematic of the processes occurring during organosolv extraction of lignin.

char-like solid that was difficult to remove from the reactor. Overall this data indicates that both the carbohydrates and lignin are susceptible to depolymerization at the reaction condition and furthermore, the depolymerization products are susceptible to further degradation and condensation, resulting in lower yields.

The model developed by Vázquez et al.[21] was fit to the lignin extraction yield data shown in Figure 3-3 while rate constants for lignin fractionation and precipitation are in Table 3-1. For extractions at temperatures of 150, 180, and 210 °C, the rate constants of fractionation are, respectively, 0.37, 0.37, and 1.1 h^{-1}, while the rate constants of precipitation are ~0, 0.01, and 0.02 h^{-1}. As shown in Figure II-2, both lignin fractionation and precipitation seem to have an Arrhenius temperature dependence with activation energies of 39 and 124 kJ/mol, respectively. The observed activation energy for lignin fractionation was similar to the activation energy of delignification reported by Vázquez et al.[21] The analysis of lignin yield as a function of time reveals that the rate

Table 3-1: Rate constants and activation energy of fractionation and precipitation.

| Rate Constants (h^{-1}) | | | | | | E_A(kJ/mol) | |
| 150 °C | | 180 °C | | 210 °C | | | |
k_F	k_P	k_F	k_P	k_F	k_P	Fractionation	Precipitation
0.37	~0	0.37	0.01	1.1	0.02	39	124
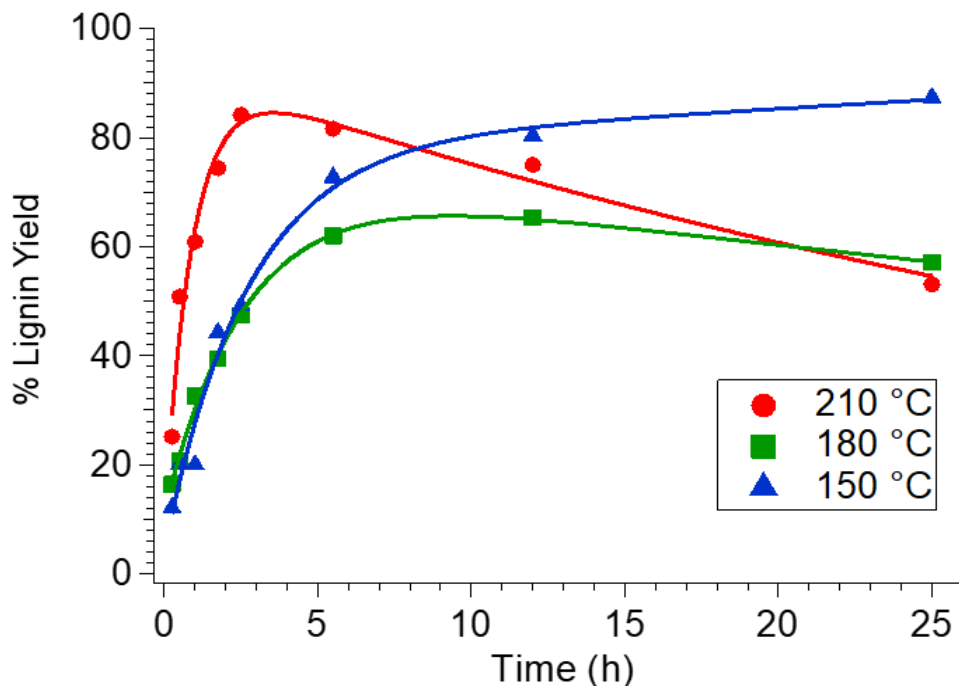
Figure 3-3: Lignin extraction yields (points) from at 150, 180, and 210 °C with fits to the kinetic model (lines) describing the rates of fractionation and precipitation.

of lignin fractionation is at least an order of magnitude larger than the rate of lignin precipitation and that there is a significant energy barrier to lignin precipitation. However, as seen in Figure 3, small rates of lignin precipitation can cause significant decreases in lignin yield at long extraction times.

3.4.2 Lignin Molecular Weight. GPC analysis was used to describe the change in the molecular weight of the fractionated lignin as a function of extraction time, as shown in Figure 4. Fractionated lignin number average molecular weight (M_n), weight average molecular weight (M_w), and dispersity (Đ) based on polystyrene standards are in Table II-1. The two competing secondary reactions pathways, fragmentation and condensation, play an important role in the resulting molecular weight of the lignin. The lignin resulting from the 150°C extraction decreased in molecular weight as extraction time increased, indicating fragmentation reactions dominated over condensation reactions. The average molecular weights of the 180°C extracted lignin initially decreased, then at the longer extraction time, the average molecular weights began to increase. The extraction conducted at 210 °C followed a similar pattern as the 180 °C extraction, initially decreasing in molecular weight, then increasing. These results suggest that condensation reactions require higher temperatures. The combined GPC and lignin yield results suggest that increases in molecular weight, likely due to condensation reactions, are related to lignin precipitation and decreases in lignin yield observed at high temperature and/or long extraction times. An additional observation is the appearance and disappearance of downfield peaks (between 31 and 35 min) that likely represent oligomers with degrees of polymerization less than four. The appearance of these peaks is a result of initial fragmentation reactions and seem to be most prominent in lignin extracted at 150 °C for 5.5 h. The disappearance of these peaks at longer extraction times and
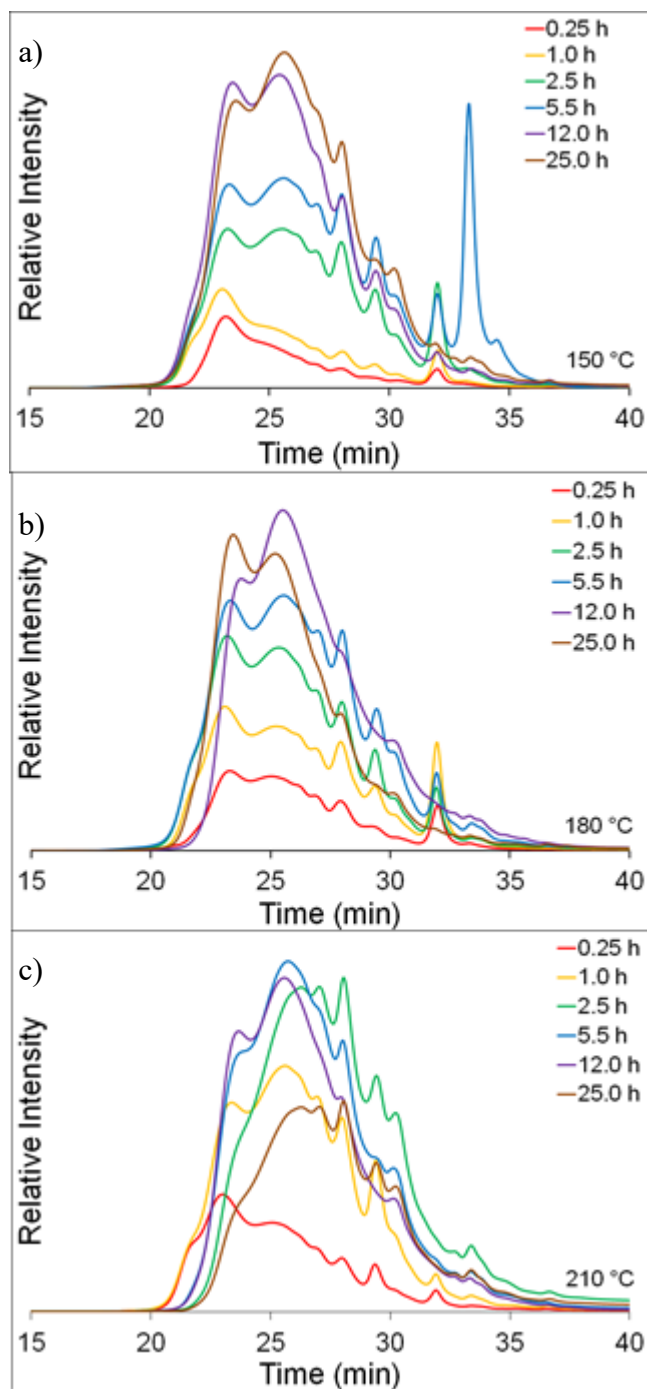
Figure 3-4: The resulting GPC chromatographs of the a) 150, b) 180, and c) 210 °C series lignin. higher extraction temperature indicates that these oligomers are not stable and likely undergone condensation reactions.

3.4.3 Lignin Chemical Moiety Modeling. Quantitative NMR was conducted to quantify a functional group or chemical moiety present within the fractionated lignin as a function of extraction time and temperature. The change in the chemical moiety concentration of the fractionated lignin was then analyzed using a pseudo-first order kinetic model for reactions in-series. It is important to realize the differences between our model and a traditional kinetic modeling approach. First, instead of considering the molarity of a chemical moiety, the concentration of a chemical moiety is expressed in mmol of that chemical moiety present on the recovered (fractionated and still soluble) lignin per gram of that lignin at a given extraction time, (i.e., mmol C or OH of moiety per gram lignin). This concentration will change as a result of (1) lignin fractionation continuously producing lignin molecules with a different chemical composition than previously fractionated lignin molecules, (2) secondary reactions that either generate or consume a chemical moiety, or indirectly concentrating or diluting a chemical moiety by changing the molecular weight, and (3) lignin precipitation that removes lignin molecules of different chemical moiety composition than current observed in solution. Additionally, the initial concentration of chemical moieties will match the chemical moiety concentration in the fractionated lignin molecules that have been initially generated at the start of the extraction ($\lim_{t \to 0} f(t)$ where $f(t)$ is the concentration of a chemical moiety), or in this case, during the time required for the reactor system to reach the desired extraction temperature.

Various hydroxyl or carbon functional groups on lignin can be attributed to phenolic groups at the end of lignin chains, aliphatic hydroxyl groups that are part of inter-monomer sub-structures, and other lignin monomeric or inter-monomer sub-structural moieties. As a result, tracking lignin hydroxyl or carbon functional groups distributions provide unique insight into fragmentation and condensation reactions. The most commonly cited lignin fragmentation reaction mechanism

involves β-aryl ether (β-O-4, Figure 3-5a; containing two aliphatic hydroxyls) linkages cleavage under mildly acidic conditions.[4, 31-33] One proposed route begins with a dehydration reaction which leads to acidolysis and formation of a carbonium ion at the C_α-position of the aliphatic side chain (Figure 3-5b) to generate a Hibbert-type ketone (Figure 3-5d). Though clearly present in the acidolysis reaction of lignin β-O-4 model compounds, in lignin recovered from organosolv extraction ketone are generally not detect in any significant amount.[4, 31-33] Although Miles-Barrett et al.[34] clearly demonstrated with 2D NMR experiments that, depending on the lignin source, both syringyl and guaiacyl moiety lignin-bound Hibbert ketone units could be found in acid-catalyzed organosolv lignin. Loss of lignin-bound Hibbert ketone units have also been explained by equilibration to other isomers via allylic rearrangement. Competing pathways to fragmentation and lignin-bound Hibbert ketone formation involves the (1) release of formaldehyde from the C_γ-position of the aliphatic side chain to form an enol ether-type linkage (Figure 3-5c) or (2) chain condensation with the 5-carbon of a guaiacyl unit to form a phenylcoumaran-type substructure (Figure 3-5g). Note that the formation, as described above, of the lignin-bound Hibbert ketone, phenylcoumaran-type substructure, and enol ether-type linkage results in not only chain cleavage and phenolic end group formation but also the loss, respectively, of one, one, and two aliphatic hydroxyls. Similar to β-aryl ether linkages, non-cyclic α-aryl ether (α-O-4) linkages are easily cleaved and result in a new phenolic end group and loss of an aliphatic hydroxyl; although, their considerably lower prevalence makes non-cyclic α-aryl ether cleavage of limited importance. Cyclic α-aryl ether (β-5 or phenylcoumaran) and dialkyl ether (β-β or resinol) linkages have been shown to be relatively more resistant to degradation at organosolv conditions. However, acidic reactions of based on model compound studies, phenylcoumaran linkages maybe susceptible to minor acidolysis. Though, unlikely to result in chain cleavage, this acidolysis could cause a

reduction in the presence of ether functionality. Lignin condensation reaction mechanisms also involve β-aryl ether linkages, and begins with a dehydration reaction which leads to acidolysis and formation of a carbonium ion at the C_α-position of the aliphatic side chain. In this case, electron-rich positions at the positions ortho or para to methoxyl groups on the aromatic ring of another lignin monomer form stable C-C bonds with carbonium ion at the C_α-position, leading to inter- or intramolecular condensation, the loss of an aliphatic hydroxyl, and formation of an aromatic carbon attached to a carbon.
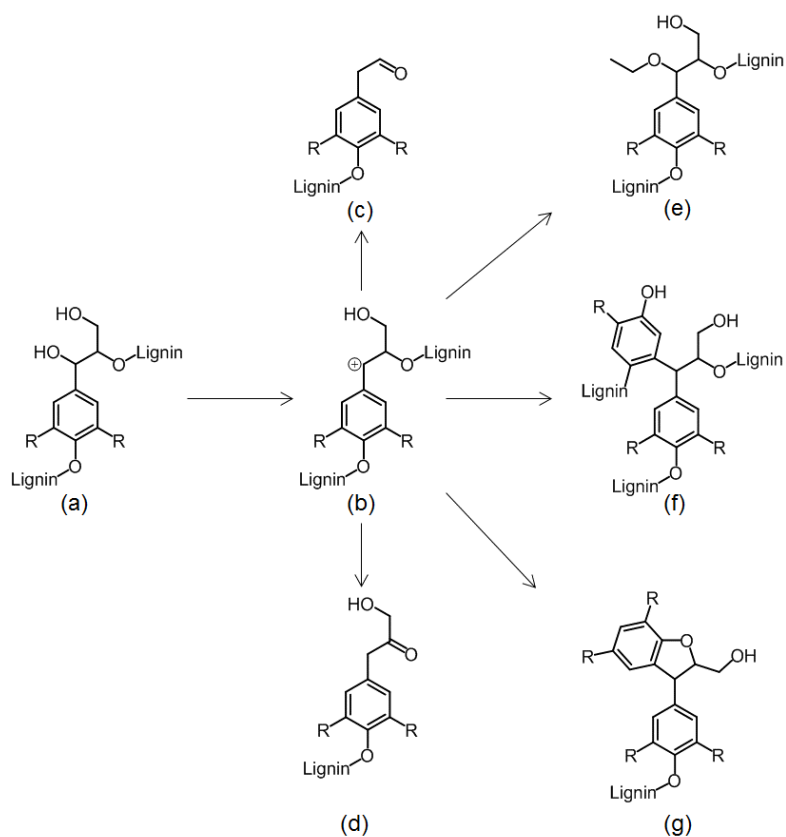
Figure 3-5: Proposed reaction routes mechanism occurring during organosolv reactions

^{31}P NMR on fractionated lignin following phosphorylation with 2–chloro–4,4,5,5–tetramethyl–1,3,2–dioxaphospholane (TMDP) can be used to quantitatively profile the distribution

of hydroxyl and phenolic groups. The ^{31}P NMR analysis focused on the appearance and disappearance of several chemical moieties: (1) aliphatic moieties based on the concentration of hydroxyls attached to aliphatic carbon (150 – 145.4 ppm), (2) terminal guaiacol moieties based on the concentration of phenolics on a guaiacyl ring (140 – 138 ppm); (3) terminal syringol moieties based on the concentration of phenolics on a syringyl ring (144.5 – 142 ppm), (4) terminal C_5-substituated guaiacol moieties, referred to as condensed phenolics, based on the concentration of phenolics on a C_5-substituated guaiacyl ring (142 – 140 ppm), and (5) carboxylic acid moieties based on the concentration of hydroxyls attached to carbonyl carbons (135.5 – 133 ppm). The ^{31}P NMR chemical shift regions for hydroxyl chemical moieties of interest are in Table II-2 and the spectra for all fractionated lignin sample are in Figures II-3 a-c. The concentrations of hydroxyl chemical moieties are plotted against extraction time along with fits to the pseudo first-order kinetic model (Figure 3-6 and Figure II-4). The rate constants for the appearance and disappearance of these hydroxyl chemical moieties are compiled in Table 3-2. Tracking the hydroxyl moieties, insight is gained into the secondary reaction pathways occurring during extraction.
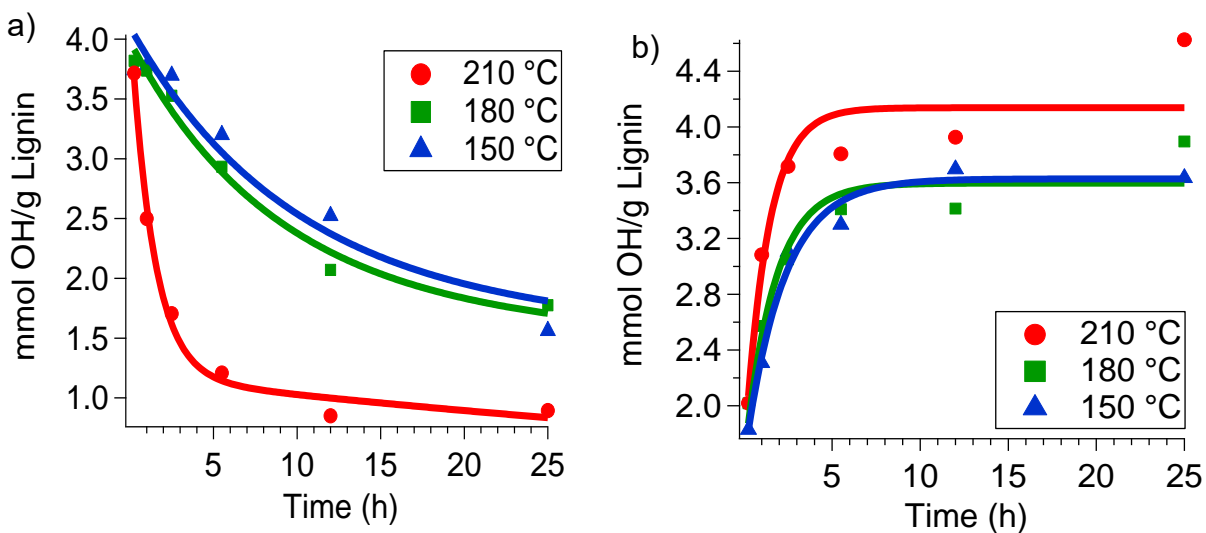
Figure 3-6: Amount of a) aliphatic OH and b) phenolic OH per gram of recovered lignin. Solid lines represent a fit to a pseudo first-order kinetic model.

71

Table 3-2: The rate constants for the chemical moieties derived from ^{31}P NMR.

| Chemical Moiety | Rate Constants(h^{-1}) | | | | | | E_A(kJ/mol) | |
| | 150 °C | | 180 °C | | 210 °C | | | |
	k_A	k_D	k_A	k_D	k_A	k_D	Appearance	Disappearance
Aliphatic	0.0035	0.11	0.0037	0.12	0.013	0.73	35	54
Phenolic	0.45		0.59		0.76		15	
Syringol	0.44		0.45		1.02		24	
Guaiacol	0.40		0.44		0.73		17	
Condensed Phenolic	0.36		0.44		0.9		26	
Carboxylic Acid	0.07		0.19		0.2		29	

Table 3-3: Rate constants for chemical moieties derived from ^{13}C NMR

| | Rate Constants(h^{-1}) | | | | | | E_A(kJ/mol) | |
| | 150 °C | | 180 °C | | 210 °C | | | |
	k_A	k_D	k_A	k_D	k_A	k_D	Appearance	Disappearance
Total Carbon	0.16	--	0.32	--	0.73	--	43	
Total Aromatic	0.20	--	0.32	--	0.63	--	33	
Aromatic C-C	0.22	--	0.48	--	0.97	--	42	
Aromatic C-O	0.21	--	0.32	--	0.63	--	31	
Aromatic C-H	0.20	--	0.24	--	0.52	--	27	
Etherified Aromatic C-O	--	0.21	--	0.26	--	0.76		37
Non Etherified Aromatic C-O	0.19	--	.26	--	.78	--	40	
Aliphatic	0.055	--	0.27	--	0.36	---	52	
O-Aliphatic	--	0.32	--	0.97	--	1.0		32

Syringol and guaiacol moieties have appear at similar rate constants (ca. 0.4 h^{-1}) at lower temperatures (150 and 180°C), but as the extraction temperature increases to 210 °C, syringol's rate constant of appearance increases by a factor of 2.3 while that of the guaiacol rate of appearance increases by only a factor of 1.7. The condensed phenolic rate of appearance is similar to that of the syringol and guaiacol moieties, displaying a comparable increase from lower to higher temperatures. The appearance of condensed phenolic moieties could result from chain cleavage at the 4-position of a lignin unit already containing a 5-5 linkage. However, a more favorable explanation supported by the difference in the rate constant of appearance increases of the syringol and guaiacol, is the condensation of two terminal guaiacol moieties. The observed rate constants of terminal phenolic moieties are the highest, confirming that aryl ether inter-monomer linkage fragmentation is a dominating feature of organosolv processing. In addition to the appearance of phenolic moieties, ^{31}P NMR suggests that carboxylic acids moieties appear as function of extraction time, which can be another product of aliphatic-aryl ether cleavage. The total aliphatic hydroxyl concentration decreases as a function of extraction time. The direct loss of aliphatic hydroxyls from aliphatic-aryl ether inter-monomer linkages can be a result of lignin chain fragmentation causing the resulting lignin to not only have a lower molecular weight but also higher carbon content (via deoxygenation). As the oxygens are removed and the carbon content is increased, the concentration of the remaining carbon-containing chemical moieties increases. Total integration of ^{13}C NMR, as well as the elemental analysis, Table II-5, indicates that the mmol of carbon per gram of lignin increases as a function of extraction severity (i.e., time and temperature). After the aliphatic hydroxyl groups were fit to the model, a rate constant of appearance was derived for the aliphatic hydroxyl, which was attributed to freshly fractionated lignin having a higher

concentration of aliphatic hydroxyls, not to secondary reactions forming new aliphatic hydroxyl moieties.

^{13}C NMR can be used to quantitatively profile the distribution of the key chemical moieties that comprise lignin. An initial assessment of the ^{13}C NMR, seen in Figure II-5 indicates that the organosolv extraction produced a lignin sample without carbohydrates. The ^{13}C NMR analysis focused on the appearance and disappearance of several key chemical moieties: (1) aliphatic moieties, based on the concentration of aliphatic carbons (0 – 28 ppm), (2) O-aliphatic moieties, based on the concentration of aliphatic carbon attached to an alcohol, ester, and/or ether (58 – 90 ppm), (3) aromatic carbon-carbon (C-C) moieties, based on the concentration of aromatic carbons attached to a carbon (124 – 142 ppm), (4) aromatic carbon-oxygen (C-O) moieties, based on the concentration of aromatic carbons attached to an oxygen (142 – 160 ppm), and (5) aromatic carbon-hydrogen (C-H) moieties, based on the concentration of aromatic carbons attached to a hydrogen (102-124 ppm). The ^{13}C NMR integrations for these chemical shift regions are in Table II-3 and the spectra for all fractionated lignin samples are in the Figure II-5. The concentration of the carbon-containing chemical moieties are plotted against extraction time along with fits to the pseudo first-order kinetic model (Figure II-6). The rate constants for the appearance and disappearance of the carbon-containing chemical moieties are compiled in Table 3-3.

The integration of the total carbon spectra with respect to the internal standard and the known amount of lignin dissolved in the NMR sample suggest that the carbon content of the extracted lignin is increasing. This trend was confirmed by total organic carbon analysis on a subset of samples as shown in Table II-4. Sannigruhi et al. and Hallac et al. have proposed β-O-4 scission mechanisms and Chakar et al. has proposed α-O-4 scission mechanisms in which O-aliphatic carbons moieties are consumed.[26, 28, 32] Beyond the deoxygenation, Santos et al.[29], proposed a β-

O-4 scission mechanism in which a hydroxylated γ carbon is lost, resulting in an increase in mmol C/ g lignin as the resulting lignin has a lower hydrogen and oxygen content. The increase in carbon content concentrates both the aliphatic and aromatic chemical moieties within the lignin. Although the increases in concentration are not equal, the aromatic chemical moieties have higher rate constants than the aliphatic, implying that the deoxygenation happens faster than the loss in aliphatic carbon groups and that aromatic groups are relatively stable, thus becoming most quickly concertated in the lignin molecules.

A deeper analysis of the aromatic carbon reveals additional details about the fragmentation and condensation reactions occurring. First, the aromatic C-O moieties have a rate constant very similar to that of the overall aromatic groups. This similarity implies that there are not significant reaction pathways that consume the methoxy groups or phenolic hydroxyl group on the aromatic or produce addition aromatic C-O groups. Although the total aromatic C-O has a similar rate constant to that of the general increase in aromatic carbon, when the region is separated into etherified (148-154 ppm) and non-etherified (145-148 ppm) aromatic C-O moieties, there are significant changes. The rate constant of appearance for non-etherified moieties and the rate constant of disappearance for etherified C-O aromatic moieties are similar, implying the direct conversion of the etherified into the non-etherified. This is in line with the observation that the breaking of aryl ether bonds is a major fragmentation pathway and reaction occurring during organosolv extraction.

Condensation reactions can be tracked by the difference between the rate constants of the aromatic C-C bonds and the aromatic C-H compared to the overall aromatic rate constants. The formation of β-5, 5-5', and to lesser extents, α-6 or β-6, consume aromatic C-H moeities and result in the formation of an aromatic C-C moiety. Although the concentrations of both the aromatic C-

C and aromatic C-H increase from the increase in carbon content, when comparing the rate constants of total aromatic (0.20, 0.32, 0.63 h^{-1}) to the aromatic C-H (0.20, 0.24, 0.52 h^{-1}) and aromatic C-C (0.22, 0.48, 0.97 h^{-1}), it can be seen that at 150 °C, there is little difference in the rate constants, but at the higher temperatures there is a dramatic difference in the rate constants. The aromatic C-H rate constants are lower than the total aromatic and the aromatic C-C is greater than the total aromatic rate constants, implying that aromatic C-C moieties are forming, and aromatic C-H moieties are being consumed, at a greater rate than the concentration effects of losing O-aliphatic or aliphatic moieties. This observation aligns with the yield, GPC, and ^{31}P NMR results that show that the condensation reactions require higher temperatures to occur.

3.5 Conclusions

Kinetic models were successfully developed to describe lignin yield as well as the appearance and disappearance of key chemical moieties of organosolv extracted lignin. As expected, higher temperature extractions had faster rates of lignin fractionation, but they also lost lignin to precipitation, at longer times resulting in lower lignin yields. ^{31}P NMR and ^{13}C NMR provide insights into secondary reaction pathways occurring after fractionation. The fragmentation pathways proceed at all temperatures, whereas condensation reactions require higher temperatures before they proceed at appreciable rates. The elucidation of rate constants for the major chemical moieties allows the processes to be designed not only for lignin yield and molecular weight, but also for desired chemical traits with the downstream use in mind.

3.6 References

1.   Parajo, J. C.; Alonso, J. L.; Santos, V., Kinetics of catalyzed organosolv processing of pine wood. *Industrial & engineering chemistry research* **1995,** *34* (12), 4333-4342.

2.   Bozell, J. J.; Black, S. K.; Myers, M.; Cahill, D.; Miller, W. P.; Park, S., Solvent fractionation of renewable woody feedstocks: Organosolv generation of biorefinery process streams for the production of biobased chemicals. *biomass and bioenergy* **2011,** *35* (10), 4197-4208.

3.   Quesada-Medina, J.; López-Cremades, F. J.; Olivares-Carrillo, P., Organosolv extraction of lignin from hydrolyzed almond shells and application of the δ-value theory. *Bioresource technology* **2010,** *101* (21), 8252-8260.

4.   Bauer, S.; Sorek, H.; Mitchell, V. D.; Ibáñez, A. B.; Wemmer, D. E., Characterization of Miscanthus giganteus lignin isolated by ethanol organosolv process under reflux condition. *Journal of agricultural and food chemistry* **2012,** *60* (33), 8203-8212.

5.   Cybulska, I.; Brudecki, G.; Rosentrater, K.; Julson, J. L.; Lei, H., Comparative study of organosolv lignin extracted from prairie cordgrass, switchgrass and corn stover. *Bioresource technology* **2012,** *118*, 30-36.

6.   Sidiras, D.; Koukios, E., Simulation of acid-catalysed organosolv fractionation of wheat straw. *Bioresource technology* **2004,** *94* (1), 91-98.

7.   Sluiter, A.; Hames, B.; Ruiz, R.; Scarlata, C.; Sluiter, J.; Templeton, D.; Crocker, D., Determination of structural carbohydrates and lignin in biomass. *Laboratory analytical procedure* **2008,** *1617*, 1-16.

8.   Pan, X.; Xie, D.; Gilkes, N.; Gregg, D. J.; Saddler, J. N. In *Strategies to enhance the enzymatic hydrolysis of pretreated softwood with high residual lignin content*, Twenty-Sixth Symposium on Biotechnology for Fuels and Chemicals, Springer: 2005; pp 1069-1079.

9.   Pan, X.; Arato, C.; Gilkes, N.; Gregg, D.; Mabee, W.; Pye, K.; Xiao, Z.; Zhang, X.; Saddler, J., Biorefining of softwoods using ethanol organosolv pulping: preliminary evaluation of process

streams for manufacture of fuel-grade ethanol and co-products. *Biotechnology and bioengineering* **2005,** *90* (4), 473-481.

10.   Goh, C. S.; Tan, H. T.; Lee, K. T.; Brosse, N., Evaluation and optimization of organosolv pretreatment using combined severity factors and response surface methodology. *biomass and bioenergy* **2011,** *35* (9), 4025-4033.

11.   Suryawati, L.; Wilkins, M. R.; Bellmer, D. D.; Huhnke, R. L.; Maness, N. O.; Banat, I. M., Effect of hydrothermolysis process conditions on pretreated switchgrass composition and ethanol yield by SSF with Kluyveromyces marxianus IMB4. *Process Biochemistry* **2009,** *44* (5), 540-545.

12.   El Hage, R.; Brosse, N.; Sannigrahi, P.; Ragauskas, A., Effects of process severity on the chemical structure of Miscanthus ethanol organosolv lignin. *Polymer Degradation and Stability* **2010,** *95* (6), 997-1003.

13.   Pan, X.; Gilkes, N.; Kadla, J.; Pye, K.; Saka, S.; Gregg, D.; Ehara, K.; Xie, D.; Lam, D.; Saddler, J., Bioconversion of hybrid poplar to ethanol and co-products using an organosolv fractionation process: optimization of process yields. *Biotechnology and bioengineering* **2006,** *94* (5), 851-861.

14.   Pan, X.; Kadla, J. F.; Ehara, K.; Gilkes, N.; Saddler, J. N., Organosolv ethanol lignin from hybrid poplar as a radical scavenger: relationship between lignin structure, extraction conditions, and antioxidant activity. *Journal of agricultural and food chemistry* **2006,** *54* (16), 5806-5813.

15.   Lu, Q.; Liu, W.; Yang, L.; Zu, Y.; Zu, B.; Zhu, M.; Zhang, Y.; Zhang, X.; Zhang, R.; Sun, Z., Investigation of the effects of different organosolv pulping methods on antioxidant capacity and extraction efficiency of lignin. *Food Chemistry* **2012,** *131* (1), 313-317.

16.   Watkins, D.; Nuruddin, M.; Hosur, M.; Tcherbi-Narteh, A.; Jeelani, S., Extraction and characterization of lignin from different biomass resources. *Journal of Materials Research and Technology* **2015,** *4* (1), 26-32.

17.   Montané, D.; Salvadó, J.; Farriol, X.; Jollez, P.; Chornet, E., Phenomenological kinetics of wood delignification: application of a time-dependent rate constant and a generalized severity parameter to pulping and correlation of pulp properties. *Wood Science and Technology* **1994,** *28* (6), 387-402.

18.   Shatalov, A. A.; Pereira, H., Kinetics of organosolv delignification of fibre crop Arundo donax L. *Industrial Crops and Products* **2005,** *21* (2), 203-210.

19.   Nguyen, K. L.; Dang, V., The fractal nature of kraft pulping kinetics applied to thin Eucalyptus nitens chips. *Carbohydrate polymers* **2006,** *64* (1), 104-111.

20.   Dang, V. Q.; Nguyen, K. L., A universal kinetic equation for characterising the fractal nature of delignification of lignocellulosic materials. *Cellulose* **2007,** *14* (2), 153-160.

21.   Vázquez, G.; Antorrena, G.; González, J.; Freire, S.; Lopez, S., Acetosolv pulping of pine wood. Kinetic modelling of lignin solubilization and condensation. *Bioresource technology* **1997,** *59* (2-3), 121-127.

22.   Donohoe, B. S.; Decker, S. R.; Tucker, M. P.; Himmel, M. E.; Vinzant, T. B., Visualizing lignin coalescence and migration through maize cell walls following thermochemical pretreatment. *Biotechnol Bioeng* **2008,** *101* (5), 913-925.

23.   Balakshin, M.; Capanema, E.; Gracz, H.; Chang, H.-m.; Jameel, H., Quantification of lignin–carbohydrate linkages with high-resolution NMR spectroscopy. *Planta* **2011,** *233* (6), 1097-1110.

24.   Sameni, J.; Krigstin, S.; Sain, M., Solubility of lignin and acetylated lignin in organic solvents. *BioResources* **2017,** *12* (1), 1548-1565.

25.   Evstigneyev, E. I.; Shevchenko, S. M., Structure, chemical reactivity and solubility of lignin: a fresh look. *Wood Science and Technology* **2019,** *53* (1), 7-47.

26.   Sannigrahi, P.; Ragauskas, A. J.; Miller, S. J., Lignin structural modifications resulting from ethanol organosolv treatment of loblolly pine. *Energy & Fuels* **2009,** *24* (1), 683-689.

27.   Chen, W.-H.; Kuo, P.-C., Isothermal torrefaction kinetics of hemicellulose, cellulose, lignin and xylan using thermogravimetric analysis. *Energy* **2011,** *36* (11), 6451-6460.

28.   Hallac, B. B.; Pu, Y.; Ragauskas, A. J., Chemical transformations of Buddleja davidii lignin during ethanol organosolv pretreatment. *Energy & Fuels* **2010,** *24* (4), 2723-2732.

29.   Santos, R. B.; Hart, P.; Jameel, H.; Chang, H.-m., Wood based lignin reactions important to the biorefinery and pulp and paper industries. *BioResources* **2013,** *8* (1), 1456-1477.

30.   Ye, Y.; Zhang, Y.; Fan, J.; Chang, J., Novel method for production of phenolics by combining lignin extraction with lignin depolymerization in aqueous ethanol. *Industrial & Engineering Chemistry Research* **2011,** *51* (1), 103-110.

31.   Sannigrahi, P.; Ragauskas, A. J.; Tuskan, G. A., Poplar as a feedstock for biofuels: a review of compositional characteristics. *Biofuels, Bioproducts and Biorefining* **2010,** *4* (2), 209-226.

32.   Chakar, F. S.; Ragauskas, A. J., Review of current and future softwood kraft lignin process chemistry. *Industrial Crops and Products* **2004,** *20* (2), 131-141.

33.   McDonough, T. J., The chemistry of organosolv delignification. **1992**.

34.   Miles-Barrett, D. M.; Neal, A. R.; Hand, C.; Montgomery, J. R.; Panovic, I.; Ojo, O. S.; Lancefield, C. S.; Cordes, D. B.; Slawin, A. M.; Lebl, T., The synthesis and analysis of lignin-

bound Hibbert ketone structures in technical lignins. *Organic & biomolecular chemistry* **2016,** *14* (42), 10023-10030.

Chapter 4: Improving the Understanding of Lignin Derived Mixtures with Fourier Transform Ion Cyclotron Resonance High Resolution Mass Spectrometry

4.1 Abstract

Understanding the chemical makeup of extracted lignin and the resulting mixture from lignin upgrading processes is of great importance for downstream uses. The complexity of the original lignin, compounded by the extraction and the upgrading processes, causes difficulty in understanding the final mixture. The combination of electrospray ionization (ESI) and atmospheric pressure photoionization (APPI) Fourier transform ion cyclotronic resonance (FTICR) high resolution mass spectrometry (HRMS) allow a near complete characterization of lignin breakdown product mixtures resulting from catalytic upgrading. Although, even with a clearer picture, thousands of data points are produced and advanced data processing methods are still required to be able to use the data quickly and efficiently.

4.2 Introduction

Previous chapters described extraction and isolation methods for lignin. Unfortunately, there are few direct uses for extracted lignin, thus further upgrading is typically required to produce base chemicals that can be 'dropped in' to current processes for producing higher value chemicals, fuels, or materials. A large range of catalytic systems for upgrading lignin have been explored.[1] Lignin streams are currently depolymerized and upgraded with various approaches: thermal methods (i.e., pyrolysis or gasification),[2-5] solvolytic cleavage,[6] and catalytic oxidative[7-9] or reductive[10-11] fragmentation. Typically, the more selective the process, the lower the yield of

desired product, although, all processes yield a large range of both desired and undesired products.[1, 12-14]

One of the major hurtles in designing effective lignin upgrading processes is accurately understanding the molecular structures and the overall composition of lignin-derived products. Currently, several methods are used to characterize lignin and lignin-derived products. Gel permeation chromatography characterizes the size distribution of the lignin molecules, indicating the progress of the depolymerization processes, but provides no chemical information. Nuclear magnetic resonance (NMR) can give very detailed structural information, but requires a large sample size and gives only averages across a sample. For sufficient sample amounts, NMR techniques are useful in characterizing lignin-derived products. Carbon (^{13}C) NMR can provide quantitative information on the types of chemical moieties and can also provide information on specific inter-unit linkages, using 2D NMR techniques such as ^{1}H-^{13}C heteronuclear single quantum coherence (HSQC). Gas chromatography (GC), typically coupled with mass spectroscopy (MS), is another commonly used technique for analyzing the volatile components of the product mixtures. Unfortunately, many components of the lignin-derived products, which are oligomeric, oxygen-rich, and polar, are not volatile enough to be separated.[15] Additionally, typical mass spectrometers do not have the resolution to separate all the components. Liquid chromatography (LC) is used to overcome the challenge of the lower volatility of many lignin breakdown products, but typically it cannot separate the mixture adequately and takes an impractically long time for a single sample. To better design catalysts and processes to produce high value chemicals, accurately understanding the complex mixture of molecules resulting from upgrading processes are crucial.

Fourier-transform ion cyclotron resonance with high resolution mass spectroscopy (FTICR-HRMS) offers a detailed understanding of lignin breakdown products. A short run time, high sensitivity, high resolution, and the ability to analyze higher molecular weight molecular analytes make FTICR-MS a powerful tool. Although FTICR-HRMS is only semi-quantitative, due to the ionization bias of individual compounds, a more complete picture of the compounds within a lignin-derived mixture can be obtained by utilizing several different ionization methods.[16]

In this study, three sets of lignin depolymerization reaction systems: (1) copper doped porous metal oxide (CuPMO) catalyst in methanol, (2) the same catalytic system with dimethyl carbonate (DMC) as a stabilizer, and (3) methanol solvolysis (MeOH), were used a model system to develop FTICR-HRMS analysis for lignin. Previous studies have used these three systems to analyze the gaseous products.[17-18] In these studies, GC-MS analysis focusing on the production of monomers and volatile products. However, there is a significant portion of the products and intermediates that are not volatile enough to be analyzed by GC-MS, thus requiring additional analysis to obtain the complete picture.

4.3 Methods
4.3.1 Organosolv Extraction: Clean poplar wood chips (600 g) and hydrochloric acid (12 mL) were added to 4.5 L of methanol, then heated to reflux and stirred for 12 days. The resulting mixture was filtered and the solution volume reduced by rotational evaporation. Ice was added to precipitate the lignin. The lignin was collected by filtration, washed with cold water, and then dried under vacuum.

4.3.2 Lignin Depolymerization: Lignin depolymerization reactions were carried out in custom-built bomb reactors comprised of a ¾ inch Swagelok union and two ¾ inch Swagelok plugs, resulting in an internal volume of ~10 mL. The reactors are described in detail in Matson et al.[19]

Three sets of reactions were run: the standard reaction, charged with 100 mg of lignin and 3 mL of methanol; catalyzed reactions, charged the same as the standard with the addition 100 mg of catalyst; and stabilized catalytic reactions, charged the same way as the catalyzed reactions with 3 mL of the mixture of methanol and dimethyl carbonate in a 2:1 ratio. The time-dependent product distribution studies were conducted by adding identical quantities of lignin, catalyst, and solvent to a set of reactors. These reactors were sealed and placed into a pre-heated furnace set to 300 °C, then removed after the given time interval (3, 6, or 9 h) and quenched in an ice water bath.

4.3.3 FT-ICR MS
4.3.3.1 Sample Preparation: Methanol and toluene solvent were LC MS grade and used as received. The samples were diluted 20-fold in 1 mL of methanol. The ESI experiments were carried out without the addition of any dopants. For the APPI experiments, toluene was added as a dopant in a 1 to 9 toluene to sample ratio.

4.3.3.2 Analysis Conditions: The measurements were performed on a Bruker SolariX 15T FT-ICR equipped with an electrospray ionization (ESI) and an atmospheric pressure photoionization (APPI) source, controlled with "FTMS" control software to optimize the different ionization methods and operating parameters. DataAnalysis software (BrukerDaltonik version 4.2) was used for peak picking and a visual data quality check.

ESI FT-ICR MS: Analysis were carried out in both positive and negative ion modes. In negative mode, the voltage at the end plate was 500 V, and the capillary was 2.4 KV. In positive mode, the voltage at the end plate was -500 V, and the capillary was -2.4 KV. The source gas was at 180 °C and held at 0.5 bar pressure. The nebulizer gas flow rate was 4.0 l/min, and the sample was injected with a flow rate of 3.0 uL/min. Ions were accumulated for 0.1 s per scan, with 300 scans summed for the final spectrum, which ranged from *m/z* 100 to 1000, with a resolution of 350K at 381 m/z.

APPI FT-ICR MS: The APPI source was equipped with a UV lamp that emitted 10 eV photons. The voltage at the end plate was 300V and at the capillary was 400V. The source gas was 220 °C and held at 4 bar pressure. The vapor temperature was 400 °C. The nebulizer gas flow rate was 2.0 L/min, and sample was injected at a flow rate of 10.0 uL/min . The ions were accumulated for 0.2 s per scan, with 300 scans summed for the final spectrum. The spectrum ranged from *m/z* 100 to 1000.

4.**3.3.3 Post-acquisition Data Processing**:

DataAnalysis software (BrukerDaltonik version 4.2) was used to convert raw spectra into lists of "m/z" and "abundance" by applying "FTMS" peak picker with the S/N threshold set to 7 and the relative and absolute intensity thresholds set to 0.001 and 100 respectively. The same peak picker parameters were used for all positive and negative mode ESI and APPI spectra. Prior to peak export, spectra were internally calibrated using an interactive function, a list of common contaminant peaks, and lignin library peaks compiled from other sources. Based on the calibration results the, estimated precision for these measurements was 0.3 ppm or better.

Molecular formulas were assigned using the Compound Identification Algorithm (CIA), described by Kujawinski et al[20-22] and implemented in PNNL-produced software Formularity[23]. All identified ions in the spectra were assumed to be singly charged; all CIA searches were performed with a mass error threshold of 0.3 ppm for m/z<500 and with elemental count filters of N<6, S<3, P<2, N*S*P=0. To analyze negative mode spectra, the presence of oxygen was also mandated (O>0). Formulas for m/z>500 were assigned exclusively through a CH_2, H_2, and O connected homologous series. When multiple formulas were matched with the same peak, the formula with the lowest number of heteroatoms, N+S+P, was selected. If multiple formulas shared this number, the formula with lowest mass error was chosen. Other than negative mode ESI

spectra, all other spectra were searched twice, assuming different ion types as summarized in the table below. Results from individual searches were consolidated into a single report using same ambiguity resolution criteria, namely the lowest N+S+P count and mass error. Isotopic peaks for many formulas confirmed by the 1.0034 Da spacing found between peaks assigned to $^{12}C_n$ and $^{12}C_{n-1}^{13}C$, were removed from final reports.

Ionization	Mode	Ions
ESI	Negative	[M-H]$^-$
ESI	Positive	[M+H]$^+$, [M+Na]$^+$
APPI	Negative	[M-H]$^-$, M*$^-$
APPI	Positive	[M+H]$^+$, M*$^+$

4.3.4 Elemental Analysis: The CNS elemental analysis was carried out using a standard protocol on a VarioEL Cube Elemental Analyzer (Elementar Analysensysteme GmbH, Langenselbold Germany). Helium carrier gas was flowed at 240 mL/min at 1150 mBar, dosed with oxygen for 210 second at a rate of 37 mL/min. The combustion was done at 1150 °C packed with granular tungsten trioxide and the reduction tube filled with copper wire (4 mm x 0.5 mm) at 850 °C. Nitrogen and carbon where detected by thermal conductivity detector, and sulfur was detected by an infrared detector.

4.4 Results

Several studies have explored the ionization bias of the various techniques and compounds. By using both (±) ESI and (±) APPI ionization to analyze the breakdown mixtures, a more complete picture of the resulting compounds is obtained. In this work, an initial analysis determined the number of peaks and the amount of the total ion current (TIC) that could be assigned to a particular chemical formula, as well as which ionization methods could ionize the

Table 4-1: Number of peaks assigned a molecular formula and the percent of TIC comprised of masses assigned a chemical formula.

		APPI_NEG		APPI_POS		ESI_NEG		ESI_POS	
		# of peaks	TIC	# of peaks	TIC	# of peaks	TIC	# of peaks	TIC
Untr-Lignin	Unassigned	601	22%	454	7%	1390	28%	306	9%
	Assigned	2471	78%	2725	93%	1152	72%	580	91%
CuPMO 9h	Unassigned	233	3%	723	2%	2296	26%	1596	36%
	Assigned	2633	97%	5944	98%	1517	74%	2082	64%
CuPMO 6h	Unassigned	436	4%	734	2%	2383	28%	1539	44%
	Assigned	3189	96%	6166	98%	1331	72%	1559	56%
CuPMO 3h	Unassigned	197	4%	589	2%	1227	17%	1223	23%
	Assigned	2278	96%	5566	98%	2189	83%	1946	77%
DMC 9h	Unassigned	590	4%	1641	7%	1081	14%	2101	36%
	Assigned	3757	96%	4531	93%	2464	86%	1915	64%
DMC 6h	Unassigned	551	4%	1486	6%	1430	12%	2018	37%
	Assigned	4030	96%	5100	94%	2233	88%	1977	63%
DMC 3h	Unassigned	764	5%	1609	7%	842	13%	1848	29%
	Assigned	4156	95%	4542	93%	2456	87%	1970	71%
MeOH 9h	Unassigned	912	6%	897	4%	818	22%	1040	19%
	Assigned	3471	94%	4332	96%	2511	78%	2454	81%
MeOH 6h	Unassigned	933	7%	943	5%	783	26%	987	21%
	Assigned	3467	93%	4264	95%	2549	74%	2349	79%
MeOH 3h	Unassigned	910	8%	1005	5%	1185	34%	555	13%
	Assigned	3160	92%	4208	95%	1967	66%	1995	87%

chemical. Table 4-1 displays the number of individual peaks, as well as the percent of the TIC that is unassigned and assigned a chemical formula and Figure 4-1 is a Venn diagram displaying the overlap of compounds detected by each ionization technique.

(±) APPI ionization averages over 80% of the individual masses being assigned a chemical formula per sample, and (±) ESI averages only 60% assignments per sample. However, over 90% of the (±) APPI TIC is assigned, and over 75% of (±) ESI TIC is assigned a molecular formula. For organosolv lignin catalytic breakdown products, (±) APPI ionization produces overall larger mass counts and total ion current (TIC), as well as chemical formula assignments, than (±) ESI ionization. Only ~10% of the identified compounds were detected by all of the ionization methods, whereas ~70% of the compounds were detected by only a single ionization method, confirming

that multiple ionization techniques are required for a complete picture of the chemical profile of the lignin breakdown products.
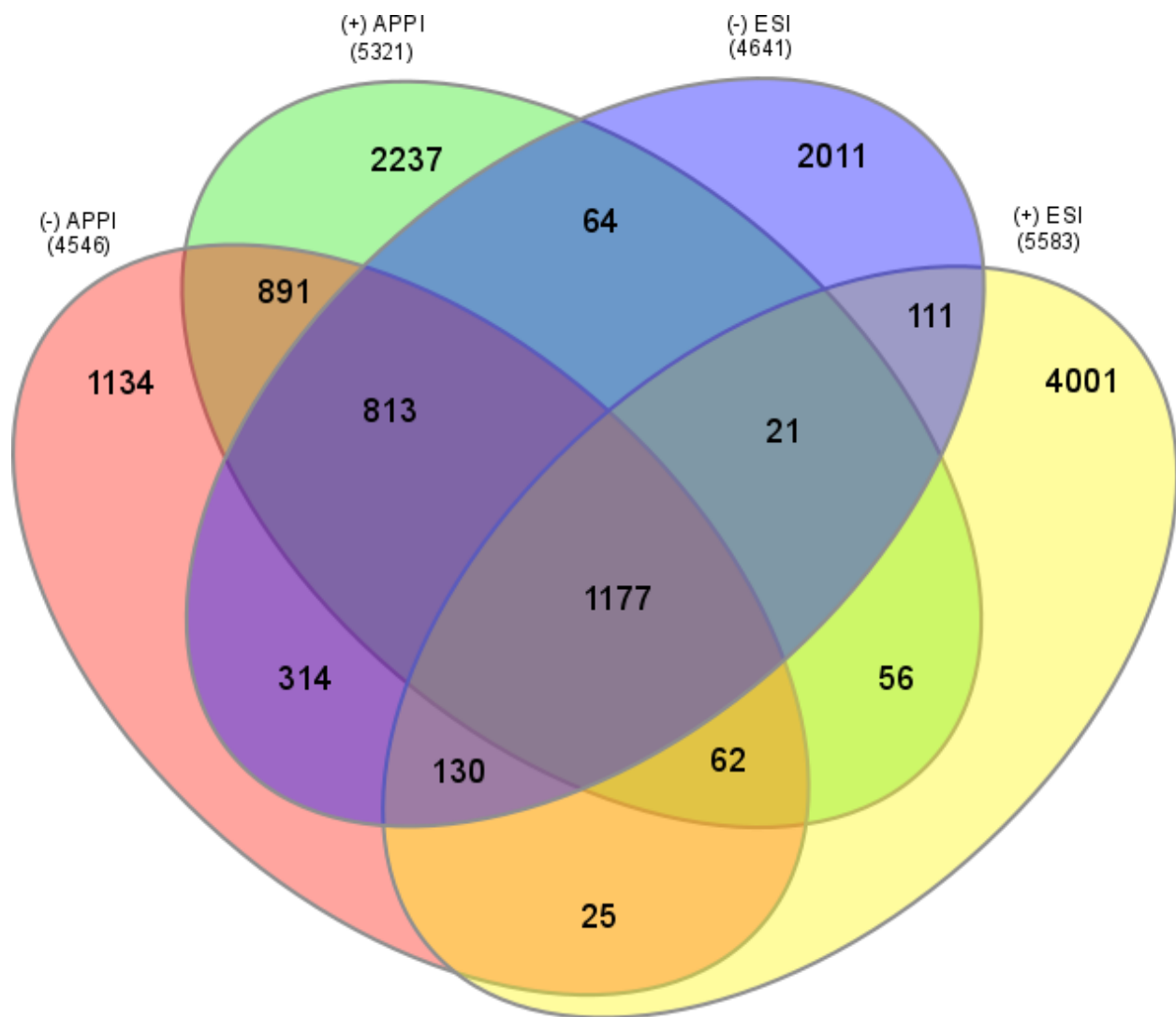

Figure 4-1 Venn diagram of the unique chemical structures detected by each ionization method. The areas are not to scale.

A closer look at the masses assigned a chemical formula is required to understand the chemical bias of the ionization methods. The majority of the chemicals, both in terms of number and TIC are comprised of C, H, and O. Non-oxygenated aliphatic (i.e., C and H) containing compounds were only detected by positive ionization methods, particularly (+) APPI. Nitrogen-containing compounds were favorably ionized by positive modes and by ESI. (+) ESI in particular

has a strong bias towards nitrogen containing compounds, and over 50% of the compounds detected by (+) ESI in some samples were nitrogen containing compounds. Sulfur followed a similar pattern, being favorably ionized by positive modes and ESI. (+) ESI had the largest portion, 36%, of assignments containing sulfur. Phosphorous was the opposite, being favored by negative modes and APPI ionization, (-) APPI had the largest portion, 4%, of assignments containing phosphorous. The heteroatom (nitrogen, sulfur, and phosphorous) chemical count distributions are tables III-1, III-2, and III-3. Elemental analysis to determine the carbon, nitrogen, sulfur content was also performed to understand the overall chemical makeup of the lignin breakdown product mixture, Table III-4. Both nitrogen and sulfur made up less than 0.1 wt% of the samples, and this small amount confirms that ionization bias occurred. The low overall mass count and TIC of (+) ESI, coupled with the disproportionate amount of nitrogen and sulfur containing compounds,
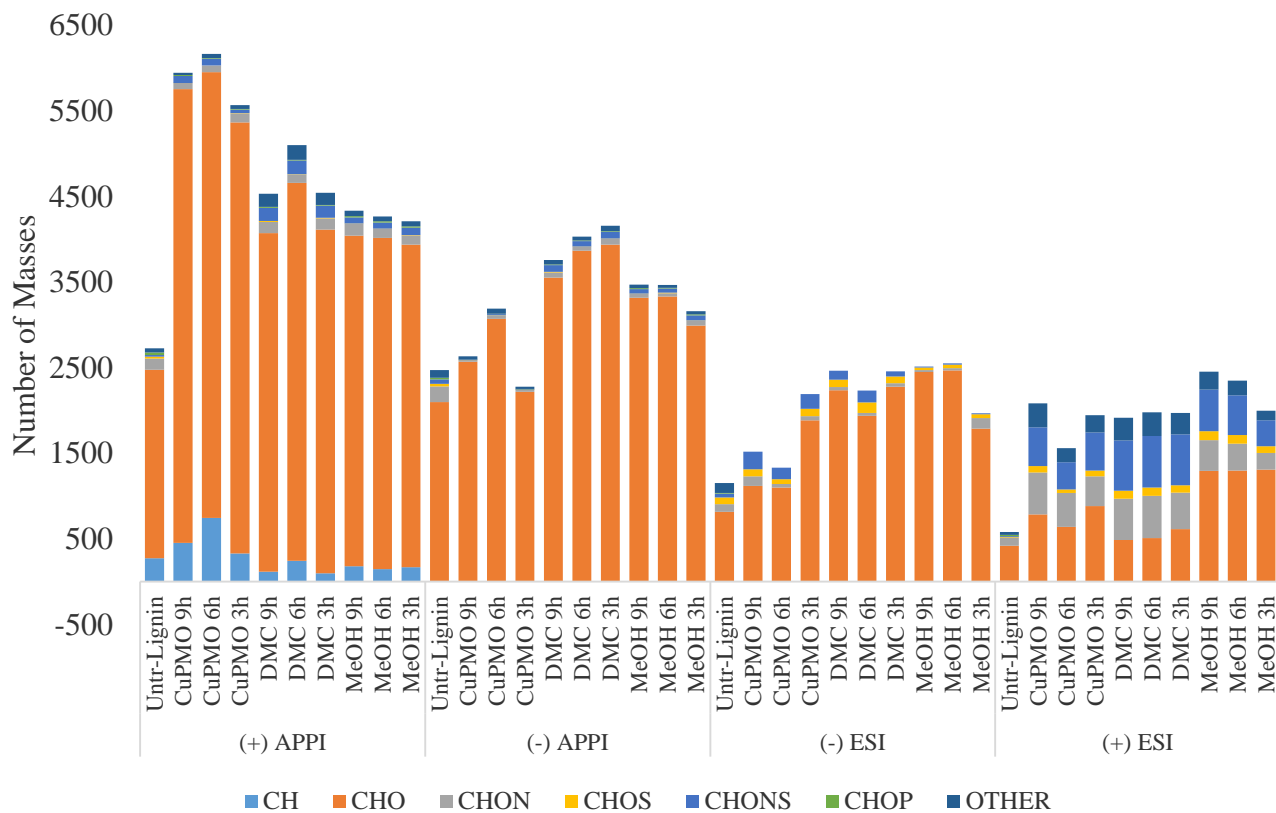

Figure 4-2: Number of unique masses assigned a chemical formula, by chemical class per ionization method and sample

90

proves the extreme ionization bias that can occur for lignin breakdown products. It is important to remember that each ionization method has a bias.

The molecular weight was calculated to insure that there isn't weight based bias in the ionization methods. The molecular weight distribution calculated from FTICR-HRMS is more accurate than the GPC. GPC relies on correlating a standard, typically polystyrene, and its interaction with chromographic columns to the lignin breakdown products and its interaction with the columns. The interactions are typically not exactly the same, and furthermore, the interaction between the columns and the difference types of lignin breakdown products is rarely the same. By using the exact masses of the FTICR-HRMS gives a more precise distribution. The average number molecular weight (Mn), average weight molecular weight (Mw), and dispersity (Đ) were calculated for each of the samples' spectra produced by the four ionization methods, considering both the unique masses and the TIC (Table III-5). The molecular weight is crucial to understanding the reactions occurring, e.g., fragmentation or condensation, as well as the physiomechanical characteristics of the breakdown products. A quick check of the Mn and Mw indicates that the ionization methods do not favor either higher or lower molecular weights. The Mn, Mw, and Đ based on the numbers indicates the increase or decrease in diversity of chemicals present. The Mn, Mw, and Đ based on the TIC indicates the most prevalent reaction pathways, i.e., whether fragmentation or condensation dominate.

The amount of data produced by a single FTIRC-HRMS can be thousands of chemical species (data points), and since at least four different runs are need to accurately characterize a single mixture, advanced analytical methods are needed to understand and track a series of reaction conditions. A slew of analyses have been developed based on FTICR spectra of crude oils and to a lesser extent, refined petrelum, named 'petroleomics', which consists of a series of

visualizations and analyses, (e.g., Van Kreveleen, DBE vs #C, oxygen distributions, and Kendrick Mass Defect) . These methods are very useful to characterize crude oils or coal, but can be labor intensive to understand the nuanced difference when trying to follow reactions.

Additional studies have been done to adopt the petroleomic techniques from oil to biomass applications.   Herein, petroleomics are adopted in a meaningful way to succinctly characterize lignin breakdown products from three different upgrading systems.

The adaption of petroleomics was performed on the signal from $C_xH_yO_z$ (x=3-72, y=1-140, z=0-25) which accounts for most of the signal, both in terms of molecular formula count and TIC. The first technique used were Van Kreveleen plots. Van Kreveleen plots were originally designed to measure the maturity of coal by plotting the amount of hydrogen per carbon versus oxygen per carbon, and were later adopted to petroleum and now lignin. Both deoxygenation and
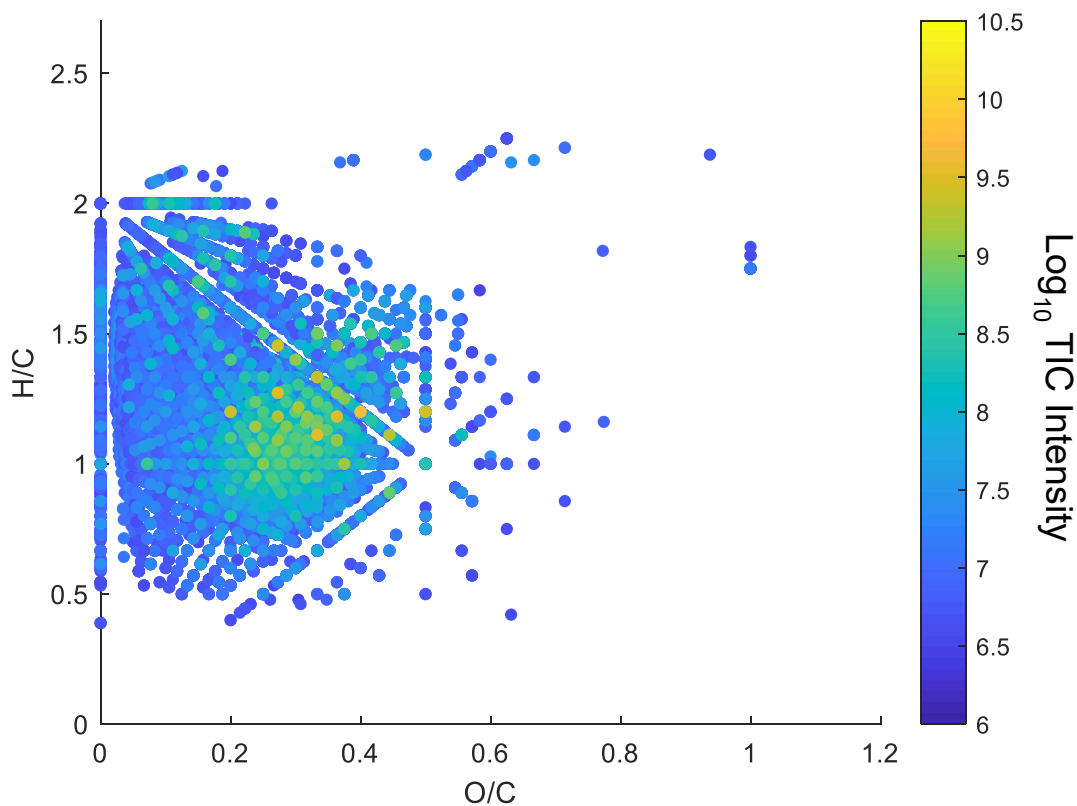

Figure 4-3:Example of Van Kreveleen plots, (+) APPI CuPMO 3h

hydrogenation are a major lignin upgrading pathways that can be tracked with the Van Kreveleen plots. An example of Van Kreveleen plot is shown in Figure 4-3 and all of the plots are in Appendix III. The amount of data is quickly too large to be easily and rapidly analyzed to monitor a reaction system. In this work, we utilize the Van Kreveleen data to calculate the center point, i.e., point (average of the O/C, average of the H/C), and spread, i.e., point(one standard deviation in the O/C, one standard deviation in the H/C), of both the number count and weighted by TIC. Similar single point Van Kreveleen plots have been generated by elemental analysis, but these plots are unable to provide the spread data, as with FTIRC-MS. This additional information is crucial to following the reaction direction. By plotting this data, it is rapidly apparent the difference between the samples and the extent of reaction. Shown here the (+) APPI center point and spread plots as an example, the other ionization techniques are in Appendix III.

All of the characterizations techniques are used to analyze our test system, three time series with only methanol as a control (MeOH), with a copper porous metal oxide catalyst (CuPMO), and finally the catalyst with the addition of a reactive co-solvent DMC (DMC). The location of the center points largely varies based on the ionization efficiency, but distinct trends do appear. First, the MeOH series has the lowest H/C ratios. This confirms that without the catalyst, little hydrogen is produced, and the hydrogenation reaction pathway is minimal. Additionally, the CuPMO series typically had the lowest O/C ratio, with the aboundance of hydrogen and without the stabilizing DMC, an additional deoxygenation reaction pathway was present. The spread plots gave additional insight into the reactions occurring. First, the untreated lignin always had the highest spread in both the H/C and O/C directions, proving that all the upgrading processes did, to some degree, narrow the product distribution. Additionally, the DMC, series typically had the
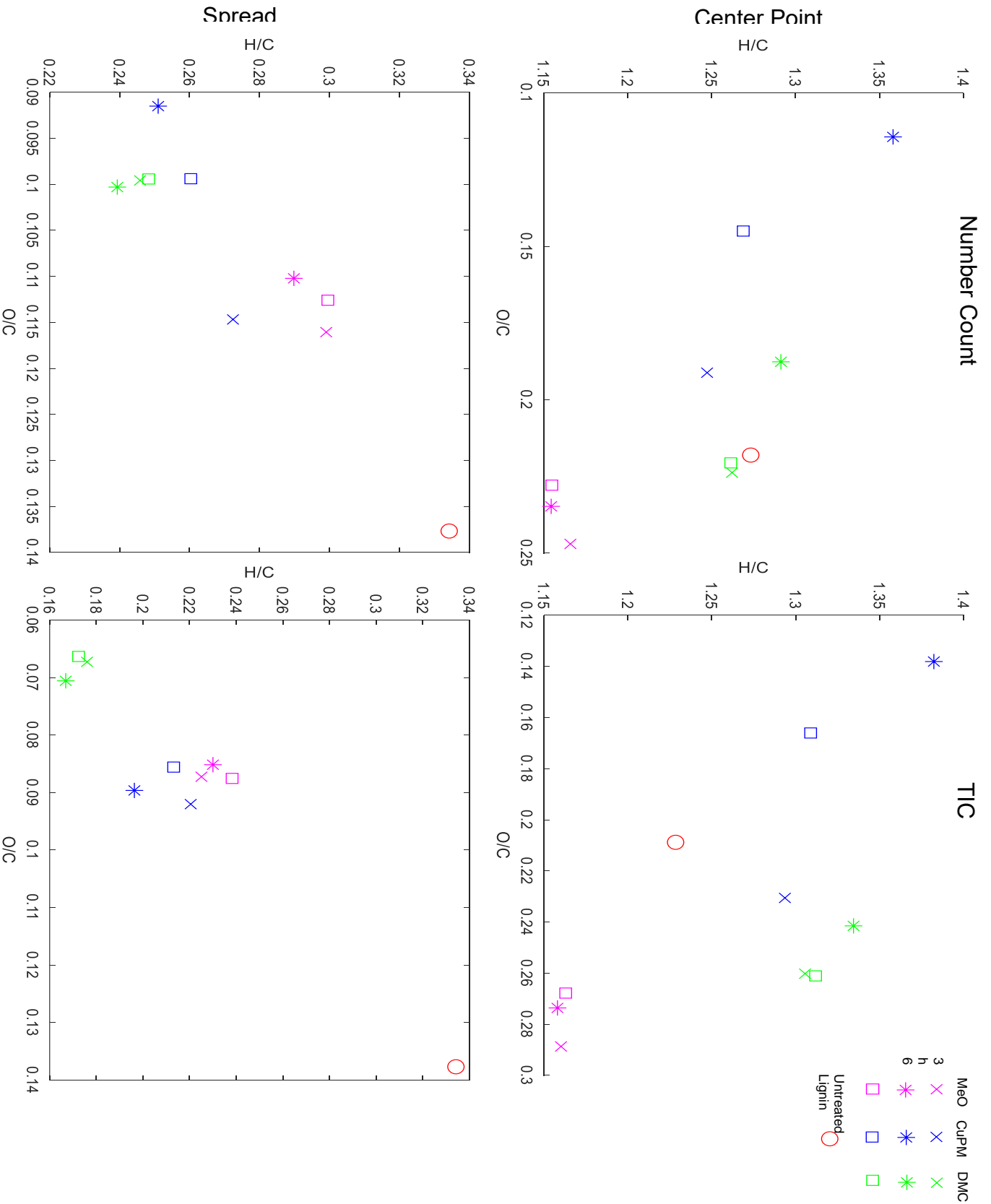
93

Figure 4-4: Example of the center point and spread plots for both mass count and TIC. (+) APPI is used as the example

lowest spread in both the H/C and O?C. This 94 indicates that the co-solvent does prevent some

secondary reactions thus producing a more narrow chemical distribution.

4.5 Conclusion:

It was demonstrated a rapid technique to characterize the chemical makeup of lignin breakdown products. (+) APPI is a preferred ionization technique for lignin breakdown products do to its ability to ionize both aliphatic and oxygenated hydrocarbons. We also proven that CuPMO with DMC as a reactive co-solvent produces a narrower product distribution which is beneficial to downstream separations. This work will help design the next generation of catalyst and upgrading processes, moving towards an economically viable biorefinery.

4.6 Refences

1.   Schutyser, W.; Renders, T.; Van den Bosch, S.; Koelewijn, S.-F.; Beckham, G. T.; Sels, B. F., Chemicals from lignin: an interplay of lignocellulose fractionation, depolymerisation, and upgrading. *Chemical Society Reviews* **2018,** *47* (3), 852-908.

2.   Fan, L.; Zhang, Y.; Liu, S.; Zhou, N.; Chen, P.; Cheng, Y.; Addy, M.; Lu, Q.; Omar, M. M.; Liu, Y., Bio-oil from fast pyrolysis of lignin: Effects of process and upgrading parameters. *Bioresource technology* **2017,** *241*, 1118-1126.

3.   Molino, A.; Larocca, V.; Valerio, V.; Rimauro, J.; Marino, T.; Casella, P.; Cerbone, A.; Arcieri, G.; Viola, E., Supercritical water gasification of lignin solution produced by steam explosion process on Arundo Donax after alkaline extraction. *Fuel* **2018,** *221*, 513-517.

4.   Brebu, M.; Vasile, C., Thermal degradation of lignin—a review. *Cellulose Chemistry & Technology* **2010,** *44* (9), 353.

5.   Christensen, E.; Evans, R. J.; Carpenter, D., High-resolution mass spectrometric analysis of biomass pyrolysis vapors. *Journal of analytical and applied pyrolysis* **2017,** *124*, 327-334.

6.   Jensen, A.; Nielsen, J. B.; Jensen, A. D.; Felby, C., Thermal and Solvolytic Depolymerization Approaches for Lignin Depolymerization and Upgrading. *Lignin Valorization: Emerging Approaches* **2018,** *19*, 74.

7.   Vangeel, T.; Schutyser, W.; Renders, T.; Sels, B. F., Perspective on Lignin Oxidation: Advances, Challenges, and Future Directions. *Topics in Current Chemistry* **2018,** *376* (4), 30.

8.   Lange, H.; Decina, S.; Crestini, C., Oxidative upgrade of lignin–Recent routes reviewed. *European polymer journal* **2013,** *49* (6), 1151-1173.

9.   Springer, S. D.; He, J.; Chui, M.; Little, R. D.; Foston, M.; Butler, A., Peroxidative oxidation of lignin and a lignin model compound by a manganese SALEN derivative. *ACS Sustainable Chemistry & Engineering* **2016,** *4* (6), 3212-3219.

10.   Huang, X.; Korányi, T. I.; Boot, M. D.; Hensen, E. J., Catalytic depolymerization of lignin in supercritical ethanol. *ChemSusChem* **2014,** *7* (8), 2276-2288.

11.   Espro, C.; Gumina, B.; Szumelda, T.; Paone, E.; Mauriello, F., Catalytic transfer hydrogenolysis as an effective tool for the reductive upgrading of cellulose, hemicellulose, lignin, and their derived molecules. *Catalysts* **2018,** *8* (8), 313.

12.   Tuck, C. O.; Pérez, E.; Horváth, I. T.; Sheldon, R. A.; Poliakoff, M., Valorization of biomass: deriving more value from waste. *Science* **2012,** *337* (6095), 695-699.

13.   Esposito, D.; Antonietti, M., Redefining biorefinery: the search for unconventional building blocks for materials. *Chemical Society Reviews* **2015,** *44* (16), 5821-5835.

14.   Li, C.; Zhao, X.; Wang, A.; Huber, G. W.; Zhang, T., Catalytic transformation of lignin for the production of chemicals and fuels. *Chemical reviews* **2015,** *115* (21), 11559-11624.

15.   Panda, S. K.; Andersson, J. T.; Schrader, W., Mass-spectrometric analysis of complex volatile and nonvolatile crude oil components: a challenge. *Analytical and bioanalytical chemistry* **2007,** *389* (5), 1329-1339.

16.   Hertzog, J.; Carré, V.; Jia, L.; Mackay, C. L.; Pinard, L.; Dufour, A.; Mašek, O. e.; Aubriet, F. d. r., Catalytic Fast Pyrolysis of Biomass over Microporous and Hierarchical Zeolites: Characterization of Heavy Products. *ACS Sustainable Chemistry & Engineering* **2018,** *6* (4), 4717-4728.

17.   Gao, Y.; Walker, M. J.; Barrett, J. A.; Hosseinaei, O.; Harper, D. P.; Ford, P. C.; Williams, B. J.; Foston, M. B., Analysis of gas chromatography/mass spectrometry data for catalytic lignin depolymerization using positive matrix factorization. *Green Chemistry* **2018,** *20* (18), 4366-4377.

18.   Barrett, J. A.; Gao, Y.; Bernt, C. M.; Chui, M.; Tran, A. T.; Foston, M. B.; Ford, P. C., Enhancing aromatic production from reductive lignin disassembly: in situ O-methylation of phenolic intermediates. *ACS Sustainable Chemistry & Engineering* **2016,** *4* (12), 6877-6886.

19.   Matson, T. D.; Barta, K.; Iretskii, A. V.; Ford, P. C., One-pot catalytic conversion of cellulose and of woody biomass solids to liquid fuels. *Journal of the American Chemical Society* **2011,** *133* (35), 14090-14097.

20.   Kujawinski, E. B.; Behn, M. D., Automated Analysis of Electrospray Ionization Fourier Transform Ion Cyclotron Resonance Mass Spectra of Natural Organic Matter. *Analytical Chemistry* **2006,** *78* (13), 4363-4373.

21.   Kujawinski, E. B.; Longnecker, K.; Blough, N. V.; Del Vecchio, R.; Finlay, L.; Kitner, J. B.; Giovannoni, S. J., Identification of possible source markers in marine dissolved organic matter using ultrahigh resolution mass spectrometry. *Geochimica et Cosmochimica Acta* **2009,** *73* (15), 4384-4399.

22.   Minor, E. C.; Steinbring, C. J.; Longnecker, K.; Kujawinski, E. B., Characterization of dissolved organic matter in Lake Superior and its watershed using ultrahigh resolution mass spectrometry. *Organic Geochemistry* **2012,** *43* (0), 1-11.

23.   Tolić, N.; Liu, Y.; Liyu, A.; Shen, Y.; Tfaily, M. M.; Kujawinski, E. B.; Longnecker, K.; Kuo, L.-J.; Robinson, E. W.; Paša-Tolić, L., Formularity: software for automated formula assignment of natural and other organic matter from ultrahigh-resolution mass spectra. *Analytical chemistry* **2017,** *89* (23), 12659-12665.

Chapter 5 Conclusions and Future Studies

5.1 Conclusions:

In a series of three studies, this dissertation explored methods to better utilize lignin in biorefineries and improve their overall economic viability. In the initial study, a lignin waste stream from a current AFEX biorefinery was extracted with various solvent systems to produce value added lignin streams. Both an ethanol and water and an acetone and water solvent system produced a high yield of carbohydrate-free, minimally altered lignin. By using a conventional waste stream, the new methods can be deployed quicker and at lower cost. In a second study, to achieve the ultimate goal of producing designer lignin, the reactions underlying organosolv extraction were explored and the rate constants for the appearance and disappearance of key chemical moieties found. An improved understanding of the fractionation and condensation reactions allows extraction processes to be designed to produce lignin streams with desired lignin structures and characteristics. Even the designer lignin streams require catalytic upgrading to produce more valuable mixtures of fine chemicals. Finally, to help guide the synthesis of novel catalytic systems, the third study focused on rapidly and accurately characterizing the complex mixture that results from catalytic upgrading. The combined results of the research presented in this dissertation can advance the economic competitiveness of biorefined lignin and increase its potential to eventually replace fossil resources.

5.2 Future Studies

5.2.1 Continuing Studies

Chapter 2 explored the use of various organic solvent systems to extract lignin from a current waste stream. Further investigation should be conducted into the chemical structure of lignin extracted by non-polar solvents. The highly non-polar solvents had lower yields, but were

99

highly selective for lignin. So even at ~3% mass yield, there is still the potential to produce around 10 thousand tons of high value products based on the DOE projection, if the lignin extracted by the non-polar solvent systems favored high value structures. Additionally, studies on extracting lignin from other pretreatments should also be conducted to determine how well the results extend to other systems. While similar trends are expected, every pretreatment alters the lignin structure differently and thus the solubility of the lignin will be different.

Chapter 3 quantified the apparent reaction rate constants of key chemical moieties for organosolv extractions. Additional studies should be done with different sizes of biomass particles to determine whether the controlling phenomenon is transport (diffusion and convection) or kinetic (reaction rates). In scaling up the extraction process, larger biomass particles will most likely be used, thus it will be crucial to understand the controlling mechanism. Studies with other feedstocks, particularly a softwood and/or grass, would be interesting to see how the rate constants change based on the initial lignin structure and monolignol ratio.

Chapter 4 used FTIRC-HRMS to analyze the lignin breakdown products from catalytic upgrading. A great deal more research is needed in this area, as catalysis development will be critical if lignin is to be converted into fine chemicals. Additional work to completely understand the bias of the ionization source, and methods to lessen the bias, are needed as well.

5.2.2 Future Directions

To fully utilize lignin, separation technologies and methods need to be developed. Due to lignin's inherent heterogeneity, even an ideal catalyst will produce a complex mixture of compounds. Many of the chemical industry's large scale separation processes (e.g., distillation) have been developed for petroleum fractionation. Lignin is less stable, more oxygen rich, and more acidic than most crude oil mixtures, so numerous adaptations will be required to effectively produce fine chemicals.

Appendix I: Supplementary Information for Chapter 2: Isolation of Lignin from Ammonia Fiber Expansion (AFEX) Pretreated Biorefinery Waste

Contains 12 pages including: 4 figures and 5 tables.

Table of Contents:

Figures

Tables

Figure I-1. Aliphatic region of 2D ^{1}H-^{13}C HSQC NMR spectra of UHS and the solids remaining after extraction of UHS with aqueous solutions of acetone, ethanol, acetic acid, and γ-valerolactone.

Figure I-2. Aromatic region of 2D ^{1}H-^{13}C HSQC NMR spectra of UHS and the solids remaining after extraction of UHS with aqueous solutions of acetone, ethanol, acetic acid, and γ-valerolactone.

105

Figure I-3. ^{31}P NMR spectral intensities of phosphitylated material extracted from UHS in aqueous solutions of acetone, ethanol, acetic acid, and γ-valerolactone.
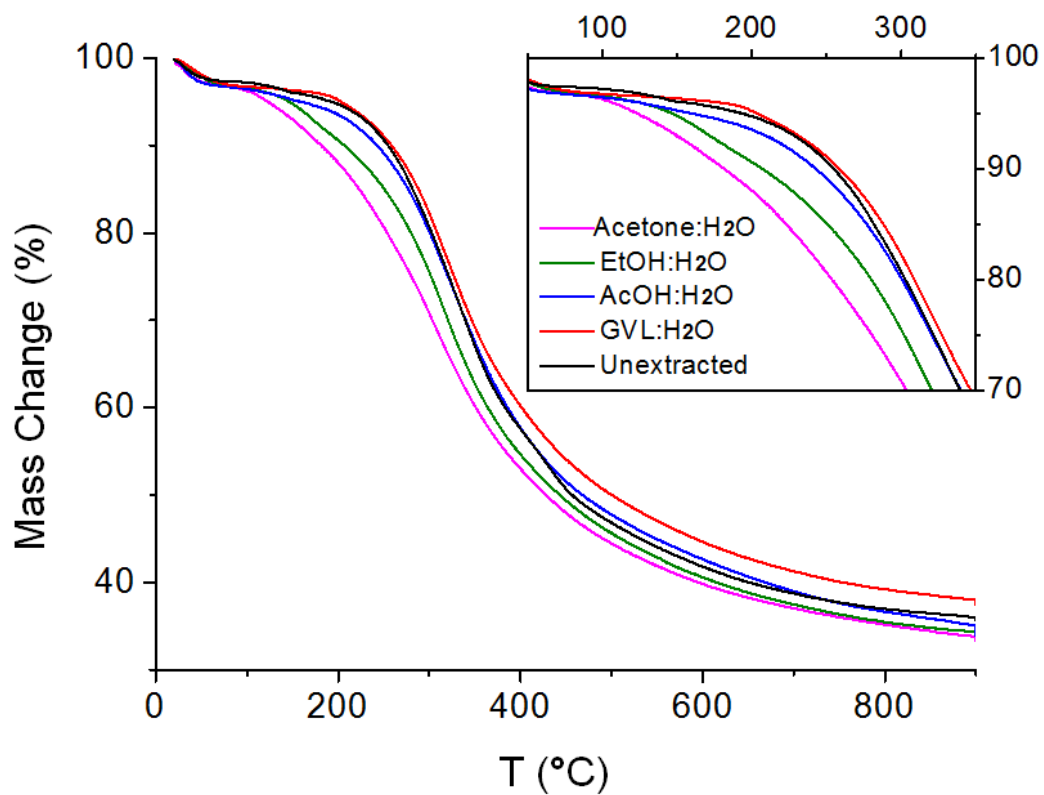
Figure I-4. Thermogravimetric analysis (TGA) cruves of material extracted from UHS in aqueous solutions of acetone, ethanol, acetic acid, and γ-valerolactone.

Table I-1. Relative compositional analysis of the material extracted from UHS with various solvents.

Solvent	Glucan (%)	Xylan (%)	Arabinan (%)	Acid insoluble Lignin (%)	Ash content (%)
Acetone:H$_2$O (2:1)	27.1	8.8	1.7	61.7	0.7
Ethanol:H$_2$O (2:1)	1.9	1.9	0.0	95.9	0.3
GVL:H$_2$O	34.5	16.6	3.6	44.5	0.9
AcOH:H$_2$O (2:1)	1.0	0.9	0.0	97.9	0.2

Table I-2. Relative compositional analysis of the residual solids after extraction of UHS with various solvents.

Solvent	Glucan (%)	Xylan (%)	Arabinan (%)	Acid insoluble Lignin (%)	Ash content (%)
Dichloromethane (DCM)	20.1	7.8	1.6	41.3	29.2
Benzene:Ethanol (2:1)	15.4	7.1	1.6	39.3	36.5
Acetone	16.0	7.4	0.0	42.7	33.9
Acetonitrile (ACN)	15.3	7.1	1.6	40.9	35.2
Acetone:H$_2$O (2:1)	**16.4**	**5.0**	**0.0**	**39.1**	**39.5**
Hexane	21.3	7.8	1.7	41.3	27.9
1,4 Dioxane	12.9	6.6	1.7	38.0	40.9
Benzene	21.4	7.6	1.5	42.1	27.5
Ethyl acetate	20.8	7.3	1.5	42.8	27.6
Ethanol	11.6	6.0	1.6	39.9	40.9
Ethanol:H$_2$O (2:1)	**13.3**	**5.5**	**1.5**	**27.3**	**52.5**
Glycerine:H$_2$O (2:1)	10.0	2.2	0.0	51.4	36.3
1,4 Dioxane:H$_2$O (24:1)	13.2	6.3	1.5	36.4	42.7
Water	9.5	2.7	0.8	51.8	35.2
γ-Valerolactone (GVL)	9.6	0.8	0.0	43.7	45.9
AcOH	10.1	4.6	0.0	45.8	39.6
GVL:H$_2$O	**0.8**	**0.8**	**0.0**	**65.3**	**33.1**
AcOH:H$_2$O (2:1)	**16.4**	**2.4**	**0.0**	**13.4**	**67.8**
UHS	**18.0**	**7.3**	**0.1**	**51.8**	**22.8**

δ_C/δ_H(ppm)	Assignment	Std	GVL :H$_2$O	AcOH :H$_2$O	EtOH :H$_2$O	Acetone :H$_2$O
55.5/3.7	C/H in methoxyl group (OMe)	s	s	s	s	s
59.6/3.4-3.7	C$_\gamma$/H$_\gamma$ in β-O-4 ether linkage (A)	s	s	s	s	s
71.5/4.9	C$_\alpha$/H$_\alpha$ in β-O-4 linked (A)	s	s	s	s	s
63.3/4.4(3.9)	C$_\gamma$/H$_\gamma$ in β-O-4 ether acetyl linkage (A)	--	--	s	--	--
83.6/4.3	C$_\beta$/H$_\beta$ in β-O-4 linked to a G unit (A)	s	m	w	s	s
85.5/4.1	C$_\beta$/H$_\beta$ in β-O-4 linked to a S unit (A)	s	w	w	s	s
103.5/6.7	C$_{2,6}$/H$_{2,6}$ in syringyl units(S)	s	s	s	s	s
110.6/7.0	C$_2$/H$_2$ in guaiacyl units (G)	s	m	w	s	s
114.3/6.7	C$_5$/H$_5$ in guaiacyl units (G)	s	s	s	s	s
118.6/6.8	C$_6$/H$_6$ in guaiacyl units (G)	s	s	m	s	s
127.9/7.2	C$_{2,6}$/H$_{2,6}$ in p-hydroxycinnamyl units (H)	s	s	s	s	s
120.7/7.0	C$_6$/H$_6$ in ferulate (FA)	s	--	--	w	w
128.6/7.4	C$_{2,6}$/H$_{2,6}$ in p-coumarate (pCA)	m	m	m	m	m

Table I-3. [1]H/^{13}C chemical shifts and assignments for the chemical substructures units as detected by HSQC NMR spectra of the material extracted from UHS in aqueous solutions of acetone, ethanol, acetic acid, and γ-valerolactone.
s: strong resonance; **m**: medium resonance; **w**: weak resonance

Table I-4. Carbon content (mmol C / g lignin) attributed to functionalities from quantitative ^{13}C NMR spectral intensities of the material from UHS in aqueous solutions of acetone, ethanol, acetic acid, and γ-valerolactone. The residual γ-valerolactone peaks were removed from the integrations.

^{13}C Chemical Shift (ppm)	Assignment	Carbon Content (mmol of C / g lignin)				
		GVL:H$_2$O	AcOH:H$_2$O	EtOH:H$_2$O	Acetone:H$_2$O	Standard
	Total C	48.0	43.9	39.2	46.3	46.0
166.2-95.8	Aromatic C	20.6	21.7	20.5	23.6	26.1
91.0-60.8 / 55.2-0.0	Aliphatic C	18.9	12.9	11.2	14.1	13.9
166.2-142.0	Aromatic C-O	7.3	5.9	6.2	7	7.1
142.0-125.0	Aromatic C-C	5.5	6.4	6.4	7.1	8.1
125.0-95.8	Aromatic C-H	7.9	9.4	7.9	9.5	10.9
91.0-60.8	Aliphatic C-O	11.9*	4.8	5.8	7.5	5.4
60.8-55.2	Methoxyl	3.3	3.8	3.8	4.9	5.2
55.2-0.0	Aliphatic C-C	7.0	8.1	5.4	6.6	7.7
215.0-166.2	Carbonyl and Carboxyl	5.2*	5.5	3.7	3.6	1.6

*The intensity of solvent related peaks were removed from the integration.

Table I-5. Hydroxyl content (mmol of OH / g of lignin) determined by ^{31}P NMR spectral intensities of the phosphitylated material extracted from UHS in aqueous solutions of acetone, ethanol, acetic acid, and γ-valerolactone.

^{31}P Chemical Shift (ppm)	Assignment	OH content (mmol of OH / g of lignin)				
		Std	GVL:H$_2$O	AcOH:H$_2$O	EtOH:H$_2$O	Acetone:H$_2$O
	Total OH	9.6	7.4	5.8	8.4	10.4
145.4-150.0	Aliphatic OH	4.7	3.6	1.9	5.4	7.6
136.0-143.5	Aromatic OH	3.8	2.6	2.8	2.2	1.9
143.5-141.5	Syringyl and Condensed Phenol OH	1.0	0.7	0.9	0.5	0.4
141.5-140.5	C$_5$-Substituted Guaiacyl OH	0.1	0.2	0.2	0.2	0.2
140.5-138.8	Guaiacyl OH	1.5	0.9	1.0	0.9	0.8
~137.8	*p*-Hydroxyphenyl OH	1.2	0.8	0.7	0.7	0.6
136.0-130.0	Carboxylic Acid OH	1.1	1.2	1.1	0.9	0.9

Appendix II: Supplementary Information for Chapter 3 Understanding Fragmentation and Condensation Reaction Kinetics during Organosolv Extractions

Contains 12 pages: 6 figures and 4 tables

Table of Contents:

Figures:

Figure II-1: Mass balance of the recovered fractions

Figure II-2: Arrhenious plot of extraction and precipitation reactions

Figure II-3: ^{31}P NMR spectra of resulting lignin

Figure II-4: Amount of key OH moieties with fits

Figure II-5: ^{13}C NMR spectra of resulting lignings

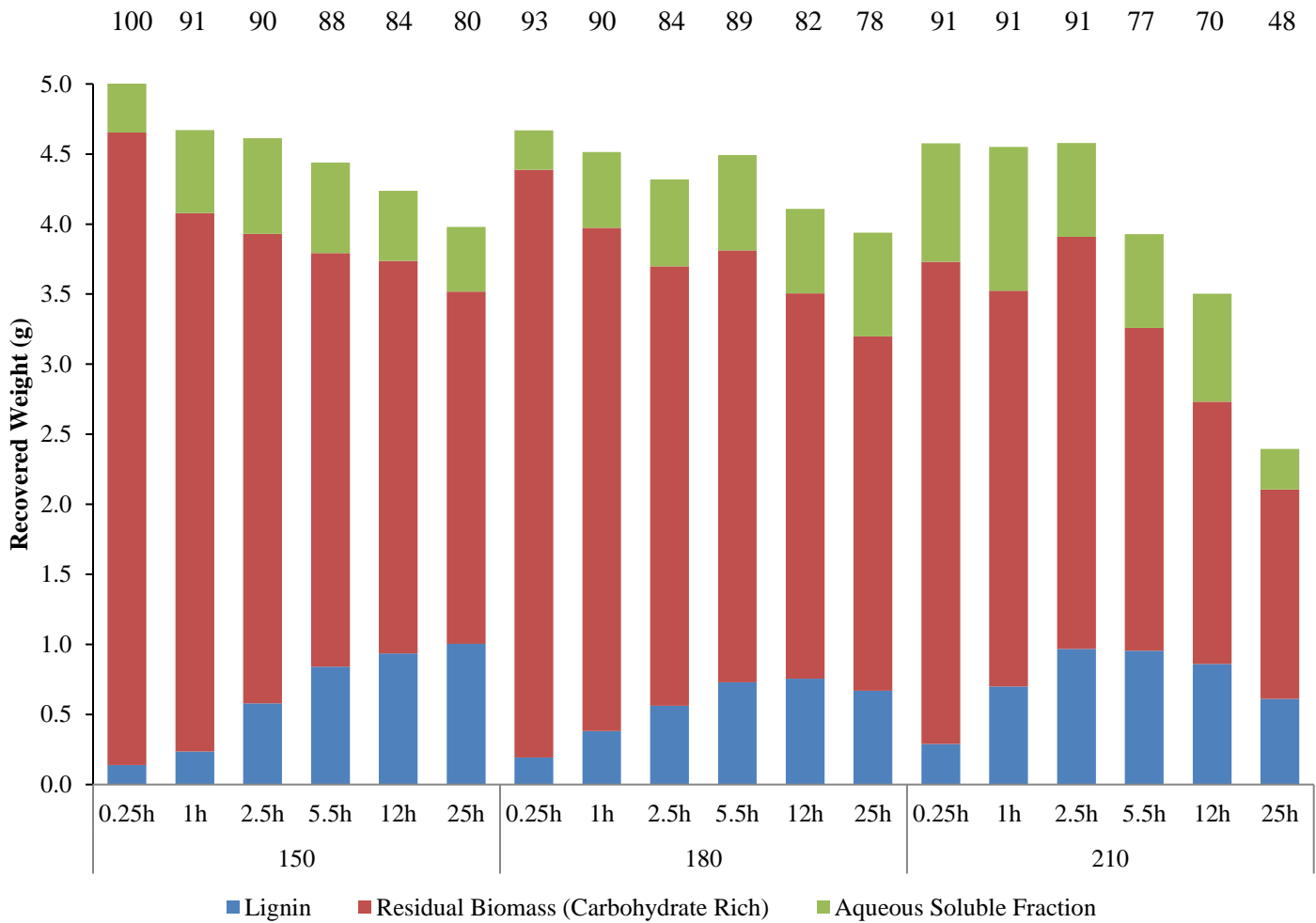Figure II-6: Amount of key carbon chemical moieties and fits

Tables:

Table II-1: GPC results of the resulting lignin

Table II-2: Chemical shifts and integration regions for lignin in a ^{31}P NMR spectrum

Table II-3: Chemical shifts and integration regions for lignin in a ^{13}C NMR spectrum

Table II-4: TOC results for select lignin

Figure II-1: Mass balance of the recovered fractions. The starting biomass was ~5g, the starting lignin within the biomass is ~1.1g (dashed line). The number above each column is the total mass percent of starting biomass recovered after the organosolv extractions.
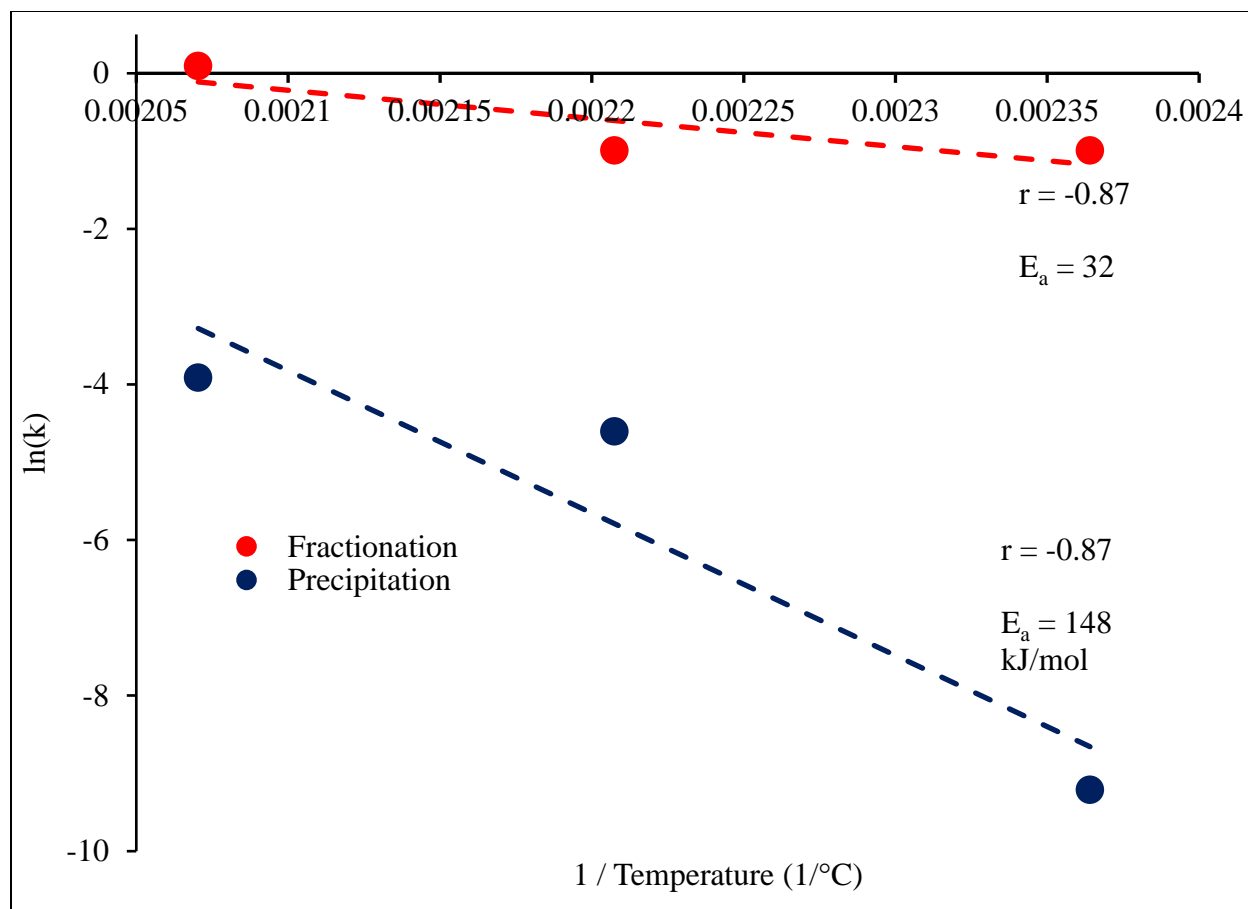
Figure II-2 Arrhenius plot of the fractionation and precipitation
reactions.

Table II-1: GPC results. The number average and weight average molecular weight and dispersity of the recovered lignins

| | 150 °C | | | 180 °C | | | 210 °C | | |
	M_n	M_w	Đ	M_n	M_w	Đ	M_n	M_w	Đ
0.25 h	1300	2500	2.0	1100	2300	2.1	1300	3500	2.7
1.0 h	1300	3300	2.7	1000	2600	2.5	1100	2300	2.1
2.5 h	1000	2200	2.2	1200	2700	2.4	800	1200	1.6
5.5 h	700	1900	2.7	1000	2400	2.4	900	1500	1.7
12 h	1200	2400	2.0	900	1500	1.6	900	1600	1.7
25 h	1000	2000	1.9	1200	2300	1.8	700	1200	1.6

Table II-2: Chemical shifts and integration regions for lignin in a ^{31}P NMR spectrum.

Structure	Δ(ppm)
Aliphatic OH	150.0-145.4
Syringyl Phenolic OH	~142.7
Guaiacyl Phenolic OH	140.2-139.0
Condensed Phenolic OH	144.7-140.2
Carboxylic Acid OH	136.0-133.6
Internal Standard	152.8-151.0
TMDP Hydrolysis Product	~132.2
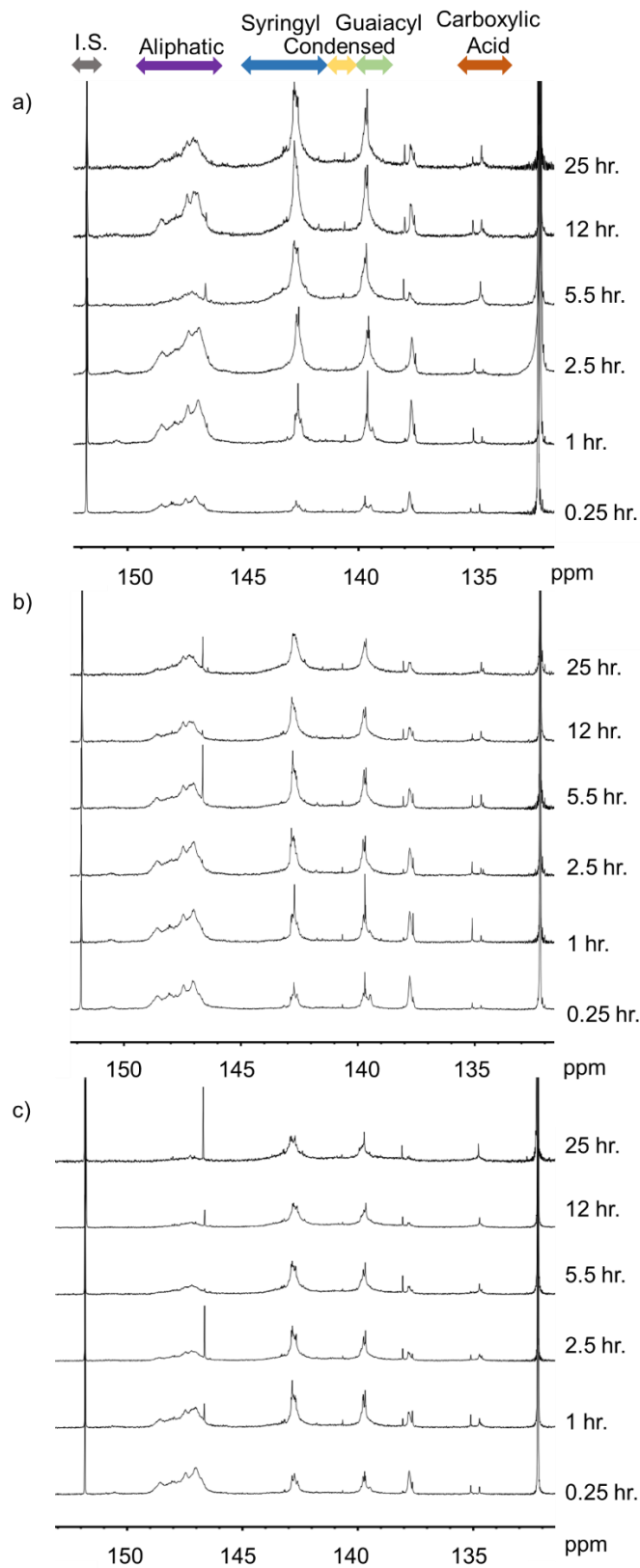
Figure II-3: ^{31}P NMR spectra for a) 150 °C b) 180 °C and c) 210 °C extraction series with integration regions for key moieties indicated by arrows.
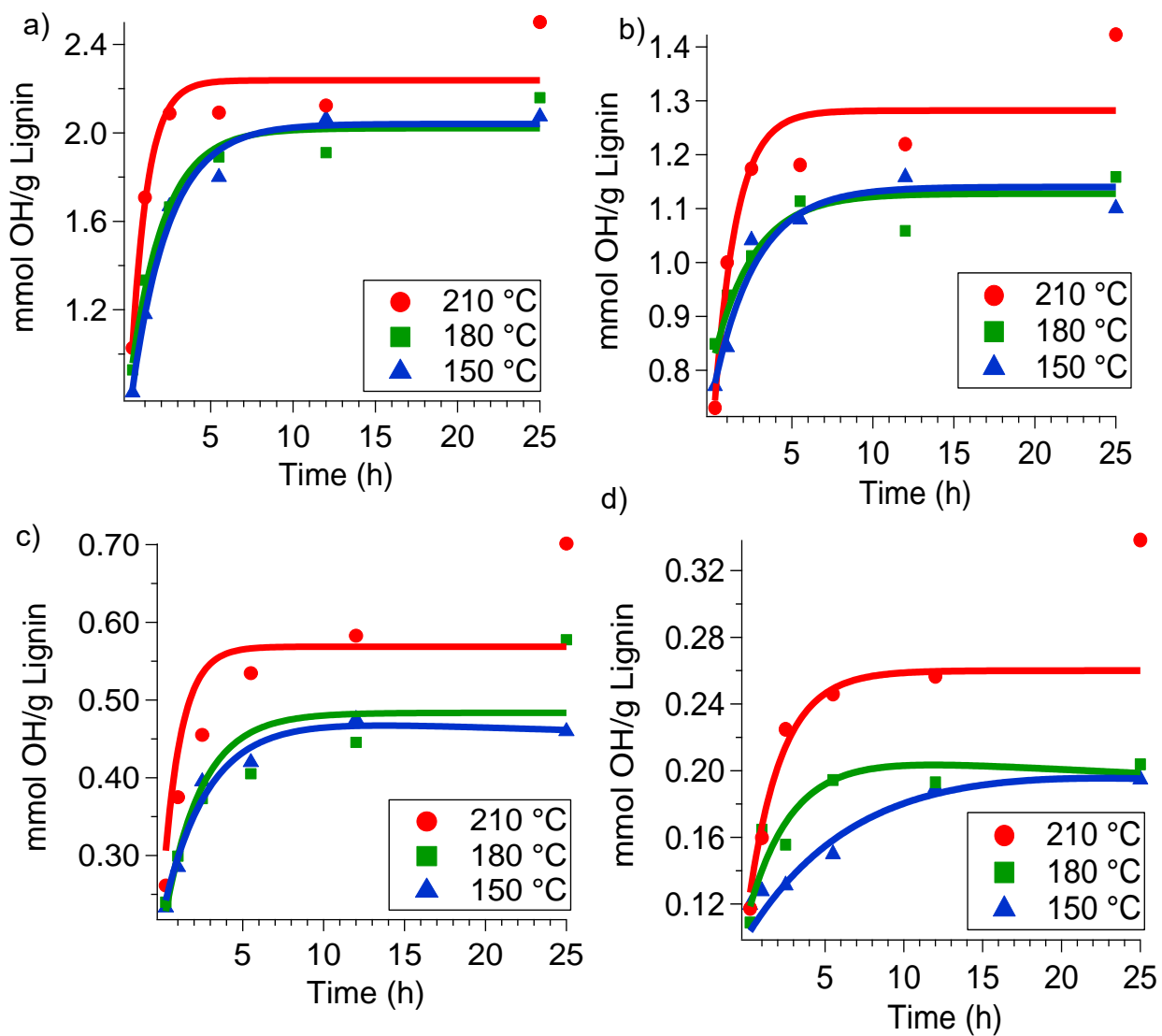
Figure II-4: Amount of a) syringyl OH b) guaiacyl OH c) condensed OH and d) carboxylic acid OH per gram of recovered lignin with fits

Table II-3: Chemical shifts and integration regions for lignin in a ^{13}C NMR spectrum.

Structure	Δ(ppm)
Aliphatic	28 - 0
O-Aliphatic	90 - 58
Aromatic	160 - 100
Aromatic C-H	124 - 100
Aromatic C-C	146 – 124
Aromatic C-O	146 - 160
Etherified Aromatic C-O	154 - 148
Non-Etherified Aromatic C-O	148 - 145
Internal Standard	93.2

Table II-4

Carbon Concentration (mmol C / g lignin)

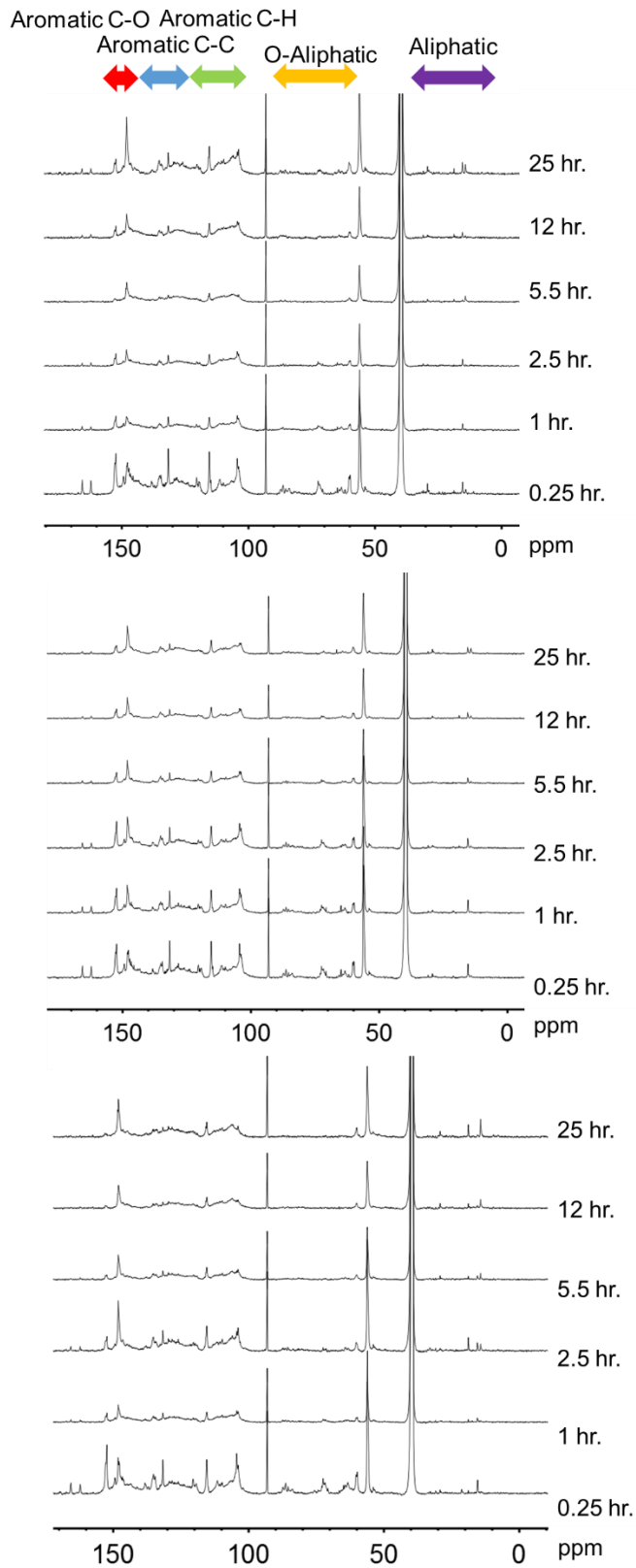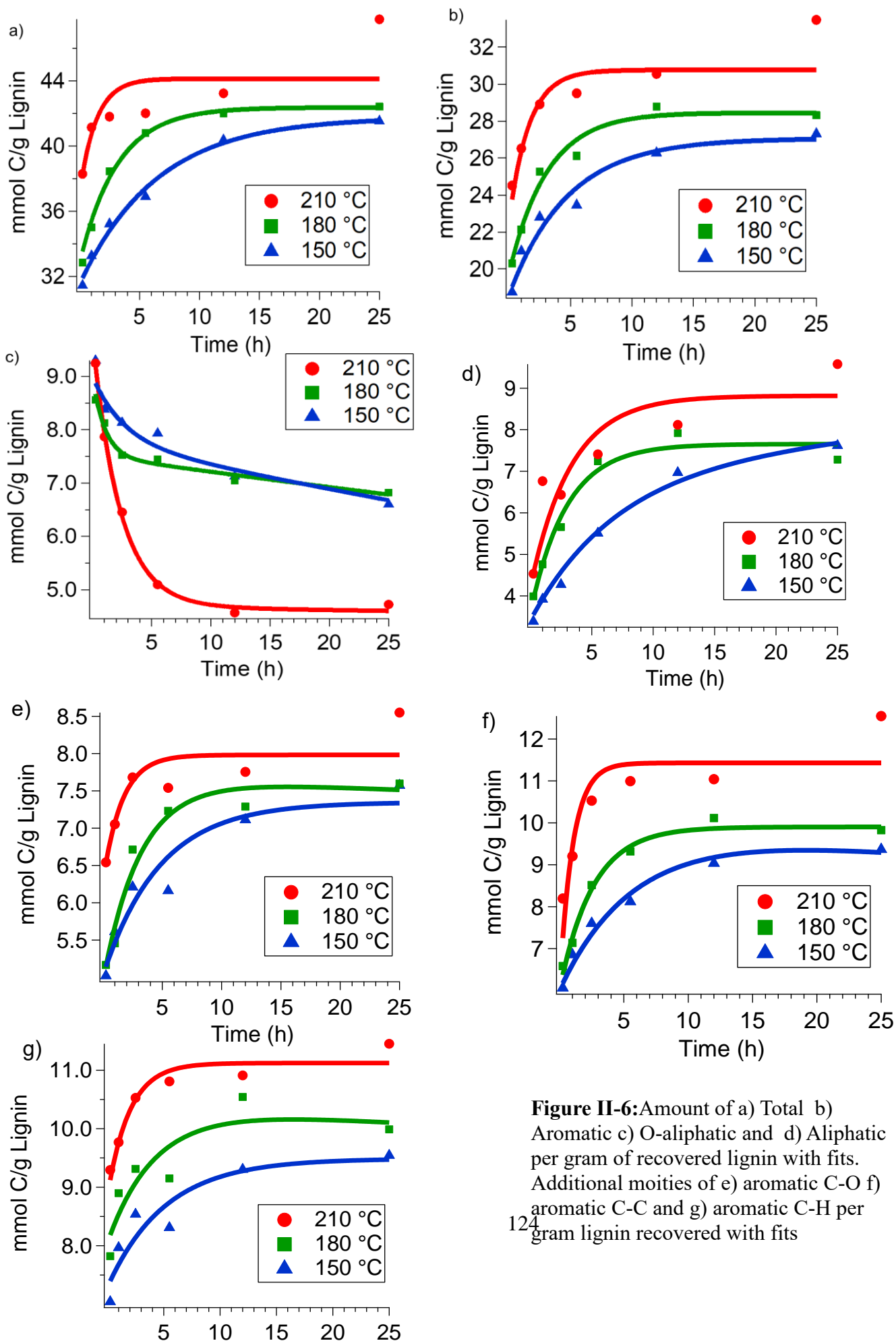|	1 h	12 h	25 h
150 °C	0.049	0.052	0.054
180°C	0.049	0.054	0.055
210 °C	0.053	0.057	0.060

Figure II-5: ^{13}C NMR spectra of a) 150
b) 180 and c) 210 °C series

23

Figure II-6: Amount of a) Total b) Aromatic c) O-aliphatic and d) Aliphatic per gram of recovered lignin with fits. Additional moities of e) aromatic C-O f) aromatic C-C and g) aromatic C-H per gram lignin recovered with fits

124

Appendix III: Supplementary Information for Chapter 4 Improving the understanding of complex lignin derived mixtures with Fourier transform ion cyclotron resonance high resolution mass spectrometry

Contains 14 pages: 7 figures and 5 tables

Table of Contents:

Count of peaks	# of N	1	2	3	4	5	6	7	8	9	10	11	12	13	14	15	16	17	18
	(-) APPI	280	85	107	178	121	0	0	0	0	0	0	0	0	0	0	0	0	0
Ionization Method	(+) APPI	366	133	57	345	159	0	0	0	0	0	0	0	0	0	0	0	0	0
	(-) ESI	253	801	172	32	20	0	0	0	0	0	0	0	0	0	0	0	0	0
	(+) ESI	772	532	356	510	620	299	50	298	49	107	62	94	38	8	5	12	6	2

% of peaks	# of N	1	2	3	4	5	6	7	8	9	10	11	12	13	14	15	16	17	18
	(-) APPI	3%	1%	1%	2%	2%	0%	0%	0%	0%	0%	0%	0%	0%	0%	0%	0%	0%	0%
Ionization Method	(+) APPI	3%	1%	1%	3%	1%	0%	0%	0%	0%	0%	0%	0%	0%	0%	0%	0%	0%	0%
	(-) ESI	3%	11%	2%	0%	0%	0%	0%	0%	0%	0%	0%	0%	0%	0%	0%	0%	0%	0%
	(+) ESI	11%	8%	5%	7%	9%	4%	1%	4%	1%	2%	1%	1%	1%	0%	0%	0%	0%	0%

Table III-1: Distribution of nitrogen containing compounds by ionization method

Count of Peaks	# of S	1	2	3	4	5	6	7	8	9
	(-) APPI	267	156	0	0	0	0	0	0	0
Ionization Method	(+) APPI	528	236	0	0	0	0	0	0	0
	(-) ESI	922	425	0	0	0	0	0	0	0
	(+) ESI	1578	668	119	79	6	8	6	4	2

% of peaks	# of S	1	2	3	4	5	6	7	8	9
	(-) APPI	3.3%	1.9%	0.0%	0.0%	0.0%	0.0%	0.0%	0.0%	0.0%
Ionization Method	(+) APPI	4.6%	2.1%	0.0%	0.0%	0.0%	0.0%	0.0%	0.0%	0.0%
	(-) ESI	12.1%	5.6%	0.0%	0.0%	0.0%	0.0%	0.0%	0.0%	0.0%
	(+) ESI	23.2%	9.8%	1.7%	1.2%	0.1%	0.1%	0.1%	0.1%	0.0%

Table III-2: Distribution of sulfur containing compounds by ionization method

Count of Peaks	# of P	1
	(-) APPI	286
Ionization Method	(+) APPI	390
	(-) ESI	125
	(+) ESI	40

% of peaks	# of P	1
	(-) APPI	4%
Ionization Method	(+) APPI	3%
	(-) ESI	2%
	(+) ESI	1%

Table III-3: Distribution of phosphorous containing compounds by ionization methods

Sample	N [%]	C [%]	S [%]
MeOH3h	0.084	59.746	0.028
MeOH 6h	0.082	68.977	0.023
MeOH 9h	0.082	60.370	0.021
CuPMO 3h	0.087	63.947	0.016
CuPMO 6h	0.075	65.955	0.008
CuPMO 9h	0.073	66.370	0.008
DMC 3h	0.056	57.793	0.002
DMC 6h	0.073	57.830	0.002
DMC 9h	0.062	61.424	0.003
Untreated Lignin	0.079	59.021	0.031

Table III-4: Elemental analysis of the lignin samples

Mass Count		Untr-Lignin	CuPMO 9h	CuPMO 6h	CuPMO 3h	DMC 9h	DMC 6h	DMC 3h	MeOH 9h	MeOH 6h	MeOH 3h
(-) APPI	M_n	374	336	352	335	433	412	433	404	410	437
	M_w	458	366	385	368	497	469	496	452	461	496
	Đ	1.22	1.09	1.09	1.10	1.15	1.14	1.15	1.12	1.12	1.13
(+) APPI	M_n	326	374	394	369	400	397	400	371	376	379
	M_w	386	414	439	410	456	451	455	417	423	431
	Đ	1.18	1.11	1.11	1.11	1.14	1.14	1.14	1.13	1.12	1.14
(-) ESI	M_n	342	319	345	366	389	362	394	391	389	372
	M_w	384	342	373	399	426	389	430	427	425	407
	Đ	1.13	1.07	1.08	1.09	1.09	1.07	1.09	1.09	1.09	1.09
(+) ESI	M_n	328	415	421	409	416	429	418	430	436	430
	M_w	372	446	450	440	441	457	445	457	464	460
	Đ	1.13	1.07	1.07	1.07	1.06	1.07	1.07	1.06	1.06	1.07

TIC		Untr-Lignin	CuPMO 9h	CuPMO 6h	CuPMO 3h	DMC 9h	DMC 6h	DMC 3h	MeOH 9h	MeOH 6h	MeOH 3h
(-) APPI	M_n	319.8	284.2	297.2	280.7	375.1	350.5	376.3	373.4	377.0	400.7
	M_w	382.8	311.5	325.2	312.4	426.4	394.6	427.6	410.3	415.6	446.0
	Đ	1.20	1.10	1.09	1.11	1.14	1.13	1.14	1.10	1.10	1.11
(+) APPI	M_n	270.0	291.1	304.3	282.1	341.2	329.6	338.7	322.8	332.2	334.1
	M_w	325.0	325.9	342.1	318.5	391.2	376.5	388.7	367.2	376.1	381.6
	Đ	1.20	1.12	1.12	1.13	1.15	1.14	1.15	1.14	1.13	1.14
(-) ESI	M_n	267.7	321.2	315.2	339.4	354.9	337.5	357.1	324.4	323.0	317.5
	M_w	291.2	334.9	324.3	362.4	382.6	359.8	386.8	355.6	354.4	349.0
	Đ	1.09	1.04	1.03	1.07	1.08	1.07	1.08	1.10	1.10	1.10
(+) ESI	M_n	310.8	383.4	376.9	373.5	391.9	395.3	393.6	395.7	400.1	385.6
	M_w	328.3	414.0	405.7	397.6	409.6	416.8	411.7	414.1	419.3	406.1
	Đ	1.06	1.08	1.08	1.06	1.05	1.05	1.05	1.05	1.05	1.05

Table III-5: Molecular weight and dispersity of the lignin samples by ionization method
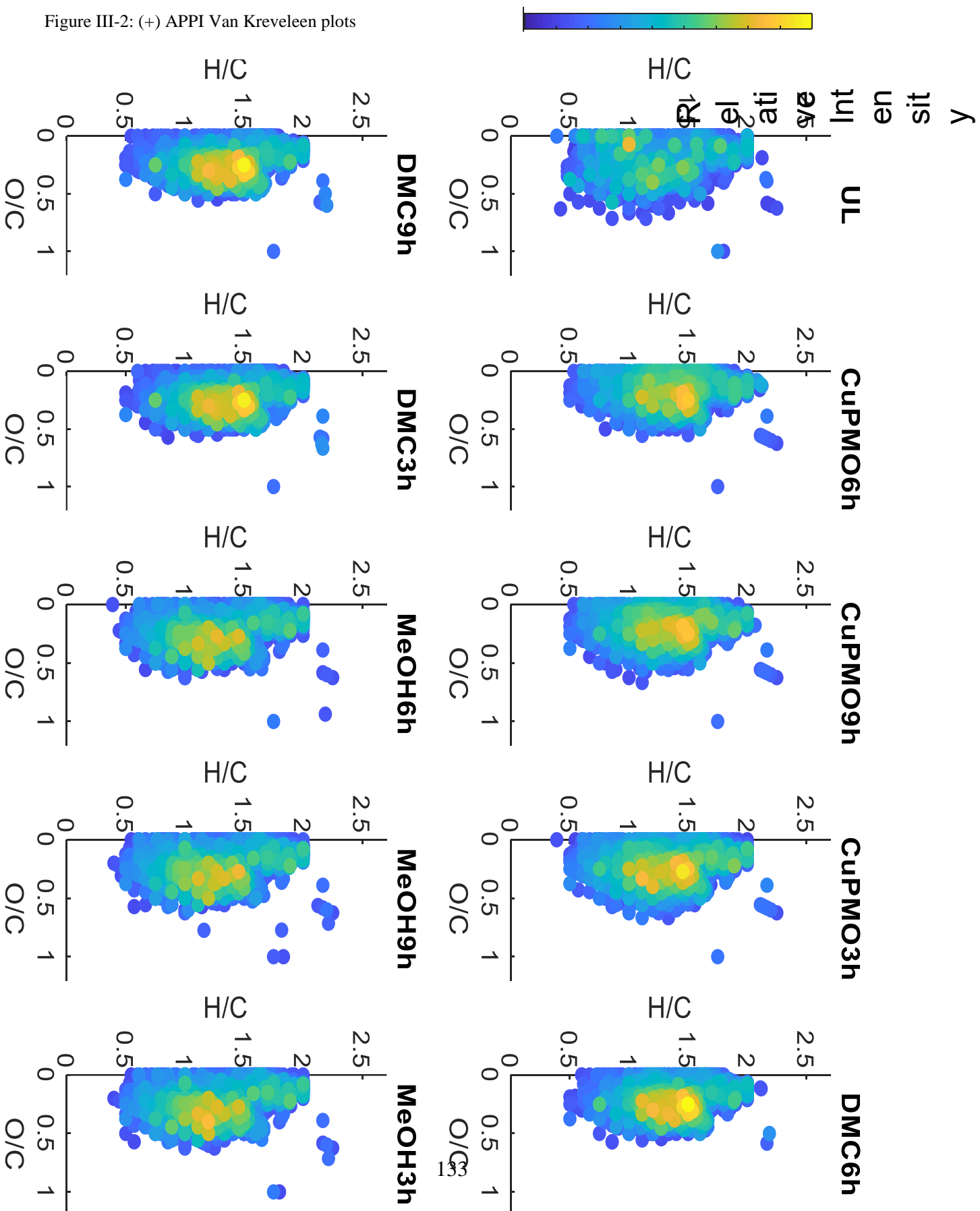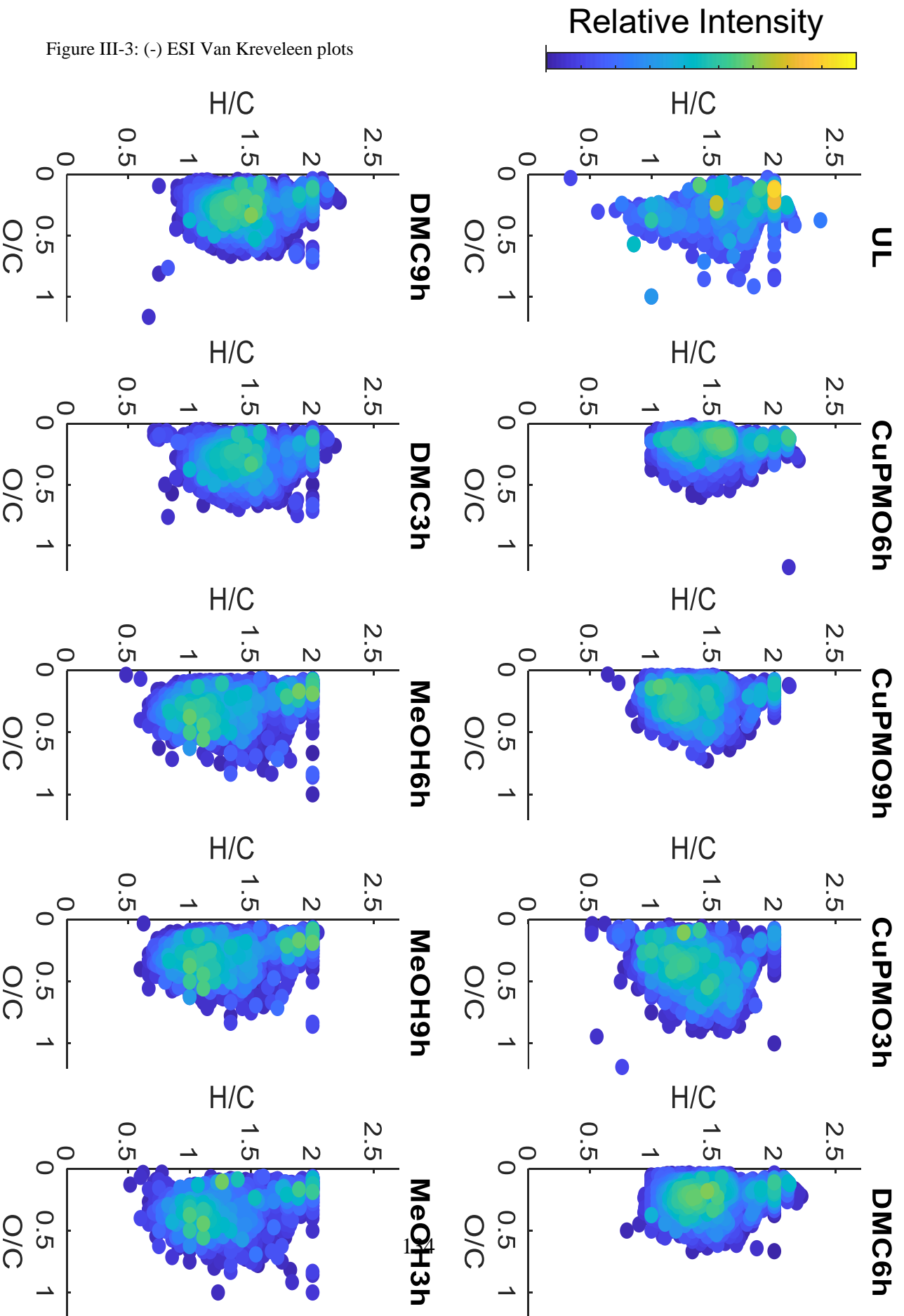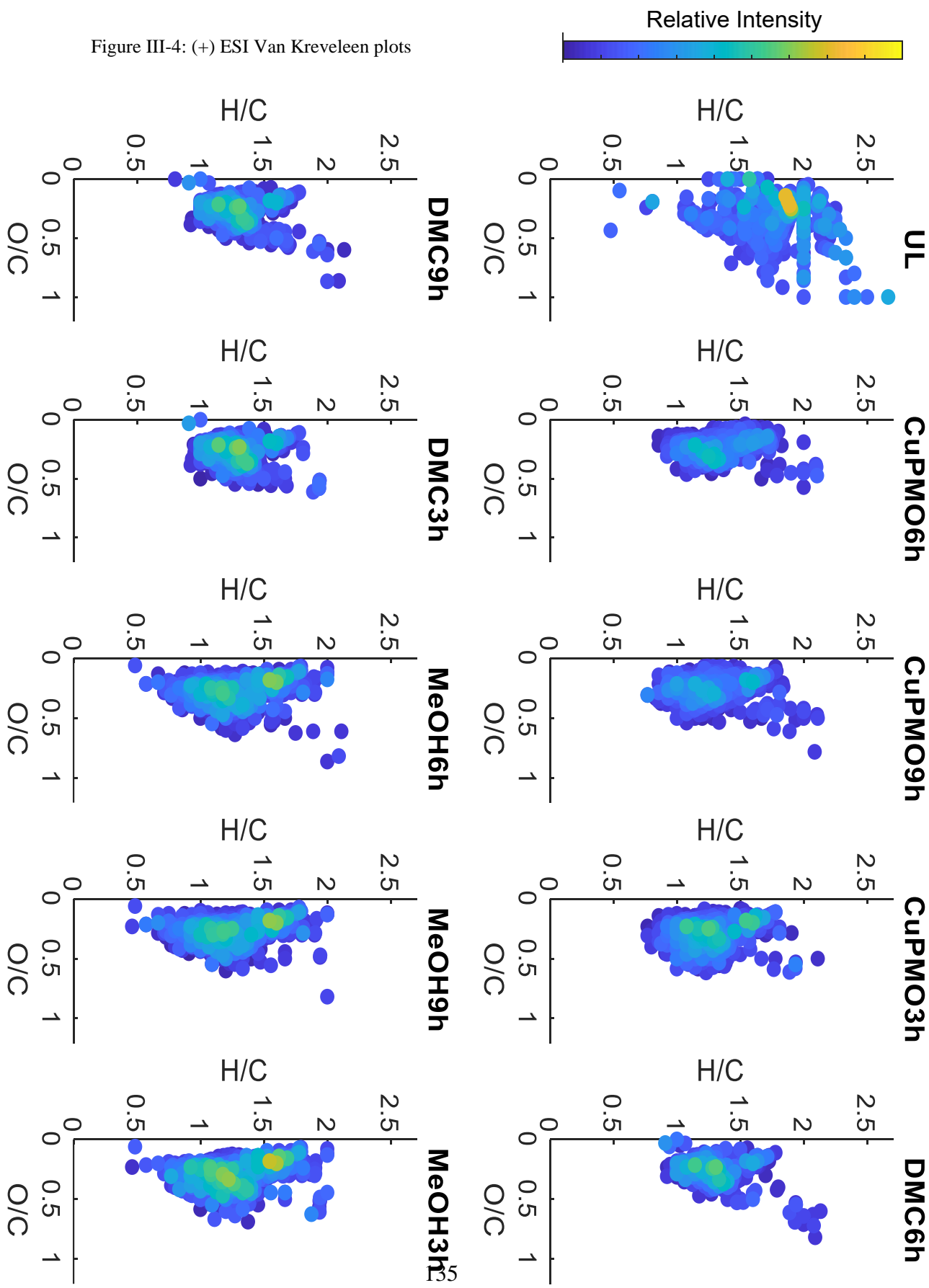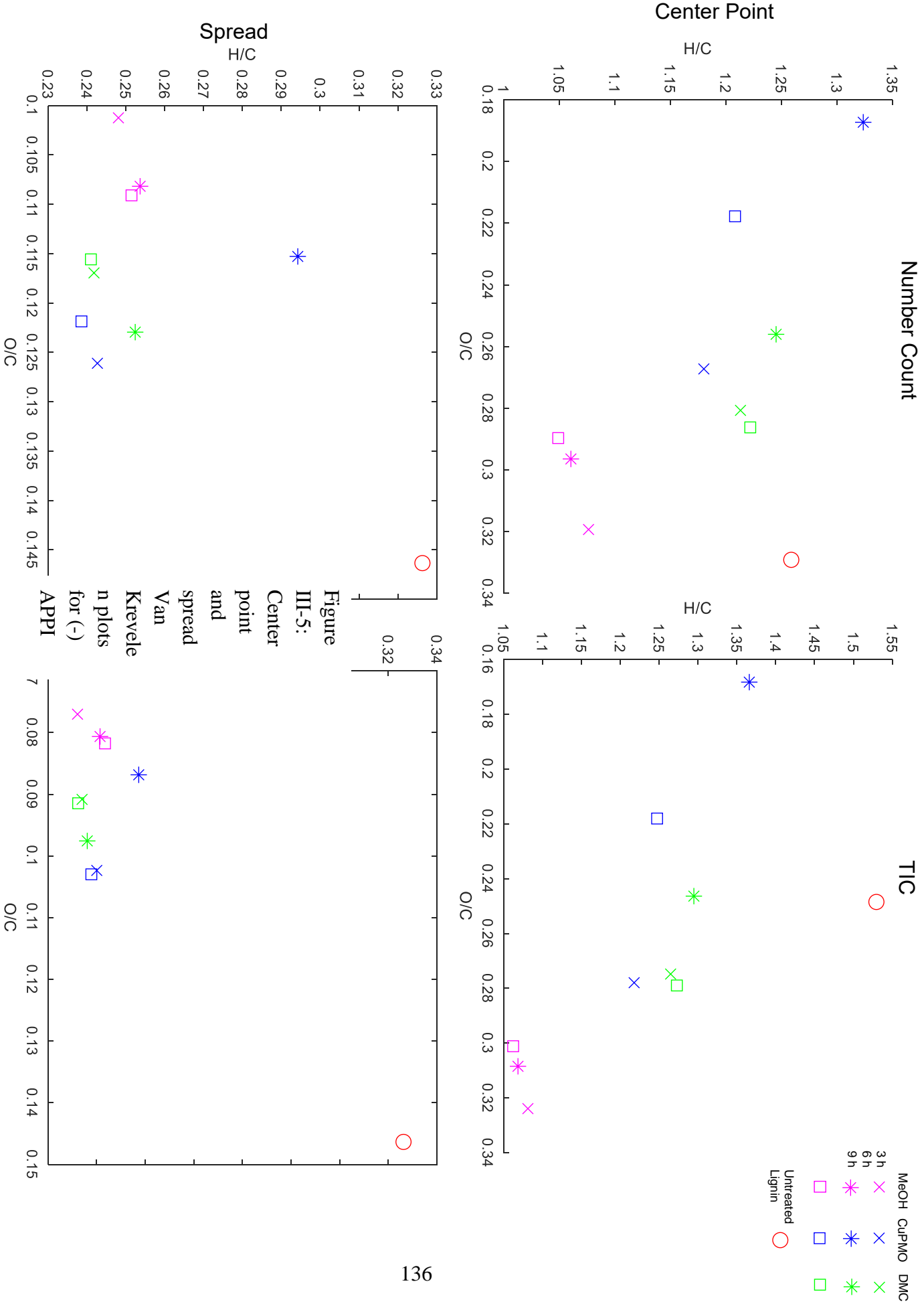
Figure III-1: (-) APPI Van Kreveleen plots
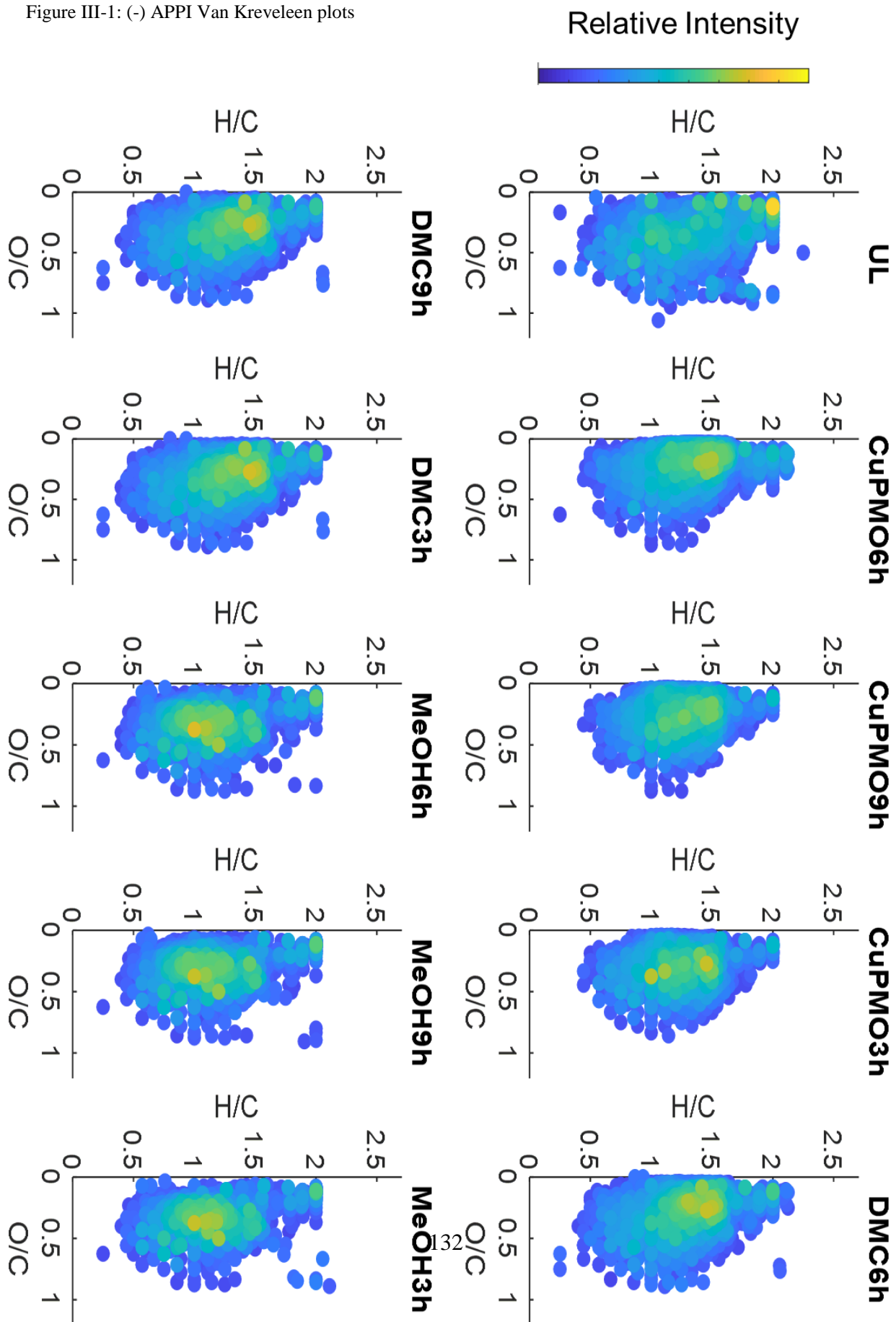
Figure III-2: (+) APPI Van Kreveleen plots

Figure III-3: (-) ESI Van Kreveleen plots

Relative Intensity

UL

CuPMO6h

CuPMO9h

CuPMO3h

DMC6h

DMC9h

DMC3h

MeOH6h

MeOH9h

MeOH3h

Figure III-4: (+) ESI Van Kreveleen plots

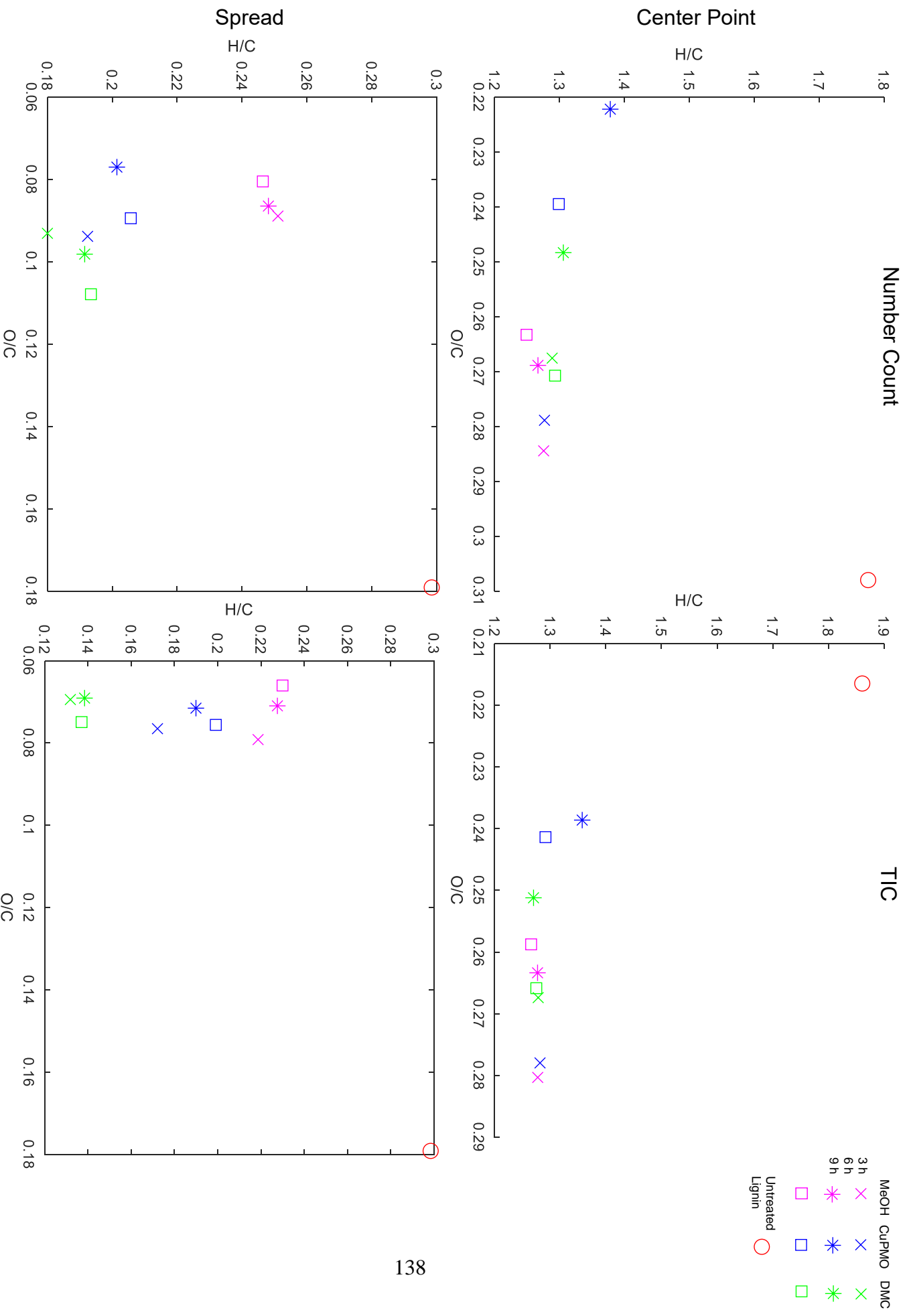Figure III-5: Center point and spread Van Krevelen plots for (-) APPI
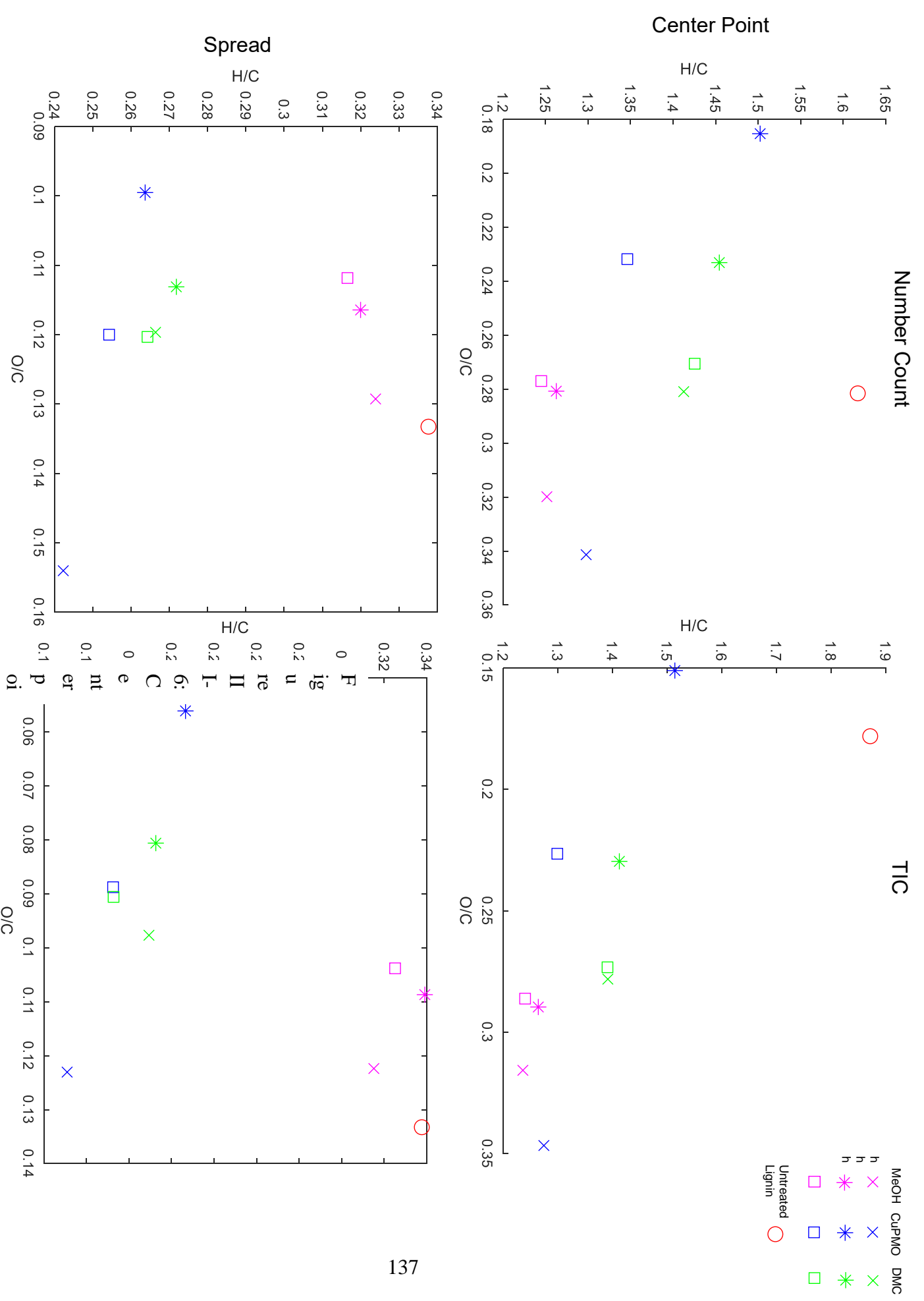
Figure III-7: Center point and spread Van Krevelen plots for (+) ESI